EFFECTS OF PARP-1 SIGNALING AND CONJUGATED LINOLEIC ACID ON BRAIN CELL BIOENERGETICS AND SURVIVAL

By

Waylon T. Hunt

A Thesis submitted to the Faculty of Graduate Studies of

The University of Manitoba

in partial fulfillment of the requirements of the degree of

DOCTOR OF PHILOSOPHY

Department of Pharmacology and Therapeutics

University of Manitoba

Winnipeg

This thesis is dedicated to my wife Iona, my son Wyatt, and my daughter Aiya

You provide purpose and meaning to my life. Iona, you have been extremely patient and supportive during my pursuit of higher education over the past decade and I will forever be grateful. Wyatt and Aiya, you are by far my most important experiments and no hypothesis could have prepared me for the results. Thank you all for blessing me with such a loving family.

TABLE OF CONTENTS

Acknowledgements

To my supervisor, Dr. Chris Anderson and to my graduate committee advisors Dr. Francis Amara, Dr. Hope Anderson, and Dr. Gordon Glazner, thank you for your mentorship and guidance throughout the course of my various projects. You each possess strengths that are necessary for demonstrating what becoming a successful PhD graduate is. Thank you for your input and for ensuring my successful development and completion.

To members of the Anderson lab, especially our research associate Dr. Zongjun (June) Shao and lab mates, Jill LeMaistre, Dr. Amit Kamboj and Dr. Kim San Tang, thank you for all of your assistance and support over the course of my graduate studies. I have been fortunate to possess your friendship and I will miss the conversations and laughter we shared.

To Dr. Jason Schapansky, thanks for all of your help troubleshooting over the years. Your experience and expertise has been an invaluable asset to the entire department. You were a great friend and fellow graduate student until you decided to move away. Your ability to understand my 80's references will be missed.

To Dr. Elena Zherebitskaya and Dr. Eli Akude, thank you for your friendship and help troubleshooting experiments. Elena, I will miss our conversations and laughter. Eli, I will not miss calling you Dr. Akude for the last few months.

To our administrative manager, Kelly Jorundson, your help with posters, award applications, general administration and even my thesis have been appreciated immensely. Thank you for lending an ear and a helping hand even when you were busy with other things; you are irreplaceable.

To all other pharmacology graduate students and faculty, thanks for the memories of Christmas parties and pizza lunches. I will always remember the HPLC grade punch.

To my parents, thank you for raising me to believe that I could accomplish anything I set my mind to and especially for supporting my decisions.

To my brothers, thank you for providing an outlet for venting frustrations or sharing successes during my graduate studies. The Catalina Rye Mixer and Skype were great inventions.

To the Alzheimer's Society of Manitoba and the James Gordon Fletcher Fellowship and the University of Manitoba, thank you for financial support.

Abstract

Glutamate is the primary excitatory neurotransmitter in the central nervous system. Extracellular glutamate concentrations are tightly regulated to avoid over-stimulation of glutamate receptors, which leads to a cascade of deleterious processes collectively known as excitotoxicity. Excitotoxicity is common to several neurodegenerative disorders and CNS injuries, including stroke and Alzheimer's disease (AD). The projects described in this thesis were designed to uncover novel protective pathways in excitotoxic neurodegeneration.

Excessive activation of the DNA repair enzyme, poly(ADP-ribose) polymerase-1 (PARP-1), is a convergence point for neuron death signaling in excitotoxic pathways. In AD, the peptide amyloid-β_{1-42} ($A\beta_{1-42}$) is aberrantly produced, leading to excitotoxic neuron death *in vitro*. To investigate links between $A\beta_{1-42}$ and PARP, we treated cultured cortical neurons with $A\beta_{1-42}$ and determined whether PARP-1 contributes to neuron death. Increased neuron death was observed after $A\beta_{1-42}$ exposure. A non-selective PARP-1/2 inhibitor significantly reduced $A\beta_{1-42}$-induced death while elimination of PARP-1 alone was not neuroprotective. This suggests that PARP-2 or combined effects of PARP-1 and PARP-2 are required for $A\beta_{1-42}$-induced neuron death.

A hallmark of PARP over-activation is depletion of intracellular NAD^+ and ATP levels, yet nearly all studies examining adenine nucleotide levels use separate biochemical samples to measure nucleotides individually. We developed two HPLC methods for simultaneous separation of NAD^+, ATP, ADP and AMP. We determined that PARP-1 activation in astrocytes leads to near complete NAD^+ depletion, followed by partial loss of ATP pools and total adenine nucleotide pools.

Finally, we hypothesized that conjugated linoleic acid (CLA), a naturally occurring polyunsaturated fatty acid, is capable of enhancing neuron survival after an excitotoxic insult. Cultured cortical neurons were exposed to glutamate in the presence and absence of CLA. CLA levels likely achievable in human plasma and brain tissue during dietary supplementation regimens, protected neurons against glutamate excitotoxicity when given during or up to five hours after glutamate exposure. Several markers of mitochondrial damage and intrinsic apoptosis were examined. CLA stabilized mitochondrial membrane potential and permeability, shedding light on the mechanism of CLA neuroprotection.

Overall, our research suggests a role for PARP in $A\beta_{1\text{-}42}$ toxicity and identifies a novel role for CLA in neuroprotection following excitotoxicity.

List of Tables and Figures

List of Abbreviations

Aβ – amyloid-β

AD – Alzheimer's disease

ADP – adenosine diphosphate

AIF – apoptosis inducing factor

ALS – amyotrophic lateral sclerosis

AMP – adenosine monophosphate

AMPA – α-amino-3-hydroxy-5-methyl-4-isoxazole propionic acid

APOE – apolipoprotein E

APP – amyloid precursor protein

ATP – adenosine triphosphate

Bak – Bcl-2 homologous antagonist/killer

Bax – Bcl-2-associated X protein

BBB – blood brain barrier

Bcl-2 – B-cell lymphoma-2

Bcl-x_L – B-cell lymphoma-extra large

BDNF – brain derived neurotrophic factor

BSA – bovine serum albumin

BSS – basic salt solution

Ca^{2+} – calcium

cAMP – cyclic adenine monophosphate

Cl^- – chlorine

CLA – conjugated linoleic acid

CNS – central nervous system

COX – cytochrome C oxidase

CREB – cAMP response element binding

Cyt C – cytochrome C

DAG – 1,2-diacylglycerol

DCD – delayed calcium deregulation

DMSO – dimethyl sulfoxide

DNA – deoxyribonucleic acid

EAAT – excitatory amino acid transporter

EPSP – excitatory post-synaptic potential

ER – endoplasmic reticulum

ETC – electron transport chain

FAD – familial Alzheimer's disease

FBS – fetal bovine serum

Glu - glutamate

GluR – glutamate receptor

HDL – high-density lipoprotein

H_2O_2 – hydrogen peroxide

HPLC – high-performance liquid chromatography

Hz – hertz

IP_3 – Inositol 1,4,5-triphosphate

JC-1 – 5,5′,6,6′-tetrachloro-1,1′,3,3′ tetraethylbenzimidazolylcarbo-cyanine iodide

K^+ – potassium

LA – linoleic acid

LDH – lactate dehydrogenase

LDL – low-density lipoprotein

LTD – long term depression

LTP – long term potentiation

MCOA – middle cerebral artery occlusion

MEM – minimal essential medium

Mg^{2+} – magnesium

mGluR – metabotropic glutamate receptor

MK-801 – [(+)-5-methyl-10,11-dihydro-5H-dibenzo[a,d] cyclohepten-5,10 -imine maleate)]

MNNG - *N*-methyl-*N*`-nitro-*N*-nitrosoguanidine

MPTP – mitochondrial permeability transition pore

N - nitrogen

Na^{+} – sodium

NAD^{+} – nicotinamide adenine dinucleotide

NADH – reduced nicotinamide adenine dinucleotide

NaCl – sodium chloride

NB - neuralbasal

NFT – neurofibrillary tangles

NGF – nerve growth factor

NMDA – *N*-methyl-D-aspartate

NO – nitric oxide

NPC – neural progenitor cell

$O_2^{\cdot -}$ – superoxide anion

$^{\cdot}OH$ – hydroxyl radical

$ONOO^{-}$ – peroxynitrite

PAR – poly(ADP-ribose)

PARP – poly(ADP-ribose) polymerase

PBS – phosphate buffered saline

PGE_2 – prostaglandin E2

PJ34 – [N-(6-oxo-5,6-dihydrophenanthridin-2-yl)-N, N-dimethylacetamide.HCl]

PPAR – peroxisome proliferator-activated receptor

PS – presenilin

PUFA – polyunsaturated fatty acid

PVDF – polyvinylidine fluoride

ROS – reactive oxygen species

RNAi – ribonucleic acid interference

shRNA – small hairpin ribonucleic acid

SMAC/Diablo – second mitochondria-derived activator of caspases encoded by DIABLO gene

SOD – superoxide dismutase

SRF – serum response factor

TCA – tri-carboxylic acid

TNF-α – tumor necrosis factor α

VGLUT – vesicular glutamate transporter

Zn^{2+} – zinc

ZDF – Zucker Diabetic Fatty

Z-DEVD-FMK – benzyloxycarbonyl-Asp(OMe)-Glu(OMe)-Val-Asp(OMe)-fluormethylketone

Chapter 1: General Introduction

1.0 Glutamate

Glutamate is the primary excitatory neurotransmitter in the central nervous system (Fonnum, 1984). It is a non-essential amino acid that is thought to be found in the cytoplasm of every human cell (Nicholls, 2004). Roughly 80% of all excitatory neurotransmission is mediated by glutamate. Since the realization that glutamate was a neurotransmitter in the 1960's (Hara & Snyder, 2007), glutamate neurotransmission has been thoroughly studied. L-Glutamate is derived from metabolism of glucose via the TCA cycle in mitochondria, and synthesized directly from α-ketoglutarate in the endoplasmic reticulum (ER) (Mark, et al., 2001). It may also be synthesized from glutamine which has been released by astrocytes and taken up into pre-synaptic nerve terminals (Anderson & Swanson, 2000).

Glutamate is ubiquitous throughout the CNS, unlike many other neurotransmitters; this paired with its excitatory nature, results in the requirement for tight control over glutamate concentrations in order to avoid over-stimulation of glutamate receptors (Hardingham, 2009; Olney, 1986). Substantial partitioning in numerous cellular compartments is responsible for maintaining the necessary low basal extracellular concentrations. For example, it is estimated that cytoplasmic concentrations are maintained at approximately 1 mM, while synaptic vesicular concentrations may reach 100 mM. Yet, concentrations found in the synaptic cleft are normally maintained below 1 μM to avoid tonic stimulation of glutamate receptors. Vesicular glutamate transporters (VGLUTs), located on synaptic vesicles, and excitatory amino acid transporters (EAATs), located on the cytoplasmic membranes of both neurons and astrocytes are responsible for glutamate uptake and maintenance of low extracellular glutamate (Fig. 1),

while Na^+/K^+-ATPase's are primarily responsible for maintaining the ionic gradient that keeps these transporters working properly (Nicholls, 2008; Shigeri, Seal, & Shimamoto, 2004). Loss of glutamate homeostasis can result in dramatic increases to as high as 100 μM extracellularly (Nicholls, 2008), producing a paradigm known as glutamate excitotoxicity. Loss of glutamate homeostasis has been linked to conditions including: stroke, epilepsy, Alzheimer's disease (AD), Lou Gehrig's disease (ALS), Huntington's disease, Parkinson's disease, among others (Castillo, Dávalos, Naveiro, & Noya, 1996; Chapman, 2000; Coyle & Puttfarcken, 1993; Mattson, 2003).

Glutamate neurotransmission is achieved via two types of glutamate receptors; ionotropic (NMDA, AMPA and kainate), and metabotropic (mGluR). Glutamate plays a vital role in numerous physiological functions including neurotransmission, CNS development, movement and breathing, learning and memory, as well as numerous deleterious processes such as those mentioned above (VanDongen, 2009).

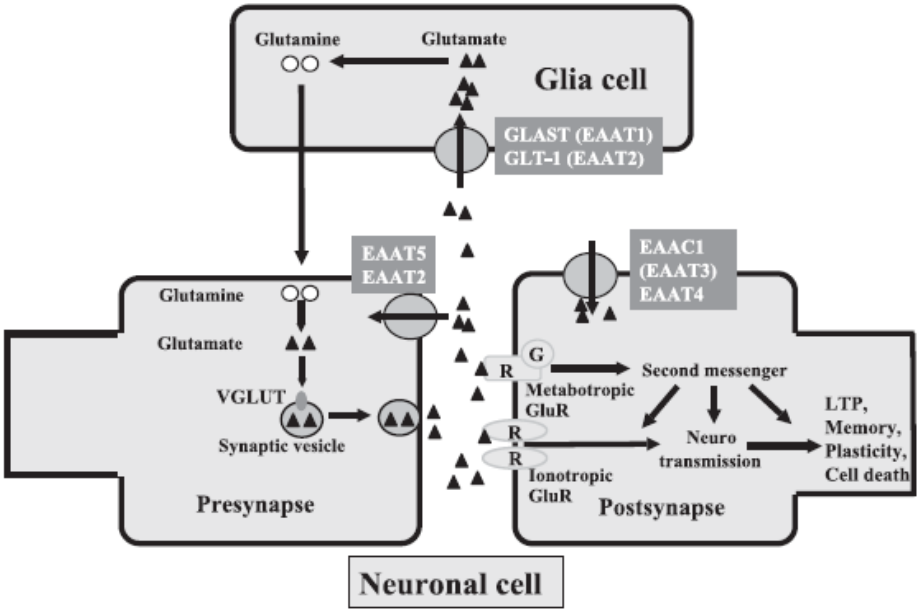

Figure 1. Mechanism of excitatory neurotransmission in the mammalian nervous system

Reprinted from "Molecular pharmacology of glutamate transporters, EAATs and VGLUTs," by Y. Shigeri, R.P. Seal, and K. Shimamoto, 2004, Brain Research Reviews, 45(3):250-265., Copyright 2004, with permission from Elsevier.

1.1 Glutamate Receptors

1.1.1 NMDA Receptors

NMDA receptors (Fig. 2) are ligand-gated ion channels named for the synthetic pharmacological agonist, *N*-methyl-D-aspartate. Known agonists besides NMDA include L-glutamate, L-aspartate, quinolinate, and homocysteate. Co-agonists include glycine and D-serine (Dingledine, Borges, Bowie, & Traynelis, 1999). NMDA receptors mediate slow-excitatory synaptic transmission and are comprised of four subunits. The combination of subunits NR1, NR2A-NR2D, NR3A and NR3B dictates several functional traits of NMDA receptors. Neuronal NMDA receptors contain two NR1 subunits, which contain the co-agonist binding site, and most receptors typically have two NR2 subunits, which contain the glutamate binding site. The presence of NR1 subunits is a functional requirement of all NMDA receptors (Hardingham, 2009), but expression of specific NR2 or NR3 subunits confers specialized functional characteristics and gives rise to differential agonist selectivity and variable channel function that is regionally specific (Lau & Tymianski, 2010). This phenomenon is especially evident during brain development (Kohr, 2006), but also in pathological states such as stroke. For example, it has been demonstrated in neuronal cell cultures that NMDA receptors containing the NR2A subunit promoted survival from excitotoxic insult, whereas receptors containing NR2B mediated neuron death under similar stimuli (Liu, et al., 2007). Another important characteristic of NMDA channels is their voltage dependent Mg^{2+} block. Under resting conditions, Mg^{2+} occludes the NMDA receptor channel pore which blocks the flux of ions through the channel. Mg^{2+} is found at millimolar concentrations in the extracellular environment and at micromolar intracellular concentrations thus providing a gradient that

promotes NMDA receptor channel block under normal conditions. Mg^{2+} block underpins the voltage requirement for receptor activation. Therefore, a voltage threshold must be achieved via activation of AMPA receptors (discussed below) in order for NMDA receptor activation to occur (VanDongen, 2009). AMPA receptor activation, which is much faster, allows for the influx of extracellular Na^{+} in order to depolarize the neuron enough to alleviate the Mg^{2+} block and facilitate a post-synaptic potential. NR2C, NR2D, and NR3 are less sensitive to Mg^{2+} block. Another unique trait of NMDA receptors is their requirement for both an agonist (NR2 subunit) and a co-agonist, glycine or D-serine (NR1 subunit) in order to allow influx of Na^{+} and Ca^{2+} and efflux of K^{+} (Dingledine, et al., 1999). Depolarization leads to subsequent activation of voltage gated Ca^{2+} channels allowing further influx of Ca^{2+} and even further depolarization.

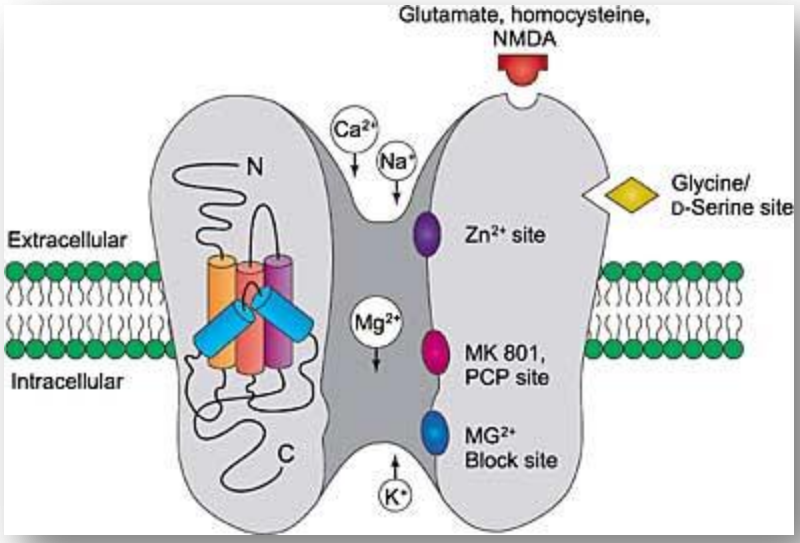

Figure 2. Schematic diagram of the *N*-methyl-D-aspartate (NMDA) subtype of glutamate receptor

The receptor, positioned in the plasma membrane of cells, has a number of subunits and controls a cation channel, which is permeable to Ca2+ as well as to Na+ and K+. The receptor is stimulated by glutamate, as well as homocysteine and the pharmacological substrate, NMDA. The opening of the channel requires extracellular glycine as a co-factor; new data has emerged indicating that D-serine is also an endogenous ligand for the receptor and binds at the glycine binding site.

1.1.2 AMPA Receptors

AMPA receptors are ligand-gated ion channels named for the pharmacological agonist, α-amino-3-hydroxy-5-methyl-4-isoxazole propionic acid (Platt, 2007). They differ from NMDA receptors in their noticeably lower affinity for glutamate and faster activation. However, similar to NMDA receptors, AMPA receptors are tetra-heteromeric; comprised of various subunit combinations, GluR1-GluR4 (Dingledine, et al., 1999). These receptors require binding by two agonist molecules in order to initiate activation. The subunit combination dictates the permeability of the pore which allows influx of Na^+ primarily but, also Ca^{2+} and Zn^{2+} while permitting efflux of K^+ (Wang & Qin, 2010). Additionally, the subunit combination dictates its permeability to Ca^{2+}. For example, AMPA receptors containing GluR1 and GluR2 subunits make the receptor almost impermeable to Ca^{2+} (Wang & Qin, 2010). The presence of the GluR3 subunit significantly increases permeability to Ca^{2+} (Platt, 2007). Furthermore, expression patterns by GluR4 are more limited than that of the other subunits allowing for localized specificity.

1.1.3 Kainate Receptors

Kainate receptors are ligand-gated ion channels named for Kainic acid, a pharmacological agonist for these receptors. Like AMPA receptors, they require binding of two agonist molecules to elicit activation. Moreover, Kainate receptors mediate fast-excitatory transmission. Permeability to influx of Na^+ and efflux of K^+ may be altered by

various combinations of subunits which make up their hetero-tetrameric structure. The subunits are GluR5-GluR7 and KA-1 or KA-2 (Dingledine, et al., 1999).

1.1.4 Metabotropic Glutamate Receptors

Metabotropic glutamate receptors (mGluRs) are monomeric G-protein coupled receptors which are linked to the second messenger molecules, phospholipase C, Inositol 1,4,5-triphosphate (IP_3), Ca^{2+}, 1,2-Diacylglycerol (DAG), and adenylate cyclase depending on their conformation. However, these receptors may also possess G-protein independent signaling (Lau & Tymianski, 2010). mGluRs generally increase intracellular IP_3 and initiate release Ca^{2+} from the ER (Wang & Qin, 2010). There are eight different isoforms, mGluR1-8, belonging to three groups; groups I, II, and III. Group association depends on pharmacology, sequence homology, and mechanism by which signal transduction occurs (Wang & Qin, 2010). While these receptors are not directly implicated in excitotoxicity, modulatory roles have been demonstrated (Conn & Pin, 1997); each of the three groups have been shown to influence various mediators of excitotoxic death (Lau & Tymianski, 2010; Wang & Qin, 2010).

1.2 Glutamate Neurotransmission and Function

1.2.1 Neurotransmission

Glutamate neurotransmission accounts for the vast majority of excitatory post-synaptic potentials (EPSP) in the CNS (Fonnum, 1984). Under basal conditions, glutamate in the synaptic cleft is maintained below 1 μM in order to avoid constant

NMDA receptor stimulation while glutamate synthesized in neurons is packaged in vesicles at concentrations of approximately 100 mM and is trafficked to the pre-synaptic membrane for release into the synaptic cleft. At release, the concentration of glutamate is estimated to reach levels of 100 μM (Nicholls, 2008). Glutamate in the cleft diffuses to the post-synaptic neuron where it stimulates AMPA and NMDA receptors to initiate an EPSP. Glutamate is reclaimed from the synaptic cleft by perisynaptic astrocyte membranes expressing high-affinity glutamate transporters. Glutamate is transferred back to neurons by conversion to glutamine, shuttling back to neurons and reconversion to glutamate.

1.2.2 Development

Glutamate has been shown to directly affect neurogenesis by increasing proliferative responses in neural progenitor cells (NPC) (Suzuki, et al., 2006). Indirectly, it has been shown to induce production of neuronal growth factors such as brain-derived neurotrophic factor (BDNF) which promotes differentiation of NPCs. Moreover, as NPC differentiation progresses, production of signaling molecules such as NO increase to further inhibit NPC proliferation, thus favoring differentiation (Cheng, Wang, Cai, Rao, & Mattson, 2003; Mattson, 2008). Glutamate can also interfere with cytoskeletal components in the growth cone and shaft of developing neurons, thereby inhibiting neurite outgrowth. However, glutamate that has been released from growth cones can act on adjacent dendrites in paracrine fashion to promote synaptogenesis (Mattson, 2008; Mattson, Dou, & Kater, 1988).

1.2.3 Neuronal Survival

Pruning of neurons is part of regular neuronal network development and is partially dependent on glutamate neurotransmission. For instance, developing neurons are dependent on release of neurotrophins such as nerve growth factor (NGF) and BDNF. Thus, in a concentration dependent manner, the presence of neurotrophins released due to glutamate stimulation of AMPA and NMDA receptors can promote neuronal survival as well as cell migration (Balazs, 2006). It is also postulated that regular release of glutamate followed by release of neurotrophins, like BDNF, may be responsible for survival of mature neurons (Mattson, 2008). Glutamate triggers glutamate receptor mediated Ca^{2+} signaling in neurons; there are numerous pro-survival targets that are activated by this process. cAMP response element binding (CREB) is one such transcription factor that is activated by $Ca2^{+}$ signaling; CREB and other transcription factors such as serum response factor (SRF) can lead to expression of other pro-survival factors and thus, enhance cell stability and survival (Balazs, 2006).

1.2.4 Synaptic Plasticity

Glutamate is involved with the initiation of strengthened neuronal responses following repeated use of specific pathways. This is referred to as long-term potentiation (LTP) and long-term depression (LTD) and is thought to represent a molecular mechanism of learning and memory. Both ionotropic receptors (NMDA and AMPA/Kainate) and metabotropic receptors (mGluRs) are mediators of LTP and LTD (Dingledine, et al., 1999; Hardingham, 2009). Glutamate, in a Ca^{2+} dependent fashion,

activates numerous substrates and transcription factors that are responsible for neuronal spine remodeling and plasticity. Initiation of LTP vs. LTD is a matter of frequency and amplitude; if the appropriate short bursts at a high frequency occur (15 Hz for 15 seconds or 100 Hz for 3 seconds) (Bliss & Gardner-Medwin, 1973), LTP will result. However, if there is a lower frequency (0.5 to 3 Hz) for longer duration, LTD is favored (Dudek & Bear, 1992). LTD is characterized by a reduced synaptic response after low frequency activity. NMDA receptor subunit composition can greatly influence the outcome of LTP vs. LTD; a larger ratio of NR2B to NR2A subunits leads to an increased probability of LTP. A larger ratio of NR2A to NR2B promotes LTD. These distinctions are based on how the subunits promote Ca^{2+} flux (Yashiro & Philpot, 2008).

1.3 Excitotoxicity

Persistent stimulation of glutamate receptors, primarily NMDA receptors (Choi, 1988; Sattler, Charlton, Hafner, & Tymianski, 1998) by excess local glutamate can lead to neuronal depolarization and initiation of Ca^{2+}-dependent cell death (Choi, 1985). This process occurs in acute pathology in instances of ischemia, brain injury and stroke as well as in chronic neurodegenerative disorders such as Lou Gehrig's disease (ALS), Huntington's disease, Alzheimer's disease, Parkinson's disease, along with many psychiatric disorders (Mattson, 2008). The term "excitotoxicity" was first used by JW Olney (Olney, 1974) to describe neuronal death caused by excess glutamate and other excitatory amino acids (Olney, 1986). Numerous reports of glutamate mediated neuronal death under a myriad of conditions have been the focus of a wealth of research over

recent years. The excitotoxic process begins with an acute insult such as a stroke or brain trauma or as a result of neurodegeneration in numerous chronic states, which results in a massive glutamate release from damaged pre-synaptic nerve terminals and astrocytes into the local environment (Platt, 2007). Impaired glutamate uptake by adjacent astrocytes further exacerbates the insult (Hardingham, 2009). Glutamate initiates depolarization of neurons by activation of AMPA and NMDA receptors (Mattson, 2007). Predominantly extrasynaptic, NR2B-containing NMDA receptors allow the influx of Na^+ and Ca^{2+} along with a minor influx of Cl^- ions, which is accompanied by water and can result in the swelling of cellular organelles as well as the cell itself (Choi, 1992). The initial depolarization leads to activation of the voltage gated Ca^{2+} channels which elicits further depolarization. Under normal homeostatic conditions, there are numerous mechanisms for handling the influx of Ca^{2+} including the plasma membrane bound Na^+/Ca^{2+} exchanger, Ca^{2+} binding proteins, Ca^{2+} -ATPases on the plasma membrane and on the endoplasmic reticulum, in addition to Ca^{2+} sequestration by the mitochondria (Mattson, 2007). The endoplasmic reticulum and mitochondria play significant roles in buffering Ca^{2+} inside the cell by their ability to sequester excess $Ca^{2+.}$ However, under pathological conditions, Ca^{2+} transport and energy production come to a halt and the cell's ability to buffer Ca^{2+} is compromised. Ca^{2+} overload contributes to pH imbalance and leads to the generation of oxygen radicals and overall oxidative stress (Mattson, 2007). Moreover, the excess Ca^{2+} activates many cysteine proteases known as caspases and notably, calpain; these proteases degrade numerous cellular constituents such as the cytoskeleton, membrane receptors, and enzymes eventually committing the cell to certain fate (Choi, 1988; Mattson, 2007). There are numerous pathways that may become active under

cellular stress but the predominant pathway involved in excitotoxicity involves Ca^{2+} overload, ROS generation, mitochondrial dysfunction, delayed Ca^{2+} deregulation (DCD), activation of Ca^{2+} dependant enzymes, formation of the apoptosome, activation of caspases, expression of pro-death genes and finally, death (Wang & Qin, 2010). Ultimately, the intensity of the insult dictates whether death by necrosis, apoptosis or autophagy ensues (Wang & Qin, 2010). If sufficient ATP is present apoptosis can proceed, while severe ATP depletion, such as that occurring in core stroke areas, prevents apoptosis and promotes necrosis.

1.3.1 Apoptosis

Apoptosis is the ability of a cell to enter a programmed, energy dependent state of organized demise (Kerr, Wyllie, & Currie, 1972). It is characterized by chromatin condensation and plasma membrane blebbing in contrast to extreme swelling and bursting into the interstitial space as occurs in necrosis. A myriad of insults may trigger apoptosis and several pathways to apoptosis exist. A summative description of apoptotic pathways would be to categorize them into extrinsic and intrinsic pathways (Fig. 3). The extrinsic pathway involves the activation of death receptors on the cell outer-membrane initiating a cascade which leads to cell death (Galluzzi, Blomgren, & Kroemer, 2009). However, the intrinsic pathway is mitochondrial mediated and represents the majority of apoptosis in brain injury and neurodegeneration. The intrinsic pathway starts with a stressful event such as excitotoxicity which leads to activation of numerous pro-death and pro-survival mediators. For instance, members of the B-cell lymphoma-2 (Bcl-2) family

of proteins, such as Bax and Bak, may be activated and may contribute to cell death by promoting mitochondrial permeability and leading to a loss of membrane potential. Other members from the same family of proteins like Bcl-x_L and Bcl-2 itself can interfere with this process by blocking pore formation and thus, promote cell survival. Ultimately, the potency of the insult will dictate which set of proteins dominates and tips the balance in favor of survival or death. If Bax and Bak are successful in overcoming the inhibitory actions of Bcl-2, they will insert themselves into the mitochondrial outer membrane, forming pores, while also binding to other protein components of the mitochondrial permeability transition pore (MPTP) (Galluzzi, et al., 2009). Formation of the MPTP allows spillage of inner mitochondrial proteins such as cytochrome *c*, SMAC/Diablo and apoptosis inducing factor (AIF) into the cytosol where they activate down-stream initiators of apoptosis (Hengartner, 2000). MPTP formation leads to a breakdown in ATP generation by the electron transport chain (ETC), loss of mitochondrial membrane potential, loss of mitochondrial function, ROS generation, and activation of caspase enzymes. At this point, cell death is a certainty (Galluzzi, et al., 2009).

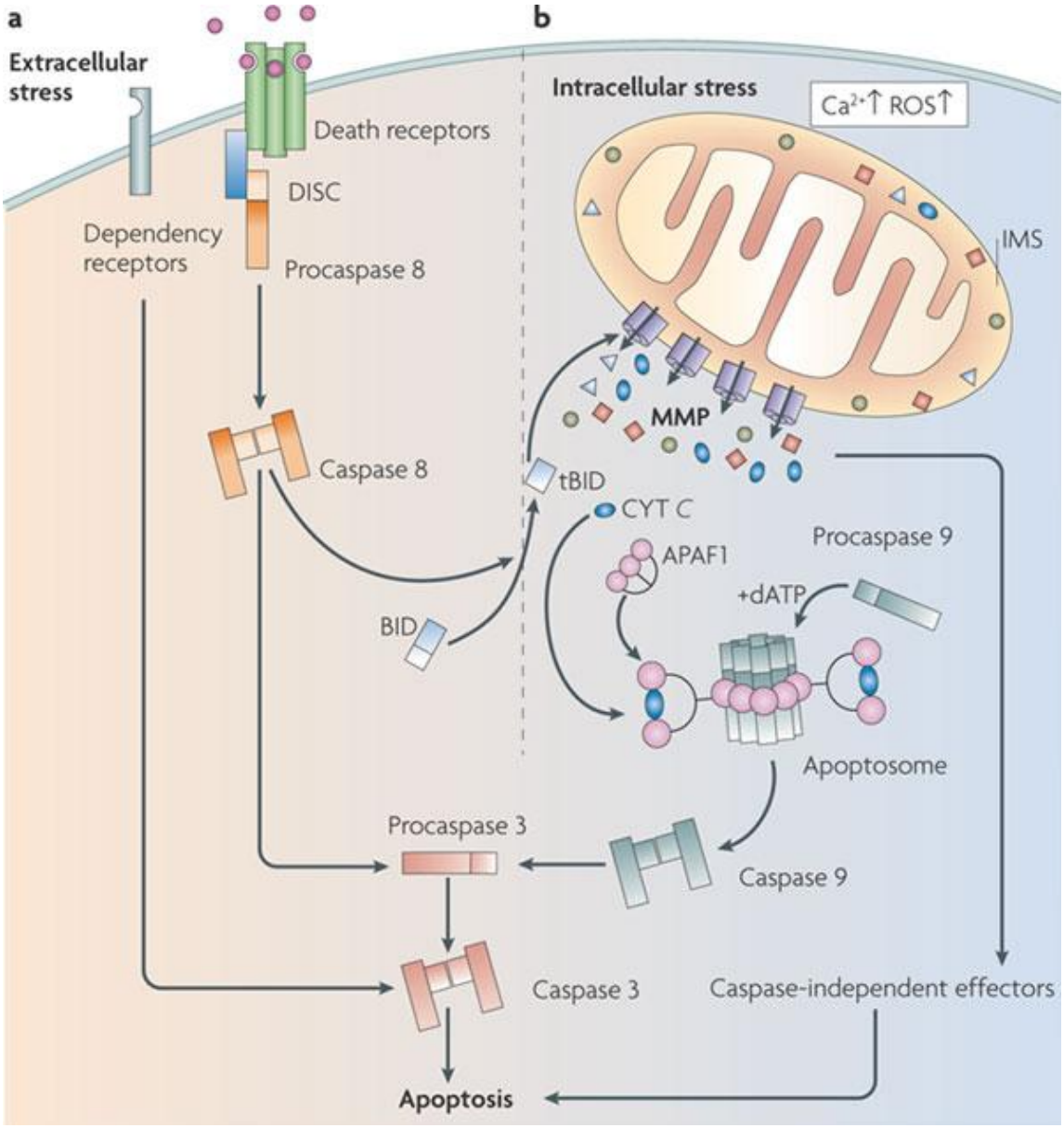

Figure 3. The extrinsic and intrinsic (mitochondrial) pathways of apoptosis

Apoptosis can result from the activation of two biochemical cascades, which are known as the extrinsic (part a) and the intrinsic (or mitochondrial, part b) pathways. The extracellular apoptotic pathway is initiated at the plasma membrane by specific transmembrane receptors, whereas mitochondrial apoptosis is triggered by intracellular stimuli such as Ca^{2+} overload and overgeneration of reactive oxygen species (ROS). In

both pathways, initiator caspases (caspase 8 and 9, respectively) are activated within specific supramolecular platforms and so can catalyse the proteolytic maturation of executioner caspases, such as caspase 3, which mediate (at least part of) the catabolic processes that characterize end-stage apoptosis. Mitochondrial membrane permeabilization (MMP) marks a point of no return in the mitochondrial pathway by activating both caspase-dependent and caspase-independent mechanisms that eventually execute cell death. For example, following MMP the mitochondrial intermembrane space (IMS) protein cytochrome c (CYT C) is released into the cytosol and interacts with the adaptor protein apoptotic peptidase activating factor 1 (APAF1) as well as with procaspase 9 to form the apoptosome. This results in the sequential activation of caspase 9 and executioner caspases, such as caspase 3, a process that is known as the caspase cascade. One of the major links between extrinsic and mitochondrial apoptosis is provided by the BCL-2 homology domain 3 (BH3)-only protein BID, which can promote MMP following caspase-8-mediated cleavage. dATP, deoxyadenosine triphosphate; DISC, death-inducing signalling complex; tBID, truncated BID.

1.3.2 Stroke

Stroke is the third leading cause of all deaths in Canada and the United States of America (Dirnagl, Iadecola, & Moskowitz, 1999). There are two types of stroke, ischemic and hemorrhagic. Ischemic stroke, which results from an embolus or a thrombus, blocks an artery in the brain leading to decreased blood flow and oxygenation with subsequent cell death; it typically accounts for 80-90% of all strokes. Hemorrhagic stroke, which results from a burst vessel in the brain, accounts for the difference. While both can be devastating, more patients survive ischemic attacks with the prospect of life-long impairment than do those who have suffered a hemorrhagic stroke. Earlier, it was mentioned that strict control over glutamate concentrations was of paramount importance to maintaining homeostasis. During a stroke, it is estimated that the concentration of glutamate spilled into the synaptic cleft may reach 100 μM in as little as 5 minutes (Benveniste, Drejer, Schousboe, & Diemer, 1984). While these concentrations cause sudden cell death by necrosis in the infarct area, adjacent neurons contained in the surrounding area, known as the penumbra, begin to undergo the initial stages of excitotoxicity as they deal with the inability to remove the copious amounts of glutamate that have been released by neurons in the acute phase. Moreover, clearance of glutamate is further stifled by presence of the blood brain barrier (BBB) since it is almost impervious to glutamate (Nedergaard, Takano, & Hansen, 2002). The excitotoxic cascade ensues exacerbating inflammation that may contribute to cell death for many days after the initial stroke (Dirnagl, et al., 1999). At the origin or core of the infarct, cells are eliminated by necrosis, resulting from complete occlusion of blood flow; however, cells in the penumbra may survive depending on how quickly blood flow is re-established and

to what extent oxidative metabolism was impaired (Hertz, 2008). It has been reported that reductions in oxidative metabolism within the penumbra which exceed 69% correlate with a much higher morbidity (Frykholm, et al., 2000). Moreover, since anaerobic metabolism of glucose can persist in the penumbra long after oxygen is exhausted, a build-up of lactate by-product can also interfere with energy generation and lead to much delayed cell death (Hertz, 2008).

1.3.3 [1]Alzheimer's Disease

Alzheimer's disease (AD) is a neurodegenerative disorder that affects nearly 30 million individuals worldwide (Selkoe, 2004). AD patients experience progressive decline in their cognitive functions and loss of short-term memory with age. The brain regions most commonly affected in AD are the hippocampus and entorhinal cortex, both of which are involved in short-term memory and learning processes (Braak & Braak, 1994). Histopathological examination of AD brain slices reveal amyloid-beta peptide (Aβ) deposits and neurofibrillary tangles (NFT), both hallmarks of AD. Amyloid deposits or amyloid plaques are mainly extra-cellular aggregates of Aβ. NFTs, which are intra-cellular aggregates of the microtubule-associated protein Tau, also contribute to AD pathology. Both these deposits contribute to the neuronal loss observed in AD. Approximately 90% of AD cases are considered to be sporadic or not genetically linked. Sporadic AD also known as late-onset is often diagnosed after 65 years of age (Lijtmaer,

[1] Adapted and reprinted from Hunt WT, Salins P, Anderson CM, Amara F. (2010) *Neuroprotective role of statins in Alzheimer Disease: Anti-apoptotic signaling.* Courtesy of Bentham Open Neuroscience Journal 2010 4:13-22.

Fuld, & Katzman, 1976). The remaining 10% of AD cases have a genetic component and are autosomal dominant in transmission (Kowalska, 2004; Selkoe, 2002). In the familial form of AD (FAD), mutations in the amyloid precursor protein (APP) gene promote enhanced Aβ production. Apart from APP, other factors such as mutations in presenilins (PS1 and PS2), and the presence of the APOE allele, APOEε4 (APOE is an apolipoprotein which transports cholesterol from the brain) promotes increased Aβ plaque load (Kowalska, 2004). Interestingly, some patients with sporadic AD also display polymorphisms for the APOE gene. Therefore, APOE is considered a risk factor rather than a genetic determinant of AD (Corder, et al., 1993; Kowalska, 2004). Alteration in APP processing leads to the accumulation of Aβ though a number of proteolytic cleavage processing products of APP. FAD is considered early-onset AD, with individuals displaying cognitive impairments often by the age of 65 (Kowalska, 2004). Aβ peptide is a neurotoxic agent, which at high concentrations promotes neuronal loss (Rauk, 2008). The neurotoxic effect of Aβ has been demonstrated *in vitro*, in animals and in humans (Moreno, et al., 2007; Takuma, Tomiyama, Kuida, & Mori, 2004). Aβ promotes neuronal loss by apoptosis (Bezprozvanny & Mattson, 2008). A number of biological mechanisms have been implicated in neuronal loss. These include inflammation, free radical formation (reactive oxygen/nitrogen species), and glutamate mediated excitotoxicity (McGeer & McGeer, 1998). For example, cortical neurons exposed to Aβ succumbed to excitotoxic death as a result of lost calcium regulation (Mattson, et al., 1992).

1.4 Mediators of Excitotoxicity

1.4.1 Mitochondria

Mitochondria are often referred to as the "powerhouses" of the cell since their primary role involves energy generation in the form of ATP (Nicholls, 2004; Niizuma, et al., 2010). In addition to ATP production, there are a number of other mitochondrial functions including ROS generation, antioxidant defenses, Ca^{2+} homeostasis, and apoptosis (Nicholls, 2004; Wang & Qin, 2010). In excitotoxicity, mitochondria are of paramount significance since they act as a substantial buffer for excess Ca^{2+} by sequestering excess Ca^{2+} in the event of Ca^{2+} overload. Buffering capacity of mitochondria is not without limits and therefore can be swamped to a point that initiates mitochondrial permeability and loss of accumulated mitochondrial Ca^{2+} to the cytosol. This enhanced permeability also leads to release of pro-apoptotic factors, including cytochrome C (Cyt C) or apoptosis inducing factor (AIF). Mitochondria are thus control centers for apoptosis, as discussed in section 1.3.1.

1.4.2 Calcium (Ca^{2+})

Ca^{2+} is integral for neuronal signaling. For example, extracellular Ca^{2+} is responsible for initiation of pre-synaptic release of neurotransmitters, while ER Ca^{2+} acts as a second messenger when released in response to G-protein coupled receptor activation. Ca^{2+} is necessary for maintaining membrane excitability as well as for processes involved with growth and differentiation of cells (Arundine & Tymianski, 2003). Paradoxically, Ca^{2+} is an essential part of excitotoxic signaling and is required for

excitotoxic neuron death. Substantial Ca^{2+} increases have been observed as part of NMDA receptor mediated glutamate excitotoxicity (Choi, 1992). Excess Ca^{2+} can activate a number of Ca^{2+} dependent enzymes including phosphatases, lipases, proteases, and endonucleases. Apart from direct structural damage, activation of these enzymes can increase ROS production and promotion of apoptosis (Arundine & Tymianski, 2003).

1.4.3 Reactive Oxygen Species (ROS)

ROS generation is part of normal respiratory cell function. However, compared to other tissues ROS production in the brain is exaggerated by the disproportionate consumption of oxygen (Coyle & Puttfarcken, 1993). The high turnover of oxygen leaves neurons especially prone to oxidative stress during NMDA receptor activation (I. J. Reynolds & Hastings, 1995; Wang & Qin, 2010). In instances of excitotoxic insult, inability to manage oxidative stress can be devastating. Oxygen radicals can interfere with numerous cellular processes including ion trafficking, membrane stability, energy production, neurotransmission, and activation/deactivation of enzymes (Wang & Qin, 2010). A number of different ROS species are produced including the superoxide anion ($O_2^{\cdot -}$), the hydroxyl radical ($^{\cdot}OH$), hydrogen peroxide (H_2O_2), nitric oxide (NO), as well as peroxynitrite ($ONOO^-$) (Beal, 1995; Coyle & Puttfarcken, 1993; Dawson & Dawson, 2004). For example, during ischemia peroxynitrite formation has been shown to oxidize lipids, nitrosylate proteins and destroy DNA thus promoting cell death (Forder & Tymianski, 2009). Moreover, increased ROS production in excitotoxicity can lead to a positive feedback cycle where there is excessive release of glutamate and reduced

reuptake capacity (Bowling & Beal, 1995). Excessive production of ROS can saturate cellular antioxidant enzymes such as superoxide dismutase (SOD) (Dawson & Dawson, 2004; Mattson, et al., 2002), glutathione peroxidase (Mattson, et al., 2002), and catalase (Mattson, et al., 2002). Moreover, other antioxidant molecules such as glutathione, thioredoxin and peroxiredoxins (Hardingham, 2009), in addition to those obtained in diet such as phenols, flavonoids, β-carotene, vitamin C, and vitamin E, have been shown to counteract oxygen radicals and provide benefit against oxidative stress (Uttara, Singh, Zamboni, & Mahajan, 2009).

1.4.4 Poly(ADP-ribose) polymerase-1 (PARP-1)

PARP-1 is a DNA repair enzyme that is found in all multi-celled eukaryotes. PARP-1 belongs to a family of 18 different PARP members based on genetic studies (Dawson & Dawson, 2004). However, PARP-1 is by far the most active enzyme in the group, accounting for as much as 85% of all nuclear PARP enzyme activity (Kauppinen & Swanson, 2007). PARP-1 works by generating ADP-ribose polymers which bind to genomic proteins like histones or PARP-1 itself, at the expense of NAD^+, in order to make it more accessible for other DNA repair enzymes; PAR polymers form long branches that act to attract and recruit DNA repair enzymes (Kauppinen & Swanson, 2007). Under regular homeostatic conditions PARP-1 activation repairs the basal levels of DNA damage occurring in the cell but energy demands for this amount of repair do not detrimentally deplete NAD^+. In conditions of extreme DNA damage, PARP-1 becomes sufficiently active to virtually eliminate NAD^+ for NADH generation and ATP synthesis,

causing energy failure. Abolition of PARP-1 activity has been shown to be protective against excitotoxic insults (Dawson & Dawson, 2004; Mandir, et al., 2000). PARP-1-induced NAD^+ depletion leads to mitochondrial permeability and AIF-dependent apoptosis, but the mechanisms of mitochondrial damage are poorly understood.

1.5 Conjugated Linoleic Acid (CLA)

CLA is a polyunsaturated fatty acid (PUFA:$C_{18:2}$); derived primarily from linoleic acid (LA). CLA describes 28 possible geometric and stereo-isomers of LA. However, it is usually synonymous with the two most biologically active species of CLA, *cis*9,*trans*11 (also known as rumenic acid) (Kramer, et al., 1998) and *trans*10,*cis*12 (Fig. 4). In humans, CLA is obtained by consuming dairy products and meat from ruminant animals as part of regular dietary requirements. However, the amounts required to elicit beneficial effects similar to those described in current research can only be achieved by aid of additional purified supplements.

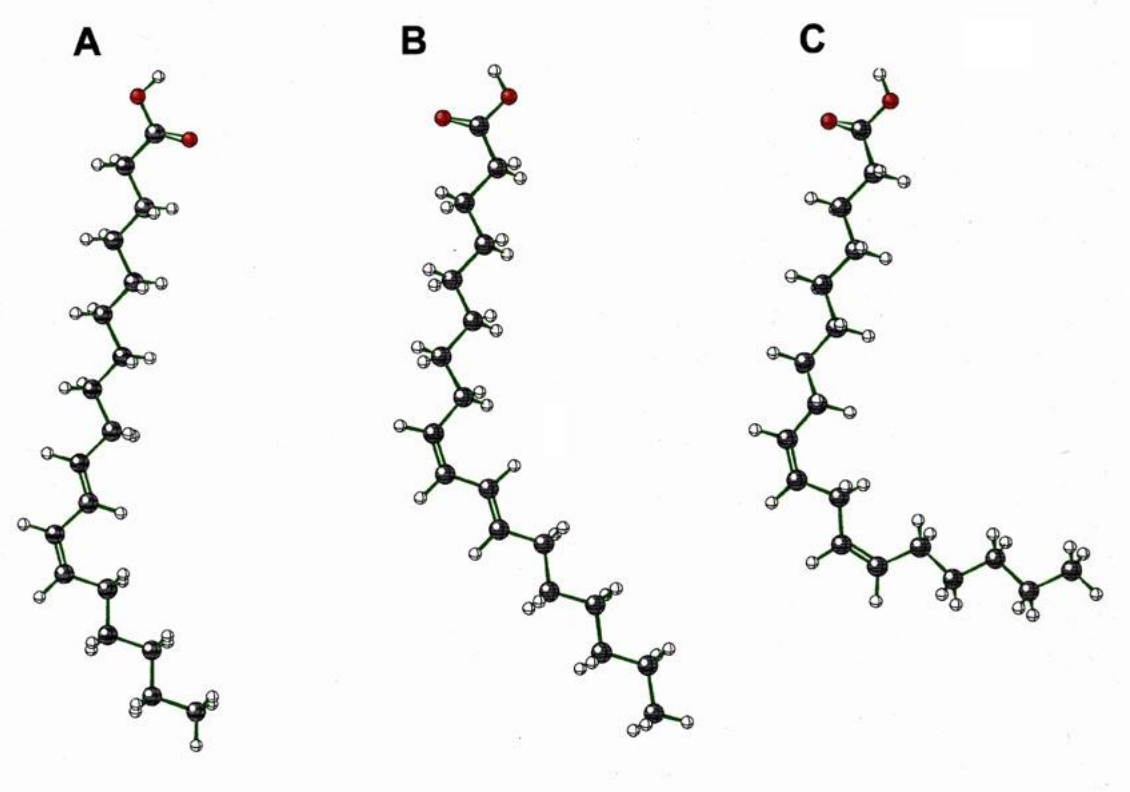

Figure 4. The two major biologically active species of CLA and LA

A. *trans*10, *cis*12 and B. *cis*9, *trans*11 depicting the conjugated double bond system present in these isomers. C. *cis*9, *cis*12 depicts linoleic acid with no conjugated double bond system

1.5.1 Synthesis of CLA

There are three modes of CLA synthesis: ruminal biosynthesis in ruminant animals by bacteria, biosynthesis in animal tissue by enzymatic conversion of vaccenic acid, and industrial synthesis by chemical means. Synthesis of CLA is accomplished by conversion of precursors; the most abundant PUFA in ruminant diets are linolenic acid ($C_{18:3}$) and linoleic acid ($C_{18:2}$). In the initial stages of CLA synthesis hydrolysis of ester linkages is accomplished by microbial lipases in order to make the fatty acids derived from plants accessible. Once available, there are two main groups of bacteria involved in the completion of CLA biosynthesis by a process known as biohydrogenation. Collectively, these bacteria are referred to as group A and group B and are comprised of various species which work synergistically to complete biohydrogenation (Palmquist, Lock, Shingfield, & Bauman, 2005). Biohydrogenation is accomplished by isomerization of the free fatty acid (C_{18}) substrate followed by reduction to generate a ($C_{18:1}$) intermediate by group A bacteria which is followed by further reduction by group B bacteria in order to generate specific conjugated diene isomers ($C_{18:2}$) (Palmquist, et al., 2005). *Butyrivibrio fibrisolvens* a group A bacterium, involved in biosynthesis of *cis*9,*trans*11 was the first to be described in the biohydrogenation process. However, it was later discovered that numerous other species were not only able to perform this process but, it required many different species to complete it and account for the numerous and diverse isomeric species produced. Apart from rumenal biohydrogenation, endogenous synthesis is thought to occur in all animals without aid of bacteria; Δ-9-desaturase (also known as stearoyl-CoA desaturase) is the enzyme responsible for endogenous synthesis of CLA. In this process Δ-9-desaturase adds a *cis*-double bond to

trans-vaccenic acid ($C_{18:1}$) in order to generate the *cis*9, *trans*11 species of CLA ($C_{18:2}$). The many health benefits associated with CLA have been the impetus for industrial synthesis; especially for use in dietary supplements. Alternate food sources have been employed in order to increase endogenous production of various desired CLA species in animals. Moreover, industrial chemical synthesis using alkali conditions have been described in order to enhance production of desired species of CLA. These methods have been especially important for generating CLA species other than the *cis*9, *trans*11 species which combined normally account for less than 25% of all naturally sourced CLA (Kramer, et al., 1998; Palmquist, et al., 2005).

1.5.2 Dietary sources of CLA

CLA is obtained primarily in diet from dairy products and meat obtained from ruminant animals (Table 1). However, the amount obtained through diet is highly variable due to both significant variation in human diets as well as variation in endogenous CLA production in ruminant animals. For example, milk sampled from numerous creameries showed an 8-fold difference in the amount of CLA found in milk fat. These differences were attributed to seasonal changes in diet throughout the year as well as the geographic locations of the animals which also impacted diet (Riel, 1963). Caloric intake in addition to dietary variability by humans results in a wide range of CLA doses acquired by diet alone. The content of CLA in ruminant animal fat has been estimated to be between 3 and 7 mg/g of fat (Bauman, Baumgard, Corl, & Griinari, 2000). It has been estimated that the average American consumes less than 500 mg of

CLA per day (Ritzenthaler, et al., 2001); as previously mentioned, beneficial effects of CLA have only been demonstrated in humans with larger doses and thus can only be achieved by supplementation with purified CLA. In healthy but overweight humans, a dose of 3.4 g/day was required over a period of 2 years in order to reduce body fat mass (Gaullier, et al., 2005). Furthermore, if enough ruminant animal products were to be consumed to reach therapeutic doses, it would result in consumption of excessive dietary fat which would most likely contribute to negative pathological outcomes such as atherosclerosis and other conditions related to obesity.

Table 1. Conjugated Linoleic Acid Content of Various Foods*

Food	mg/g fat	Food	mg/g fat
Dairy Product		Meats/Fish	
Homogenized milk	5.5	Fresh ground beef	4.3
2% milk	4.1	Veal	2.7
Butter fat	6.1	Lamb	5.8
Condensed milk	7.0	Pork	0.6
Cultured buttermilk	5.4	Chicken	0.9
Butter	4.7	Fresh ground turkey	2.6
Sour cream	4.6	Salmon	0.3
Ice cream	3.6	Egg yolk	0.6
Low fat yogurt	4.4		
Custard style yogurt	4.8	Vegetable Oils	
Plain yogurt	4.8	Safflower oil	0.7
Frozen yogurt	2.8	Sunflower oil	0.4
Medium Cheddar	4.1		
American processed	5.0		

* Based on values reported by Chin *et al.* [16] and Lin *et al.* [17]

1.5.3 Benefits of CLA

CLA was first recognized to possess beneficial traits as a food constituent in the late 1980's when it was discovered to have been responsible for anti-carcinogenic properties in a study examining the effects of cooking temperatures on levels of carcinogens in hamburger beef performed almost 10 years earlier (Ha, Grimm, & Pariza, 1987; Pariza, Ashoor, Chu, & Lund, 1979). This discovery spurred much research into putative benefits of CLA in many cancer models and other disease models. Overall, findings of the vast majority of studies investigating health benefits of CLA in disease states are similar; while there seems to be clear benefits, the variability between studies seems to be a product of a myriad of experimental conditions examined. Additionally, almost all current research has been quite successful in implicating mechanistic mediators of CLA action while, none have been able to completely substantiate a complete mechanism underling observed benefits.

1.5.3.1 Adipogenesis

CLA has been demonstrated to reliably decrease body fat mass in numerous animal models including rats, mice and pigs. However, the *trans*10, *cis*12 species seems to be primarily responsible for this effect (Kennedy, et al., 2010). Data from human studies however, have been quite mixed in this regard. For example, many studies involving healthy but obese volunteers have shown only changes to serum markers and not to overall body fat mass whereas other studies have shown that CLA supplementation does decrease body fat mass (Bhattacharya, Banu, Rahman, Causey, & Fernandes, 2006). Some reasons for the discrepancy maybe the different CLA doses used, CLA isomer

mixtures and differences in experimental design (Kennedy, et al., 2010). Interestingly, it has been proposed that decreases in body fat mass may be due to decreased food consumption caused by intake of CLA but, this has only been observed in mice (Park, et al., 1997). Studies in mice have also shown that metabolic rate has been increased and thus, more calories burned as a result of CLA intake (Terpstra, et al., 2003). In addition, the *trans*10, *cis*12 species of CLA has also been shown to inhibit adipogenesis by way of molecular mediators; inhibition of the transcription regulator peroxisome proliferator-activated receptor γ (PPAR-γ) and CAAT/enhancer binding protein by the *trans*10, *cis*12 species of CLA have been shown to decrease adipogenesis (Brown, et al., 2003; Kennedy, Chung, LaPoint, Fabiyi, & McIntosh, 2008).

1.5.3.2 Atherosclerosis

Studies initiated in rabbits were first to show benefits of mixed isomer CLA intake on markers of atherosclerosis (Lee, Kritchevsky, & Pariza, 1994). A number of follow-up studies have both confirmed these results and disputed them. However, experimental model and design have been cited as possible reasons for the discrepancy (McLeod, LeBlanc, Langille, Mitchell, & Currie, 2004; Mitchell & McLeod, 2008). In addition, conflicting data have been obtained when measuring cholesterol and triglycerides in CLA fed animal studies. However, a reduction in atherosclerotic lesions has been observed in the majority of cases (McLeod, et al., 2004). Human studies have also shown significant variability when it comes to impact of CLA on atherosclerotic markers such as blood lipid profiles. Many studies have shown no impact on cholesterol while others have demonstrated decreases in LDL cholesterol. In any case, both animal and human studies suggest that CLA impact on cholesterol may be unrelated to its effects

on atherosclerosis (Nakamura, Flintoff-Dye, & Omaye, 2008). More specifically, it has been postulated that protective effects of CLA against atherogenesis may be the result of pro-antioxidant actions vs. that of direct impact on cholesterol mediated protection (Nakamura, et al., 2008). For example, CLA has been shown to influence transcription of NF-κβ which can lead to decreased expression of pro-inflammatory signaling via mediators such as Cox-2 and prostaglandins (Ringseis, et al., 2006). Isolated isomer experiments have shown differential roles for both *cis*9, *trans*11 and *trans*10, *cis*12 species of CLA on plaque formation demonstrating anti-atherosclerotic action by the *cis*9, *trans*11 isomer and pro-atherosclerotic activity by the *trans*10, *cis*12 isomer (Arbones-Mainar, et al., 2006). However, synergy between both isomers has also been postulated which may be dose dependent (McLeod, et al., 2004). More study is required to ascertain the validity of claims made with regard to the benefits of CLA in atherosclerosis.

1.5.3.3 Cancer

The identification of CLA as an anticarcinogenic substance (Ha, et al., 1987) sparked the genesis of numerous investigations into CLA and cancer which is one of the most prominently studied areas of CLA and health. Cancer prevention in the form of tumorigenesis has been demonstrated with both mixed-isomer and individual-isomer preparations. Overall, there have been positive benefits observed in breast cancer, colon cancer, skin cancer, and stomach cancer in animal models treated with mixed-isomer preparations (Kelley, Hubbard, & Erickson, 2007). However, to date there have been no significant findings for beneficial effects of CLA intake in humans and the incidence of cancer. Moreover, results from animal model studies become confusing when individual

isomers are administered as isomer specific effects on tumors and metastasis have been observed. For example, in a study examining the effect of individual CLA isomers in a colon cancer mouse model, both major isomers of CLA prevented metastasis. Repeat of the experiment in colon cancer cell lines showed that the *cis*9, *trans*11 was able to stop cell migration whereas the *trans*10, *cis*12 isomer did not (Soel, Choi, Bang, Yoon Park, & Kim, 2007). However, in addition to isomer specific differences, experimental model, dose, and temporal aspects of administration have also been cited as confounding factors in these studies (Kelley, et al., 2007). So, while it is generally accepted that CLA is beneficial in numerous cancer cell lines and animal models, a thorough understanding of the mechanism(s) of action by CLA in cancer protection still eludes us. There is numerous evidence to suggest that a common theme is a reduction in prostaglandin synthesis by CLA which leads to decreased signaling through various transcription mediators that control inflammation, cell cycle and apoptosis (Bhattacharya, et al., 2006).

1.5.3.4 Diabetes

CLA has shown the most promise in diabetic rat models as compared to mice or humans. However, there have been numerous inconsistencies between experimental protocols which complicate interpretation of the results. In a feeding study using Zucker diabetic fatty (ZDF) rats, an equal mixture of both CLA isomers (*cis*9t, *trans*11 and *trans*10, *cis*12) were administered and markers of diabetes were assessed after 14 days. The authors found that CLA was able to stabilize glucose tolerance and insulin sensitivity (Houseknecht, et al., 1998). Studies with individual CLA isomers have led to speculation that the *trans10*, *cis*12 species of CLA may be beneficial for insulin resistance while the *cis*9t, *trans*11 species has little effect since mixed isomer experiments demonstrated

enhanced glucose tolerance in ZDF rats while enriched *cis*9, *trans*11 experiments did not (Ryder, et al., 2001). However, the opposite has been observed in other transgenic mouse models. For example, in a study using leptin-deficient obese mice *trans*10, *cis*12 CLA promoted insulin resistance and hyperlipidemia (Roche, et al., 2002). Human clinical trials with obese men, performed for 12 week periods, with enriched individual CLA isomers demonstrate similar findings to mice; the *cis*9, *trans*11 species was beneficial in reducing insulin resistance whereas, the *trans*10, *cis*12 species increased insulin resistance (Riserus, Arner, Brismar, & Vessby, 2002; Riserus, Vessby, Arnlov, & Basu, 2004). Again, there has been evidence to support benefits of CLA against insulin resistance but, which isomer is responsible for such protection requires further study.

1.5.3.5 Inflammation

The benefits of CLA on inflammation have evolved, partly due to research regarding CLA in other disease models that correlate with inflammatory status such as atherosclerosis and diabetes. In fact, discovery of the mechanism responsible for CLA protection in other pathologies may be a byproduct of our understanding of the benefits of CLA in inflammatory states. Studies in cell culture models such as RAW264.7 mouse macrophage cells have demonstrated a reduction in pro-inflammatory mediators such as prostaglandin-E_2 (PGE_2), tumor necrosis factor-α (TNF-α), NO, interleukin-6 (IL-6), IL-1β, Cox-2, and nitric oxide synthase (NOS) upon treatment with CLA (Y. Yu, Correll, & Vanden Heuvel, 2002). A subsequent investigation performed in bone marrow derived dendritic cells (BMDC) suggests that many of the anti-inflammatory mediators down-regulated upon treatment with CLA are mediated by the action of the *cis*9, *trans*11 species which has been shown to reduce activation of NF-κβ (Loscher, et al., 2005). In

animal and human studies, results have been mixed; confounding factors such as study duration, dose, inflammatory marker, and CLA preparation have resulted in studies which demonstrate beneficial effects of CLA on inflammatory markers while also producing conflicting study results in similar models (Bhattacharya, et al., 2006). However, similar to other disease states CLA seems to impact inflammation by reducing prostaglandin production leading to possible reductions in ROS production. Regulation of NF-κβ may be at the heart of this mechanism via activation of PPARγ (Bhattacharya, et al., 2006; C. M. Reynolds & Roche, 2010). Moreover, decreases in inflammatory markers observed in one study found that Crj:CD-1 (ICR) mice treated with CLA exhibited lower TNF-α levels which correlated to decreases in fat mass (Akahoshi, et al., 2002). These results suggest that the impact of CLA on inflammatory mediators may be secondary to its impact on obesity. More investigation is needed to uncover the actual direct benefits of CLA on inflammation. However, any benefits obtained directly or indirectly by CLA will provide positive therapeutic impact.

1.6 Thesis Objectives

The central objective of the thesis work was initially to characterize the role of PARP-1 in neurodegeneration models. Our first specific goal was to determine whether PARP-1 plays a critical role in neuron death produced by amyloid-β. Results showed that PARP activity does partially mediate neuron death in these conditions but that ablation of PARP-1 by itself does not reduce toxicity in our hands. A second objective was to characterize the effects of pathological PARP-1 activation on cell energy currencies in

neural cells for the first time. We developed novel HPLC methods for adenine nucleotide quantification using astrocyte cultures as a model and found severe bioenergetic depletion and astrocyte death dependent on PARP-1 activity.

At this stage, preliminary data prompted our hypothesis that the dietary polyunsaturated fatty acid, CLA, might protect neural cells from excitotoxic and PARP-1-mediated death. We showed evidence that CLA protected astrocytes from PARP-1-dependent death and used these data as fuel for further hypotheses involving protection of neurons by CLA in glutamate excitotoxicity. The objectives of the final 2 data chapters (4 and 5) were to test for neuroprotection by CLA and probe for potential mechanisms by which this may occur, respectively.

Chapter 2: Role of Poly(ADP-ribose) polymerase in Amyloid-β toxicity

2.1 Introduction and Rationale

One of the hallmarks of Alzheimer's disease is deposition of insoluble plaques rich in Aβ. While there are numerous protein components comprising amyloid plaques, the primary constituent is Aβ protein. Aβ peptides of 36 – 43 amino acids are generated by γ-secretase activity and differ in function and toxicity (Querfurth & LaFerla, 2010). $A\beta_{(1-42)}$ exists in soluble and insoluble, aggregated form in plaques. Appearance of Aβ plaques is associated with memory loss, progressing to other cognitive deficits and finally, to an overall loss of motor function and death (Querfurth & LaFerla, 2010; Yagami, et al., 2004).

It has been well established that $A\beta_{(1-42)}$ can trigger excitotoxic neuronal death (Camandola & Mattson, 2010). Activation of the DNA repair enzyme, Poly(ADP-ribose) polymerase-1 (PARP-1), by $A\beta_{(1-42)}$ has also been reported (Love, Barber, & Wilcock, 1999; Strosznajder, Jesko, & Strosznajder, 2000). PARP-1 is activated by nicked or broken DNA and works by generating Poly(ADP-ribose) polymers as a means of flagging the damaged DNA for repair by DNS specific repair enzymes. PARP-1 uses NAD^+ as a substrate in order to perform this function. However, this can lead to problems. For instance, persistent activation of PARP-1 has been shown to cause severe bioenergetic depletion and lead to cell death by mitochondrial dysfunction (Alano, et al., 2010). While PARP-1 activation is necessary for cell survival, it comes at a cost if cellular DNA damage is extensive. Therefore, we hypothesized that blocking PARP-1 activity under conditions of $A\beta_{(1-42)}$ exposure protects neurons from death. To test this hypothesis, we used a primary fetal cortical neuron culture model treated with insoluble

$A\beta_{(1-42)}$. We also used PARP-$1^{-/-}$ primary neuron cultures to assess the role of PARP-1 in Aβ induced neuron death.

2.2 Materials and methods

2.2.1 Primary neuron cultures

Primary neuron cultures were prepared from embryonic day 16 CD-1 mouse cortices in accordance within guidelines set forth by the *Canadian Council on Animal Care*. Cultures were plated on poly-D-lysine coated plastic at $2.5x10^5$ cells/cm^2 in neurobasal medium (NB) with B27 supplement (Invitrogen, Carlsbad, CA), 1.2 mM glutamine, and 5% Fetal Bovine Serum (FBS; Hyclone, Logan, UT). The following day (day 1), media was changed to NB with B27 and glutamine. Cytosine arabinofuranoside (2 μM) was added on day 2 to prevent glial proliferation, and replaced on day 3 with NB/B27/glutamine. Cultures were maintained at 37°C/5% CO_2, and given a partial media change on day 6. Cultures were used on day 8 post-culture for all experiments and contained less than 2% glial fibrillary acidic protein immunopositive astrocytes.

2.2.2 Assessment of neuron death by Amyloid-β

To determine neuron death in response to Amyloid-β insult, neurons were treated with a range of concentrations of Amyloid-β protein (1-42) (Bachem Bioscience Inc., H-1368.1000) in order to achieve consistent neuron death, solubilized in double-distilled

H_2O to a stock concentration of 100 µM and incubated for 48 hours at 37°C to promote aggregate formation. Aβ stock was later diluted in Hibernate®-E media with 2 mM glucose and NaCl added to achieve an osmolarity of 290 ± 5 mOsm, to a final concentration of 20 µM for cell treatments. Wells were rinsed and media was changed to PBS pH 7.4. Cell survival was assessed by counting live cells at the outset of each experiment, t_i, and then again at the end of each experiment, t_f using a method that allows repeated measurements in single cells. At t_i, cell culture wells were etched with cross-bars in each well, making 4 quadrants. The visual field was lined up using two etch marks for each field and a bright-field picture was obtained. Therefore, pictures were obtained for 4 fields in each well. Duplicate wells were used for each treatment in each plate. Each experiment was repeated at least 4 times. At t_f, live cells were quantified by assessing intracellular calcein acetoxymethyl ester (calcein/AM; Roche, Eugene, OR) fluorescence. Fields were matched using the identical 2 etch marks for each field in similar fashion to t_i. Once fields were located, 2-channel, bright-field and fluorescence (excitation at 485 nm and emission at 530 nm), images were captured using a Zeiss LSM-510 confocal microscope. This was repeated to match all 8 fields (2-wells) and the t_i and t_f images were counted and compared for loss of live cells. Control wells were treated the same way.

2.2.3 Immunocytochemistry

Neuron cultures were treated with 300 µM of DNA alkylating agent, *N*-methyl-*N*`-nitro-*N*-nitrosoguanidine (MNNG) for 15 minutes in Hibernate®-E media. Cells were rinsed post-treatment with PBS (pH 7.4) and fixed with 4% paraformaldehyde in PBS for

1 hour. Cells were washed with PBS and permeabilized with 0.2% Triton X-100 in PBS for 5 minutes. Next, cells were bathed in a blocking solution of 1% BSA in PBS for 1 hour. Anti-Poly (ADP-ribose) mouse monoclonal antibody (Trevigen Inc., 4335-MC-100, 1:40,000) in a PBS solution containing 1% BSA was applied overnight at 4°C. Cells were washed 3 times with PBS and exposed to Alexa-Fluor-coupled anti-mouse antibody in a PBS solution containing 1% BSA for 1 hour at room temperature.

2.2.4 Materials

Amyloid-β protein (1-42) was purchased from Bachem Bioscience Inc. (King of Prussia, PA). Calcein/AM was purchased from Roche (Eugene, OR). Anti-Poly (ADP-ribose) mouse monoclonal antibody was purchased from Trevigen Inc. (Gaithburg, MD). Except where noted, all other reagents were purchased from Sigma Chemical (Oakville, Ontario).

2.3 Results

2.3.1 $A\beta_{(1-42)}$ causes cortical neuron death

To investigate Amyloid-β induced neuron death, wild-type, neurons were treated with 20 μM $A\beta_{(1-42)}$ for 20, 30, and 48 hours in neurobasal medium lacking B27 supplement and glutamine (NBB). B27 contains neuroprotective factors and glutamine rescues neurons from PARP-1 toxicity. Both were omitted to allow isolation of the

protective effects of PARP-1 inhibition/deletion. Control groups were NBB without $A\beta_{(1-42)}$ and a theoretical 100% survival control, represented by neurobasal medium with all supplements and no experimental media changes (C). No significant decline in cell survival was attributable to replacing NB with NBB (Fig. 5), indicating no toxic effects of either neuronal media changes or changing to medium lacking B27 supplement and glutamine for the maximum 30 hour experimental period. In contrast, 20 μM $A\beta_{(1-42)}$ exposure caused significant reductions in cell survival at all three time points (Fig 5; $p < 0.001$). These data show that $A\beta_{(1-42)}$ causes neuron death in our cortical cultures.

2.3.2 PARP-1 is not required for Aβ-induced neurotoxicity

To evaluate the role of PARP-1 in neuron death induced by $A\beta_{(1-42)}$, we exposed both wild-type and PARP-$1^{-/-}$ cortical neuron cultures to 20 μM $A\beta_{(1-42)}$ for 48 hours. $A\beta_{(1-42)}$ significantly reduced cell survival in both genotypes and produced no difference in neuron death between Aβ treated groups in wild-type vs. PARP-$1^{-/-}$ (Fig. 6). These results do not support the hypothesis that PARP-1 is involved in $A\beta_{(1-42)}$ toxicity, in our hands. To investigate this further, we tested for PARP activity by performing immunocytochemistry for the enzymatic product of PARPs, ADP-ribose polymer (PAR), in response to the PARP activator and DNA alkylator, *N*-methyl-*N*`-nitro-*N*-nitrosoguanidine (MNNG). MNNG treatment of wild-type cultures produced dense puncta of immunofluorescence signal that were localized to neuronal nuclei (Fig. 7A). Since PARP-1 is a nuclear enzyme, nuclear PAR-staining is the expected result. PARP-$1^{-/-}$ neurons display diffuse immunoreactivity with a more cytosolic distribution (Fig. 7B).

Quantification of nuclear specific PAR fluorescence shows that nuclear PAR is reduced by 63% in PARP-$1^{-/-}$ cultures (Fig. 8). This indicates that PARP activity is significantly reduced in PARP-$1^{-/-}$ neurons, but that this partial reduction is not sufficient to protect from Aβ-induced death.

2.3.3 Non-selective PARP inhibition reduces Aβ neurotoxicity

We considered the possibility that PARP-2, which offers some functional redundancy with PARP-1 (Li, et al., 2010; Yelamos, Schreiber, & Dantzer, 2008), accounts for incomplete elimination of PARP activity and failed neuroprotection in PARP-$1^{-/-}$ cells. To test this, wild-type neuron cultures were exposed to $A\beta_{(1-42)}$ for 24 hours in the presence and absence of the PARP-1/PARP-2 inhibitor, [N-(6-oxo-5,6-dihydrophenanthridin-2-yl)-N, N-dimethylacetamide.HCl] (PJ34). PJ34 (10 μM) significantly reduced $A\beta_{(1-42)}$-induced neuron death (Fig. 9). This suggests that PARP-2 compensates sufficiently well for PARP-1 loss to produce neurotoxic effects in response to DNA damage. Data for Fig 9 were produced by Anderson lab member, Dr. Amit Kamboj. My contributions to Fig. 9 were experimental design, SOP generation, training of Dr. Kamboj, and data analysis.

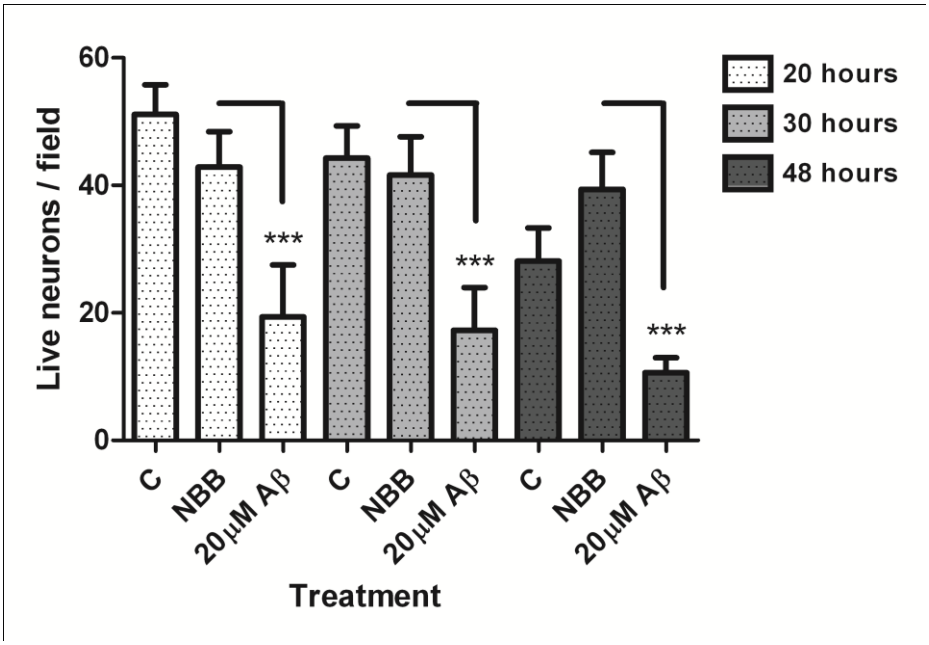

Figure 5. A significant reduction in live cells is observed as a result of Amyloid-β exposure for 20, 30 and 48 hours

Mouse cortical CD-1 primary neurons were treated in neural basal medium containing no supplements (NBB) with insoluble 20 μM $A\beta_{(1-42)}$ for 20, 30, and 48 hours. Live cells were labeled with calcein-AM and manually counted via fluorescence microscopy to assess survival. Wells with $A\text{-}\beta_{(1-42)}$ treatments contained significantly less live cells when compared to both the (C) and (NBB) controls. *** $p < 0.001$ using Bonferroni's Multiple Comparison Test for treatments at each time point. $n = 8$ for all experiments.

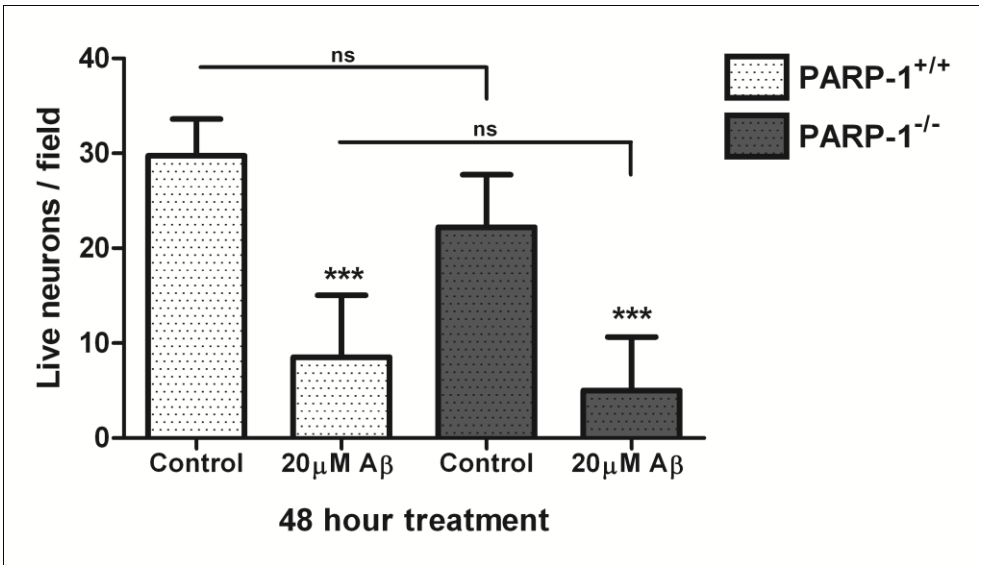

Figure 6. No difference in cell death is observed between wild-type and PARP-1$^{-/-}$ neuron cultures exposed to A$\beta_{(1-42)}$ for 48 hours

Mouse cortical primary neurons from wild-type and PARP-1$^{-/-}$ mice were exposed to A-$\beta_{(1-42)}$ for 48 hours in defined Hibernate media lacking pyruvate but containing 2 mM Glutamine. Neuronal death as a result of A$\beta_{(1-42)}$ exposure was not prevented by the loss of PARP-1 when compared to controls. *** $p < 0.001$ using Bonferroni's Multiple Comparison Test. n = 4 for wild-type and n = 5 for PARP-1$^{-/-}$. ns = not statistically significant.

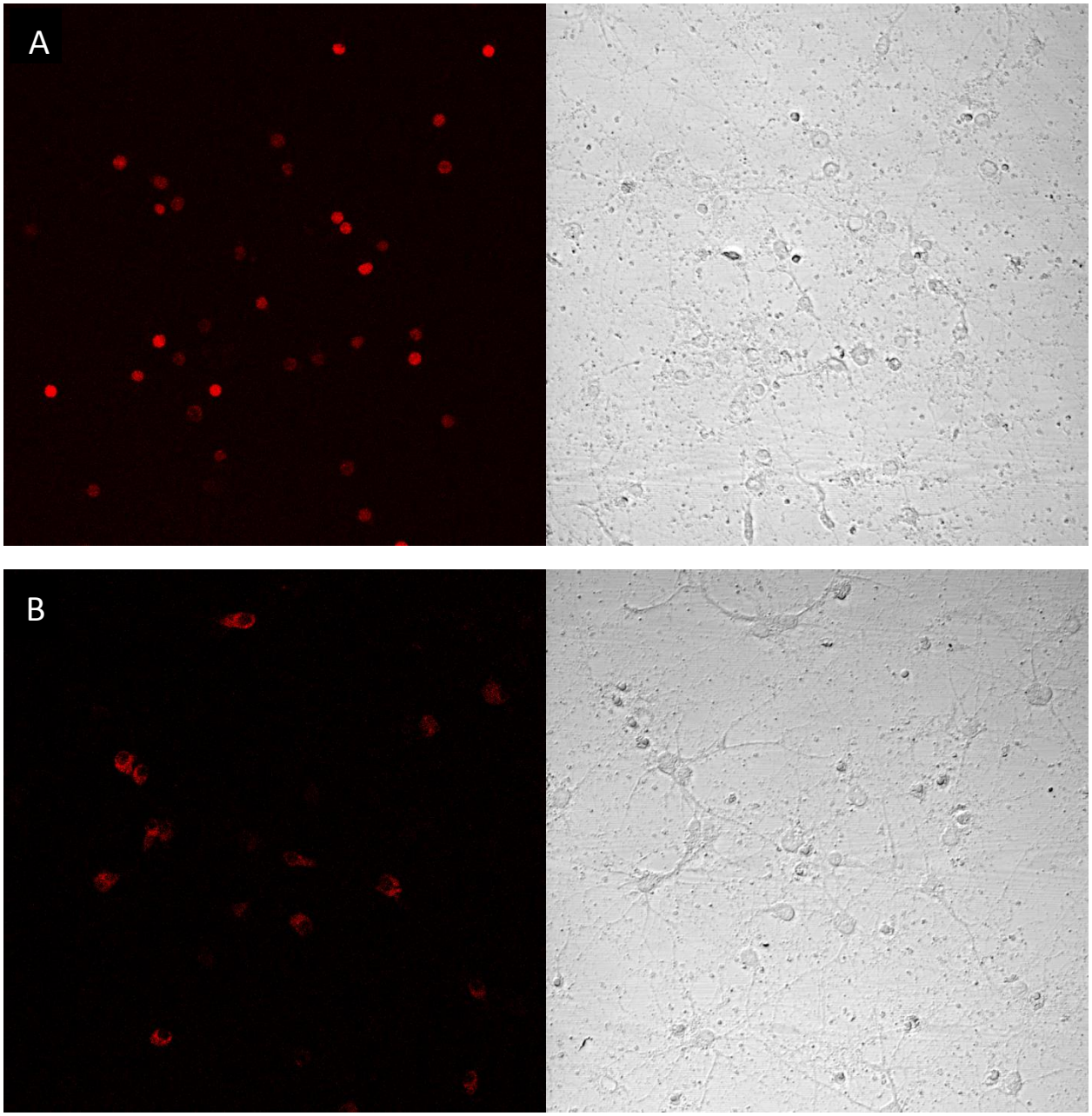

Figure 7. Wild-type and PARP-1$^{-/-}$ neurons treated with MNNG show differential PAR staining

Mouse cortical primary neurons from wild-type and PARP-1$^{-/-}$ mice were exposed to 300 µM MNNG for 15 minutes in order to induce PARP activity and PAR formation. (A) Wild-type neurons show significant nuclear PAR formation as a result of PARP-1 activation. (B) PARP-1$^{-/-}$ neurons have significantly reduced PAR formation.

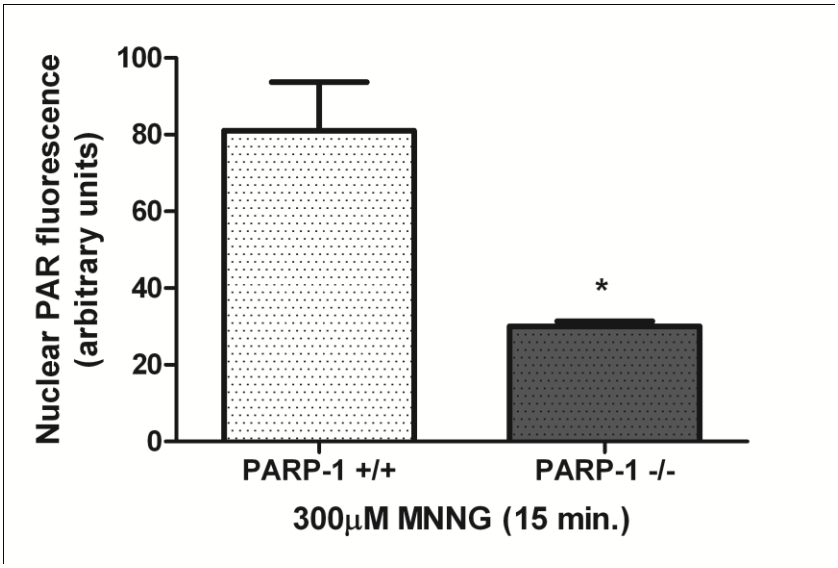

Figure 8. PARP-1$^{-/-}$ neurons treated with MNNG show significantly reduced nuclear PAR staining

Mouse cortical primary neurons from wild-type and PARP-1$^{-/-}$ mice were exposed to 300 μM MNNG for 15 minutes in order to induce PAR formation. Densitometry of nuclear PAR fluorescence shows a significant reduction with the loss of PARP-1 as expected. * $p < 0.05$ using The Student's t-test with $n = 2$.

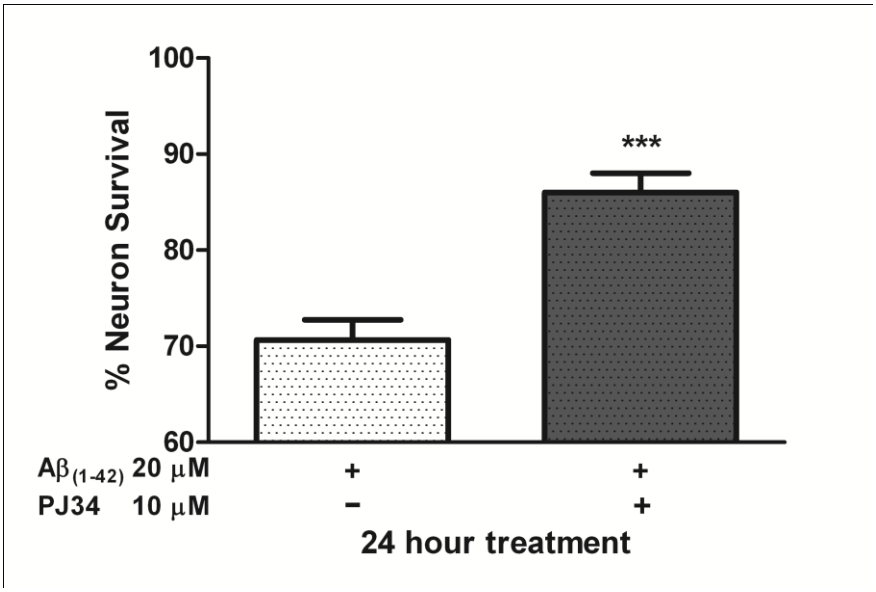

Figure 9. Protection from $A\beta_{(1-42)}$-induced death by PJ34 in wild-type neurons

Mouse cortical primary neurons from wild-type mice were exposed to A-$\beta_{(1-42)}$ in the presence and absence of 10 μM PJ34, a non-specific PARP inhibitor for 24 hours in Neural Basal media lacking supplements. Neuronal death by exposure to $A\beta_{(1-42)}$ was significantly attenuated in the presence of PJ34 when compared to control. *** $p < 0.001$ using Student's t-test with $n = 3$.

2.4 Discussion

The objective of this study was to establish an *in vitro* model of neurodegeneration in Alzheimer's Disease, and use it to determine whether PARP-1 contributes to neuron death. We successfully developed a reproducible model of A-$\beta_{(1-42)}$-induced neuron death. We also showed that combined inhibition of PARP-1 and PARP-2 significantly reduced Aβ-induced neuron death while elimination of PARP-1 alone was not neuroprotective.

We observed significant reduction of PAR immunostaining (PARP activity) in PARP-$1^{-/-}$ cultures exposed to MNNG. These results agree with other studies showing PAR staining is reduced by PARP inhibitors such as PJ34 (Kauppinen, Suh, Berman, Hamby, & Swanson, 2009). In our study, approximately 1/3 of nuclear PAR staining fluorescence observed in wild-type neurons persisted in PARP-$1^{-/-}$ neurons. This suggests that there may be one or more redundant systems in operation and that these systems may act to compensate for the loss of PARP-1. One possibility is that PARP-2 compensates partially since it is functionally similar to PARP-1 and represents up to 15% of total nuclear PARP activity (Huber, Bai, de Murcia, & de Murcia, 2004). In support of this, double PARP-1/2 knockouts are embryonic lethal, whereas single PARP-1 or PARP-2 knockouts are not. In addition, PARP-2 inhibition is neuroprotective in focal cerebral ischemia (Li, et al., 2010). It is therefore conceivable that the toxic effect of Aβ we observed in PARP-$1^{-/-}$ neurons (Fig. 6) may be mediated by compensatory activity of PARP-2. In our hands, non-selective PARP inhibition (PJ34) significantly mitigated Aβ-induced cell death in conditions where the PARP-$1^{-/-}$ genotype could not. This suggests that suppression of both PARP isoforms is required to achieve neuroprotection. This must

be reconciled with observations showing that elimination of PARP-1 alone is sufficient to protect neurons from several distinct neurodegenerative insults in other models (Cavone, et al., 2011; Pacher & Szabo, 2005; Sodhi, Singh, & Jaggi, 2010). The relative roles of PARP-1 vs. PARP-2 need to be probed further in neurodegeneration models. Future studies in Aβ toxicity could focus on investigation of Aβ-induced neuron death in PARP-2 knockouts or a conditional PARP-1/2 knockout model. For example, if double knockout of PARP-1/PARP-2 reduces Aβ toxicity, then this would be strong evidence that PARP-2 plays an obligatory role in Aβ toxicity.

Overall, we have shown that $A\beta_{(1-42)}$ exposure leads to significant neuron death. We also showed that despite Aβ-induced PARP activity, neuronal death was not dependent on PARP-1 alone. These data suggest that both PARP-1 and PARP-2 may contribute to neuron death but we cannot rule out the possibility that PARP-2 alone may be responsible. These data contribute to an important and growing body of knowledge regarding the relative importance of nuclear ADP-ribosylating PARP isoforms in neurodegeneration.

[2]Chapter 3: Poly(ADP-ribose) polymerase-1 (PARP-1) causes adenine nucleotide depletion and astrocyte death sensitive to protection by conjugated linoleic acid (CLA)

[2] Reprinted and adapted with permission by John Wiley and Sons from Tang KS, Suh SW, Alano CC, Shao Z, Hunt WT, Swanson RA, Anderson CM. (2010) *Astrocyte poly(ADP-ribose) polymerase-1 (PARP-1) activation leads to bioenergetic depletion and inhibition of glutamate uptake capacity*. Glia 58 446:457.

3.1 Introduction and Rationale

Poly(ADP-ribose) polymerase-1 (PARP-1) is a nuclear DNA repair enzyme activated by DNA strand nicks. PARP-1 works by recruiting a host of DNA repair enzymes to sites of DNA damage. These sites are marked by attaching ADP-ribose polymers (PAR) to the nick sites, using NAD^+ as a substrate. In pathological conditions, when DNA damage is substantially more severe than baseline DNA damage, PARP-1 activity increases on a large scale to a point that causes massive NAD^+ depletion and bioenergetic deficits that are thought to lead to cell death (Pieper, Verma, Zhang, & Snyder, 1999). Despite reports that NAD^+ and ATP levels are reduced after pathological PARP-1 activation (Tanaka, et al., 2005), there are several questions about the bioenergetic effects of PARP-1 that are yet to be answered. First, the temporal association between NAD^+ and ATP depletion has not been resolved adequately. It is postulated that NAD^+ depletion leads to ATP loss by reducing mitochondrial function and stimulating ATP-dependent NAD^+ synthesis *de novo*, but this has not been definitively demonstrated. Second, nearly all reports of PARP-1-induced bioenergetic depletion document changes in NAD^+ or ATP. It is not clear, however, whether there is overall adenine nucleotide depletion, or if there is an increase in AMP concomitant to declines in ATP levels, as occurs in ischemia. This is an important question because, for example, elevated AMP in ischemia activates AMP kinase, which initiates compensatory gene transcription. Loss of AMP in PARP-1 toxicity is likely to prevent AMP kinase associated genomic effects, thus significantly distinguishing PARP-1 energy failure from ischemic energy failure. To study these issues, our objective was to design HPLC paradigms that allow simultaneous detection of ATP, ADP, AMP and NAD^+ in cell

homogenates. Since PARP-1 activity causes NAD^+ depletion and cell death in astrocytes, we used astrocyte cultures as a CNS cell model. Both weak anion exchange and reverse-phase HPLC methods were optimized and produced sufficient adenine nucleotide separation to facilitate determining the effects of PARP-1 activation on astrocyte nucleotide levels.

Our second study objective was to determine whether astrocyte survival after PARP-1 activation could be rescued by the dietary polyunsaturated fatty acid, conjugated linoleic acid (CLA). CLA (described in section 1.5) refers to a combination of positional and geometric isomers of the 18-carbon polyunsaturated fatty acid, linoleic acid (LA). Whereas LA has *cis* double bonds at carbons 9 and 12, CLA has a double bond configuration whereby there is a conjugated double bond system which may be in *cis* or *trans* orientations. To date, 28 isomers have been described. However most of the biological properties associated with CLA are based on experiments involving the *cis*-9, *trans*-11-, and *trans*-10, *cis*-12-CLA species. CLA has been shown to exhibit protective benefits in a number of disease models, including cancer, diabetes, and atherosclerosis (Bhattacharya, et al., 2006). CLA can be absorbed and metabolized in the brain (Fa, et al., 2005), but there has been little work examining protective effects of CLA in the CNS. We hypothesized that CLA protects astrocytes from PARP toxicity. There is further mechanistic rationale to hypothesize that CLA is protective in brain ischemia. This rationale is reserved for Chapter 4, which presents a comprehensive examination of neuroprotection by CLA in simulated brain ischemia. To test this hypothesis, we treated astrocyte cultures with the DNA alkylator and PARP-1 activator, MNNG, in the presence and absence of CLA.

3.2 Materials and Methods

3.2.1 Astrocyte cultures

Astrocyte cultures were prepared from postnatal day 1 mice, in accordance with the guidelines set forth by the *Canadian Council on Animal Care*. Cultures were plated on tissue culture plates at $1.0x10^4$ cells/cm^2 in Eagle's Minimal Essential Medium (MEM) with 10% Fetal Bovine Serum (FBS) (Invitrogen, Carlsbad, CA) and 2 mM glutamine (Hyclone, Logan, UT). Cultures were maintained at 37°C/5% CO_2. At approximately day 14, cultures were treated with 10 µM cytosine 1-β-D-arabinofuranoside for a period of 48 hours in order to suppress proliferation of other competing cell types, followed by replacement with fresh MEM containing only 3% FBS and 2 mM glutamine. Cultures were selected for experiments between days 25 and 40 post-culture date. Cultures were approximately 95% pure astrocytes based on glial fibrillary acidic protein staining with the remainder microglia based on immunoreactivity for ionized calcium-binding adaptor molecule 1.

3.2.2 Cell death

Astrocytes were equilibrated in balanced salt solution (BSS) containing 140 mM NaCl, 3.1 mM KCl, 1.15 mM $CaCl_2$, 1.2 mM $MgSO_4$, 15.7 mM HCO_3, 0.5 mM KH_2PO_4, and 2 mM glucose (pH 7.2) for 30 minutes at 37°C. They were then treated with varying concentrations of the DNA alkylating agent, MNNG, for 30 min in BSS. BSS/MNNG was replaced with fresh BSS and nucleotide levels and cell death were measured at specified time points following MNNG washout. Astrocyte death was evaluated by

assessing cell permeability to lactate dehydrogenase (LDH) as described previously (Anderson, et al., 2002). Intracellular LDH activity was measured 18-24 hours after removal of MNNG and normalized to 0% death controls corresponding to cells maintained unperturbed in growth medium. Trends were verified by morphological examination of cultures.

3.2.3 Cell preparation for nucleotide measurements

Cells were rinsed and harvested by scraping into ice-cold phosphate-buffered saline (PBS, pH 7.2), followed by centrifugation at 400 x *g* for 10 min at 4^{o}C. Perchloric acid (0.5 N) extracts were neutralized with 1 N potassium hydroxide, and the supernatant was used as the sample for nucleotide analysis using high performance liquid chromatography (HPLC). Results were normalized to total protein, measured by the bicinchonic acid method and BSA standards. Each HPLC experimental treatment was performed in duplicate 3-5 times. Each sample replicate was derived from a separate tissue culture preparation.

3.2.4 Materials

Cell culture reagents were purchased from Invitrogen (Burlington, ON, Canada), [N-(6-oxo-5,6-dihydrophenanthridin-2-yl)-N, N-dimethylacetamide.HCl] (PJ34) was purchased from Calbiochem (San Diego, CA). All other chemicals were purchased from Sigma-Aldrich (Oakville, ON, Canada) unless otherwise stated.

3.3 Results

3.3.1 Separation of adenine nucleotide standards by weak anion-exchange HPLC

Separation of nucleotide standards NAD^+, AMP, ADP, and ATP was performed by a novel method of weak anion-exchange HPLC using a PolyWAX LP™ Column in combination with a salt gradient. In this method, we equilibrated the columns for 10 minutes with phosphate buffer (HPLC grade, $HNa_2O_4P.2H_2O$ mixed with H_2NaO_4P, adjusted to pH = 6.7), injected samples into the moving solvent phase consisting of 100 mM phosphate buffer at pH = 6.7 and steadily transitioned to 300 mM phospahate buffer at pH = 6.7 over a period of 20 minutes. Nucleotides were eluted in order of increasing charge or in order of the least number of phosphate groups to the most phosphate groups (i.e. $NAD^+ \rightarrow$ ATP), and separation was completed in approximately 28 minutes (Fig. 10).

3.3.2 Separation of adenine nucleotide standards by reverse-phase HPLC

Separation of adenine nucleotides ATP, ADP, AMP, and NAD^+ was performed by reverse-phase HPLC using a Supelcosil LC-18 HPLC column (5 µm particle size, L × I.D. 25 cm × 4.6 mm) and a Waters 600E Multisolvent Delivery System. The mobile phase and chromatographic conditions were described previously (Crescentini & Stocchi, 1984). Briefly, sample was injected into a mobile phase comprised of phosphate buffer (HPLC grade, HPLC grade, $HNa_2O_4P.2H_2O$ mixed with H_2NaO_4P, adjusted to pH = 6). In contrast to the method described above in (section 3.3.1), this method employs 100 mM phosphate buffer at pH = 6 and a methanol gradient starting at 0% and transitioning

to 10% over a period of 20 minutes. Nucleotides were eluted in order of increasing hydrophobicity and thus, nucleotides with the most phosphate groups eluted first (i.e. ATP → NAD^+). Separation was completed in approximately 20 minutes (Fig. 11).

3.3.3 PARP-1-induced astrocyte death

Primary mouse astrocyte cultures were incubated with MNNG (10-300 µM) for 30 min to induce DNA damage and PARP-dependent astrocyte death. Astrocyte death was assessed 18-24 hr after MNNG removal by measuring LDH retention. MNNG induced a concentration-dependent increase in cell death (Fig. 12A and B, E) in wildtype astrocyte cultures with an EC_{50} of 78.2 ± 2.7 µM. Maximal cell death was significantly less in PARP-$1^{-/-}$ astrocytes at 100 and 300 µM MNNG (Fig. 12C and D, F; $p < 0.001$, 2-way ANOVA), indicating that MNNG-induced astrocyte death is PARP-1-dependent. MNNG was used at 100 µM in subsequent determinations of bioenergetic status as a concentration that produces a strong but submaximal death response at 18-24 hours. At 100 µM, no significant astrocyte death was observed up to 4 hours after MNNG removal, but survival was reduced by approximately 75% between 4 and 12 hours (Fig. 12F). Thus, bioenergetics determinations were made up to 4 hours after MNNG with confidence that cultures were near 100% survival.

3.3.4 PARP-1 activation causes adenine nucleotide depletion in astrocytes

Using the reverse-phase HPLC method, NAD^+, ATP, ADP and AMP were measured up to 4 hours after MNNG treatment of astrocyte cultures (100 µM, 30 min). No significant changes in adenine nucleotide levels were seen at time 0, immediately

after MNNG removal, but significant large magnitude declines were observed at 1-4 hour time points (Fig. 13A, C, E, G). NAD^+ depletion was most severe, declining from 11.0 ± 1.3 to 2.9 ± 0.2 nmol/mg protein (74%, $p < 0.01$) at 1 hour and from 13.4 ± 2.5 to 0.3 ± 0.2 nmol/mg protein (98%, $p < 0.001$) at 3 hours post-MNNG (Fig. 13A). ATP levels experienced a smaller magnitude but significant decline as early as 1 hour after MNNG, falling from 13.8 ± 0.1 to 7.5 ± 0.9 nmol/mg protein (Fig. 13C; 46%, $p < 0.05$); maximal ATP depletion was observed 4 hours post-MNNG, declining from 18.3 ± 0.8 to 5.8 ± 0.5 nmol/mg protein (71%, $p < 0.001$). ADP and AMP levels also fell in response to MNNG, with ADP declining by 73% (Fig. 13E and F, $p < 0.001$) and AMP by 66% (Fig. 13G and H; $p < 0.01$) after 4 hours. Also when compared at 4 hours, MNNG did not change ATP:ADP ratios and produced a significant decline in ATP + ADP + AMP, indicating a net loss of adenine nucleotides.

To assess PARP-1 involvement in MNNG-induced bioenergetic depletion, PARP-$1^{-/-}$ astrocytes were exposed to MNNG. MNNG (100 μM, 30 min) still caused a significant reduction of NAD^+ levels in PARP-$1^{-/-}$ astrocytes (Fig. 13B), but the overall magnitude of response was smaller than in wildtype astrocytes, producing a statistically insignificant decline at 1 hour post-MNNG and a maximal 70% decline at 4 hours ($p < 0.01$). A direct comparison for MNNG-induced NAD^+ depletion in wildtype and PARP-$1^{-/-}$ astrocytes is shown in Fig. 14A and indicates significantly improved NAD^+ content in the PARP-$1^{-/-}$ cells at 1, 2, 3 and 4 hours after MNNG exposure (2-way ANOVA). Genetic deletion of PARP-1 also protected ATP levels as MNNG failed to produce a statistically significant decline in ATP in PARP-$1^{-/-}$ astrocytes (Fig. 13D) while percent control comparisons yielded significant differences between wildtype and PARP-$1^{-/-}$ ATP

levels at 2, 3 and 4 hours (Fig. 14B; $p < 0.001$, 2-way ANOVA). These results indicate that MNNG activation leads to NAD^+ and ATP depletion in a partially PARP-1-dependent manner. For ADP, although there is statistically significant MNNG-induced depletion in wild-type cells, there is no significant departure from untreated controls in PARP-$1^{-/-}$ astrocytes (Fig. 13F), suggesting ADP depletion is at least partially PARP-1-dependent. This effect appears to build over time as the only statistically significant difference in percent control ADP levels between wild-type and PARP-$1^{-/-}$ astrocytes was observed at the 4 hour time point (Fig. 14C; $p < 0.01$, 2-way ANOVA). A precipitating role for PARP-1 in AMP depletion was not observed in the current study as indistinguishable AMP depletion was seen in both wild-type and PARP-$1^{-/-}$ astrocytes from 0-4 hours post-MNNG (Figs. 13H and 14D). Figures 12-15 were produced by Dr. Kim San Tang, who was a postdoctoral fellow in the Chris Anderson Lab. My role was to develop the anion exchange HPLC protocol, provide HPLC training to Dr. Tang and to participate as an equal partner in intellectual development of the project. Results are published, in part, in Tang, Hunt et al., *Glia* 58(4):446-57.

3.3.5 Conjugated Linoleic Acid protects astrocytes from PARP toxicity

To determine if CLA is capable of enhancing astrocyte survival after PARP activation, cultures were exposed to 100 µM MNNG for 30 min in the presence and absence of CLA, and cell death assessed 18 hours later by measuring LDH retention. MNNG significantly increased astrocyte death ($p<0.05$) in a manner sensitive to inhibition by the PARP inhibitor, PJ34 (10 µM, $p<0.01$). CLA significantly reduced cell

death from 29% to 19% ($p<0.05$), indicating a protective role for CLA. This is the first demonstration that CLA can protect against PARP-induced death of any cell type.

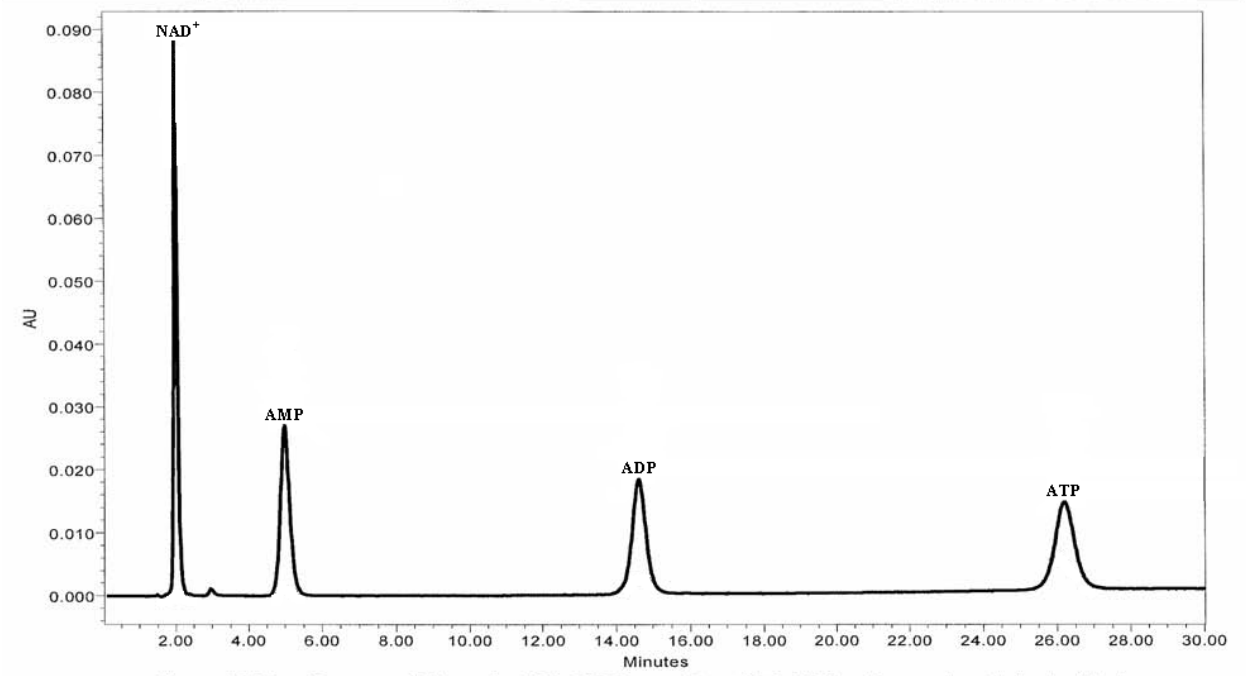

Figure 10. Weak anion-exchange HPLC separation of nucleotide standards NAD^+, AMP, ADP, and ATP

Separation of known concentrations of standards were performed by weak anion-exchange HPLC using a PolyWAX LP™ Column (5 µm particle size, 100 Å pore size; L x I.D. = 10 cm x 4.6 mm; The Nest Group, Inc., Southborough, MA). 100 mM phosphate buffer with pH = 6.7 is used for equilibration and injection of samples with a gradient transition to 300 mM phosphate buffer over 20 minutes. Separation of nucleotides is based on molecular charge and is completed by approximately 28 minutes using the Waters 600E Multisolvent Delivery System at a flow rate of 1 ml/minute coupled with a photo-diode array detecting absorbance differential between solvent and sample at 268.8 nm.

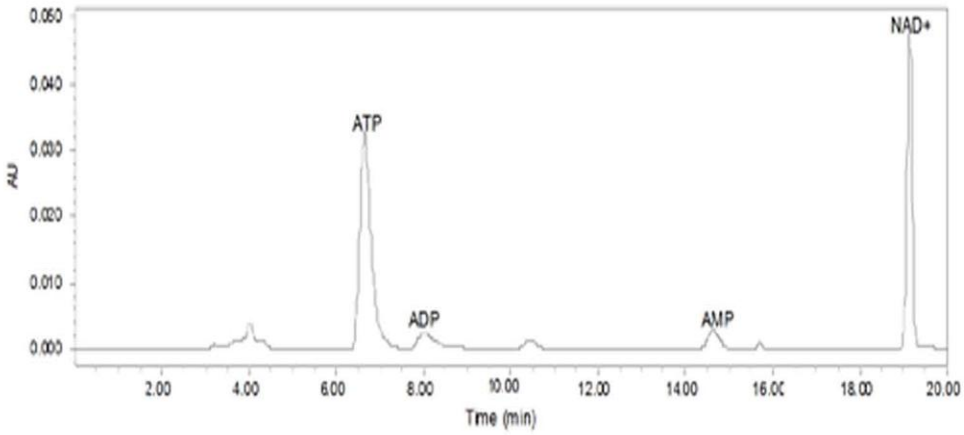

Figure 11. Reverse-phase HPLC separation of adenine nucleotide standards

Separation of adenine nucleotides was performed by reverse-phase HPLC using a Supelcosil™ LC-18 HPLC Column (5 µm particle size, 120 Å pore size; L x I.D. = 25 cm x 4.6 mm; Sigma-Aldrich, Oakville, ON). 100 mM phosphate buffer with pH = 6 is used for equilibration and injection of samples and a methanol gradient is used starting with 0% and transitioning to 100 mM phosphate buffer with 10% methanol in order to separate the nucleotides based on hydrophobicity. Separation is complete in approximately 20 minutes using the Waters 600E Multisolvent Delivery System with a flow rate of 1 ml/minute, NAD^+, ATP, ADP, and AMP were detected with a photo-diode array by monitoring the absorbance differential between sovent and sample at 254 nm.

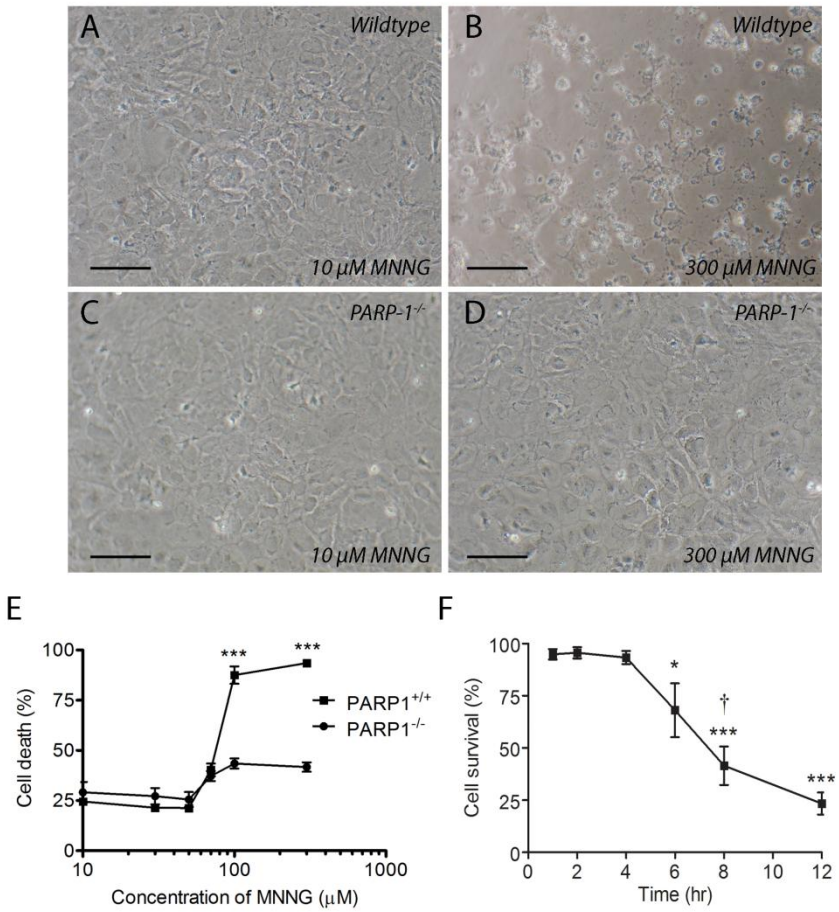

Figure 12. MNNG reduces astrocytes survival in a concentration and time-dependent fashion

Confluent astrocyte cultures were exposed to increasing MNNG concentrations (30 min, 10-300 µM) and cell death was assessed after 18-24 hours by LDH retention. A and B are representative photomicrographs of wild-type cultures treated with MNNG showing increased cell death with higher MNNG concentration. C and D are photomicrographs from PARP-$1^{-/-}$ astrocytes and show resistance to MNNG. E shows cumulative graphical data demonstrating that MNNG concentration-dependently increases astrocyte death in cells with the wild-type but not PARP-$1^{-/-}$ genotype. MNNG (100 µM) does not cause significant wild-type astrocyte death until after 4 hours post-MNNG exposure (F). Data for (E) are means ± SEM (n = 3-6). *** $p < 0.001$ compared to PARP-$1^{-/-}$ using 2-way

ANOVA with Bonferonni post-test. Scale bars (A-D) = 25 μm. Data for (F) are means ± SEM (n = 3-6). * $p < 0.05$, *** $p < 0.001$ compared to 30 minutes. † < 0.05 compared to 6 hours using ANOVA with Newman-Keuls post-test.

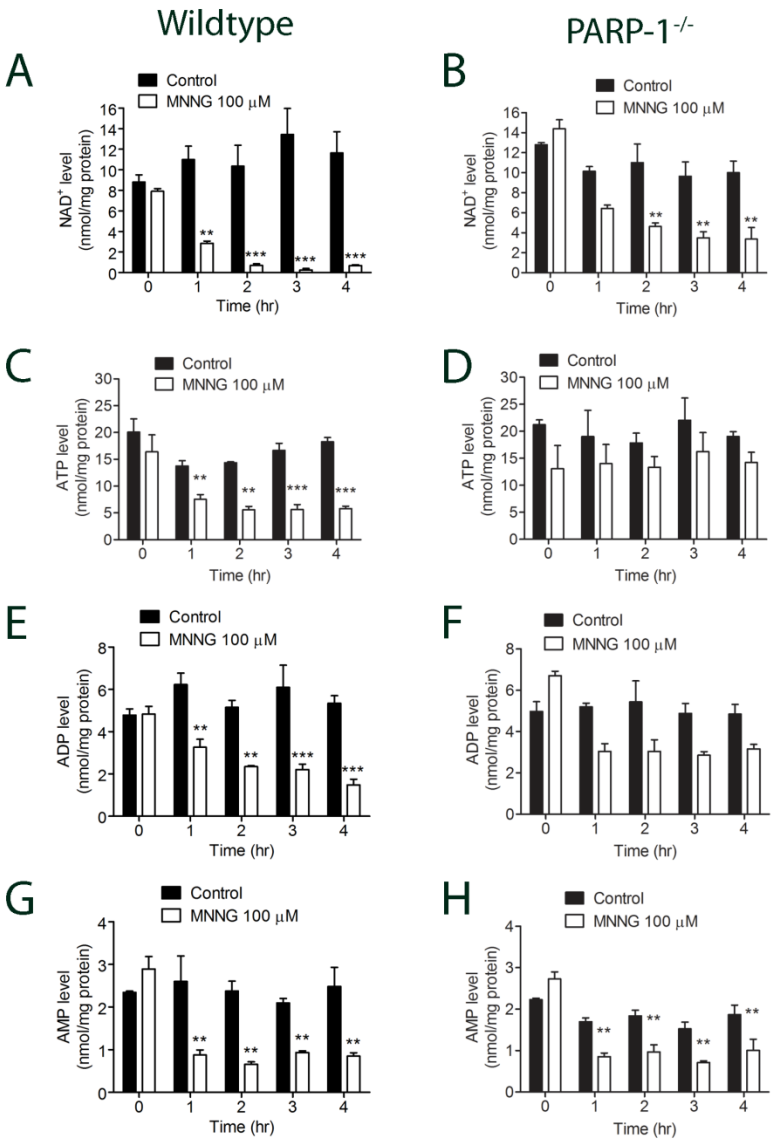

Figure 13. MNNG causes PARP-1-dependent bioenergetic depletion

MNNG (100 μM) caused significant depletion of NAD^+ (A), ATP (C), ADP (E) and AMP (G) at all time points from 1 to 4 hours after MNNG exposure. The same experiments performed in PARP-$1^{-/-}$ astrocytes show reduced but significant NAD^+ depletion (B), insignificant ATP (D) and ADP (F) depletion, and AMP depletion not distinguishable from wild-type cells (H). Data are means ± SEM (n = 4-6). ** $p < 0.01$, *** $p < 0.001$ compared to respective untreated controls using ANOVA with Newman-Keuls post-test.

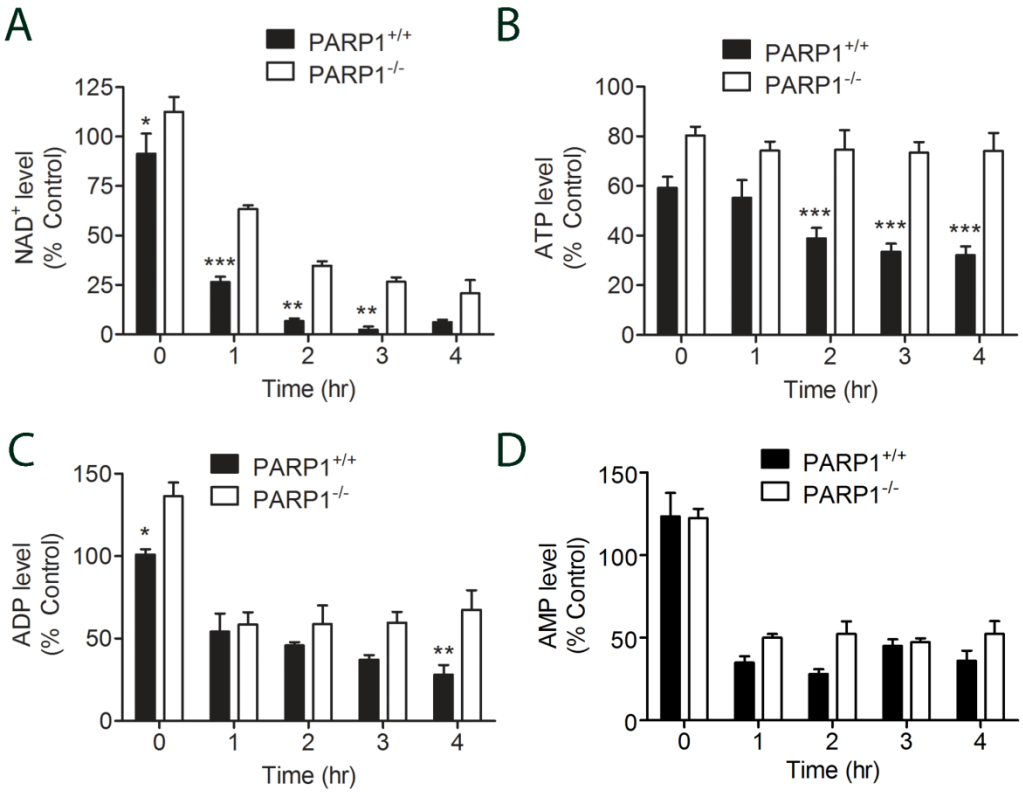

Figure 14. Direct comparisons of MNNG-induced bioenergetic depletion in wild-type and PARP-1$^{-/-}$ astrocytes

MNNG (100 µM)-induced changes in adenine nucleotide levels were expressed as percent of respective untreated controls to directly compare results between wild-type and PARP-1$^{-/-}$ astrocytes. NAD^+ levels were significantly protected in PARP-1$^{-/-}$ cells at time 0, 1, 2 and 3 hours after MNNG treatment (A) and ATP levels were protected at 2, 3 and 4 hours after MNNG (B). ADP levels were improved only at 4 hours after MNNG in PARP-1$^{-/-}$ astrocytes while AMP levels were not changed significantly by the PARP-1$^{-/-}$ genotype. Data are means ± SEM (n = 4-6). * $p < 0.05$, ** $p < 0.01$, *** $p < 0.001$ compared to respective PARP-1$^{-/-}$ groups using ANOVA with Newman-Keuls post-test.

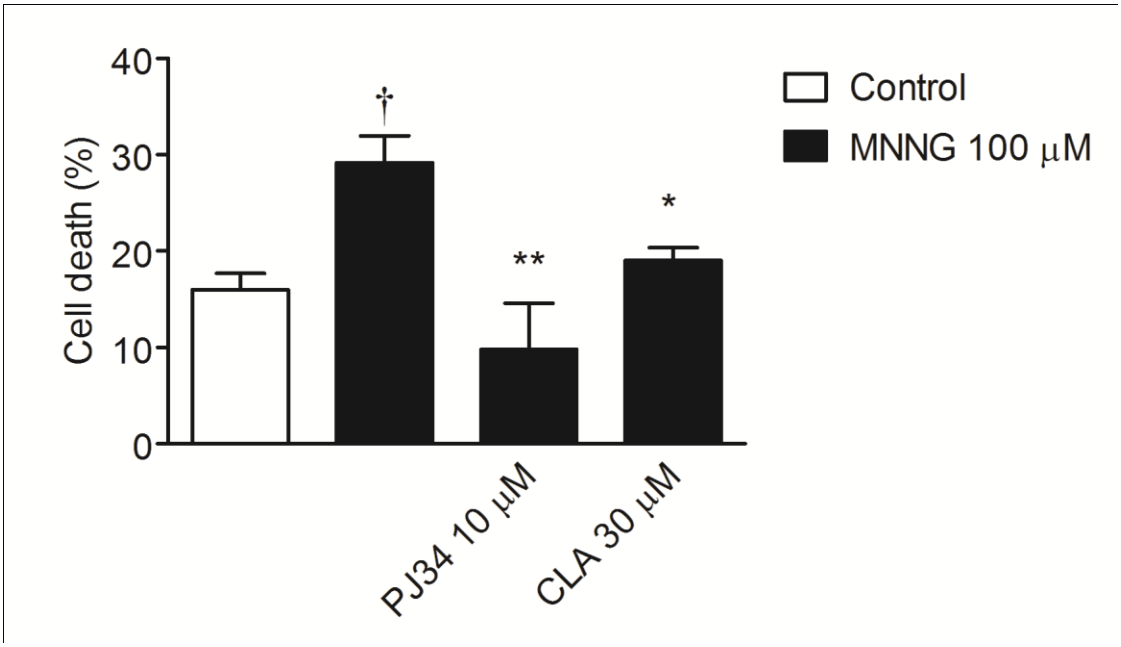

Figure 15. Conjugated Linoleic Acid protects astrocytes from PARP toxicity

Astrocyte cultures were exposed to 100 μM MNNG for 30 minutes in the presence and absence of 30 μM CLA and cell death assessed 18 hours later by measuring LDH retention. MNNG significantly increased astrocyte death ($p < 0.05$) in a manner sensitive to inhibition by the PARP inhibitor, PJ34 (10 μM, $p < 0.01$). CLA significantly reduced cell death from 29% to 19% ($p < 0.05$), indicating a protective role for CLA. Data are means ± SEM (n = 4-6). * $p < 0.05$, ** $p < 0.01$, when compared to the MNNG (100 μM) group. † $p < 0.05$, when compared to control using ANOVA with Newman-Keuls post-test.

3.5 Discussion

The objectives of the current study were 1) to design HPLC paradigms that can be used to quantify ATP, ADP, AMP and NAD^+ levels in single samples, 2) to analyze the temporal dynamics of adenine nucleotide depletion after PARP-1 activation but before cell death, and 3) to determine whether CLA is capable of protecting astrocyte survival after direct PARP-1 activation. We successfully developed two HPLC methods to simultaneously determine NAD^+, ATP, ADP and AMP levels in primary astrocyte cultures and used one of those methods to discover that PARP-1 leads to depletion of the total adenine nucleotide pool. We also found that PARP-1-induced astrocyte death is partially reversed by CLA.

Weak anion-exchange HPLC separations are based on a differential of charge between the column and the sample running through it. In our separation of adenine nucleotides the weakest charged particle, NAD^+ is eluted and detected first as the slightly negative charge of the phosphate buffer competes with the slightly positive charge of the silica inside the column allowing for attraction of the positively charged nucleotide in the column to move with the solvent phase. As the salt gradient is increased, the attractive force of the solvent phase is greater and is able to aid in the elution of even more positively charged particles such as ATP. This allows for separation to be completed in approximately 28 minutes with clear separation between peaks and reproducible results when using nucleotide standards. However, when we introduced our cell extracts, we noticed substantial noise and much less clarity of peaks of interest. Therefore, we decided to employ reverse-phase HPLC which separated our sample based on hydrophobicity. With this method, the nucleotides are eluted in the opposite order with increasing organic

mobile phase (methanol) gradient but we believe it was much less sensitive to cell extract preparations which involved pH adjustments. The result was cleaner separations of crude extract with sufficient peak separation and additionally, separations were completed within 20 minutes which saved time and money in comparison to the weak anion-exchange method.

The bioenergetic consequences of PARP-1 activation in astrocytes were modeled using MNNG as a PARP activator between the time of MNNG removal and 4 hours after MNNG, at which time significant astrocyte death began. Baseline NAD^+ levels were 8.8-13.4 nmol/mg protein at various time points, in agreement with previous studies that found baseline NAD^+ levels in astrocytes to range from 7-19 nmol/mg protein (Alano, et al., 2007; Pieper, et al., 2000; Verderio, et al., 2001). MNNG caused a time-dependent decline in NAD^+ levels reaching 98% depletion at 3 hours after MNNG. Despite reduced NAD^+ depletion in PARP-$1^{-/-}$ astrocytes (Fig. 13B), significant depletion was still observed. This indicates that PARP-1 is not the only mechanism responsible for MNNG-induced NAD^+ consumption. Although we cannot identify the alternate MNNG targets with certainty, reasonable possibilities are PARP-2, which is also activated by DNA strand breaks and catalyzes formation of ADP-ribose polymers (Ame, Spenlehauer, & de Murcia, 2004), and/or NAD^+ dependent protein deacetylases known as sirtuins, which are activated during cell stress and serve largely protective rolls in neurons by mechanisms including repression of p53-mediated apoptosis and maintenance of mitochondrial function (Gan & Mucke, 2008).

ATP levels also declined following NAD^+ depletion, in agreement with previous studies in astrocytes (Suh, et al., 2007) and brain tissue (Cosi & Marien, 1999; Zeng, et

al., 2007), reaching minimums at 3-4 hours post-MNNG. In contrast to NAD^+ declines, ATP depletion was less complete (maximum 68%) and was completely blocked in the PARP-$1^{-/-}$ genotype. The reason for significant ATP generation (~30% normal) in the apparent absence of total cell NAD^+ is not known; one might expect a more robust depletion of ATP given that PARP-1-induced NAD^+ depletion inhibits glycolysis (Goodwin, Lewis, Davies, Skidmore, & Shall, 1978; Sheline, Behrens, & Choi, 2000; Ying, Garnier, & Swanson, 2003) and compensatory NAD^+ synthesis consumes ATP. One possible explanation is that NAD^+ loss was cytosolic, with sufficient mitochondrial NAD^+ remaining to protect oxidative phosphorylation. This scenario is consistent with the failure of PARP-1 to access mitochondrial NAD^+ in the absence of mitochondrial permeability transition in astrocytes (Alano, et al., 2007).

MNNG-treated cells exhibited a PARP-1-mediated net decline in the total adenine nucleotide pool, as reported previously (Cosi & Marien, 1999; Paschen, Olah, & Mies, 2000; Zeng, et al., 2007; J. Zhang, Dawson, Dawson, & Snyder, 1994). The most obvious consequences of this are inhibition of glycolysis by NAD^+ loss and loss of adenine equivalents to massive PARP-1-mediated ADP-ribose polymer formation. Both of these effects are obstacles to replenishing ATP levels, even in the presence of adequate glycolytic substrate, and result in a PARP-1-mediated downward bioenergetic spiral. In contrast, bioenergetic depletion resulting from reduced substrate delivery (cerebral ischemia, for example) is reversible to a point, open for repair by re-supply of substrate or alternative metabolic pathways, including activation of AMP-activation protein kinase (AMP kinase). AMP kinase is highly expressed in astrocytes and is activated in hypoglycemia/hypoxia by accumulating AMP, resulting is astrocytic ketogenesis, which

can be used to produce acetyl-CoA for oxidative phosphorylation in the absence of glucose (Blazquez, Woods, de Ceballos, Carling, & Guzman, 1999). AMP kinase is likely not activated in PARP-1-mediated bioenergetic depletion as AMP levels decrease (Fig. 13G) rather than increase.

The final point for this chapter is that CLA protected astrocytes from MNNG-induced and PARP-1-dependent death. This is the first demonstration of such an effect. CLA activates peroxisome proliferator-activated receptors (PPAR) that, in turn, regulate the balance of pro- and anti-apoptotic factors, such as Bax and Bcl-2, respectively. Thus, we speculate that CLA is protective by mitigating intrinsic mitochochondrial apoptosis. The mechanism of protection was not investigated in this chapter but will be addressed comprehensively in the context of neuronal protection in simulated ischemia in subsequent chapters.

Overall, we discovered and optimized two distinct HPLC paradigms that allow simultaneous separation of ATP, ADP, AMP and NAD^+. These methods allowed temporal resolution of changes of all these nucleotides after PARP-1 activation in a way not performed previously. We also identified a novel neuroprotective function of a dietary compound, CLA, that may have therapeutic implications in brain ischemia.

[3]Chapter 4: Protection of cortical neurons from excitotoxicity by conjugated linoleic acid

[3] Reprinted and adapted with permission by John Wiley and Sons from Hunt WT, Anderson, HD and Anderson CM. (2010) *Protection of cortical neurons from excitotoxicity by treatment with conjugated linoleic acid after glutamate exposure.* J Neurochem. 115(1):123-30. Copyright 2010 by John Wiley and Sons.

4.1 Introduction and Rationale

Glutamate is the primary excitatory neurotransmitter in the mammalian central nervous system (CNS), and tight control of post-synaptic glutamate receptor activation is critical for normal physiological neurotransmission (Coyle & Puttfarcken, 1993; Fonnum, 1984). Elevated glutamate concentrations can produce hyperstimulation of N-methyl-D-aspartate (NMDA)-type glutamate receptors and lead to neuron death by a cascade of events, including membrane depolarization, excessive Ca^{2+} influx, protease activation, oxidative stress and mitochondrial permeabilization, collectively known as excitotoxicity (Choi, 1988). Excitotoxicity has been implicated in stroke and CNS trauma, as well as neurodegenerative diseases including Amyotrophic Lateral Sclerosis (Corona, Tovar-y-Romo, & Tapia, 2007), Huntington's Disease (Estrada Sanchez, Mejia-Toiber, & Massieu, 2008), and Alzheimer's Disease (Riederer & Hoyer, 2006).

Conjugated linoleic acid (CLA) refers to a mixture of positional and geometric isomers of linoleic acid (LA), an 18-carbon polyunsaturated fatty acid with *cis* double bonds at carbons 9 and 12. CLA double bonds are conjugated and may be *cis* or *trans* in orientation. Although 28 isomers have been identified, most biological actions are attributable to *cis*-9, *trans*-11-, and *trans*-10, *cis*-12-CLA (Bhattacharya, et al., 2006). CLA is receiving attention as a dietary constituent and nutraceutical (Palmquist, et al., 2005) with salutary effects on the immune system as well as against cancer, diabetes, and atherosclerosis (Bhattacharya, et al., 2006). Despite a well-developed literature describing the potential for therapeutic effects of CLA in peripheral organ systems and disorders, there have been few reports of CLA effects in the CNS. It is known that CLA crosses the blood-brain barrier and is incorporated and metabolized in the brain (Fa, et

al., 2005), that chronic dietary CLA can reduce cerebral prostaglandin E2 (Nakanishi, Koutoku, Kawahara, Murai, & Furuse, 2003), and that CLA exerts anti-angiogenic actions in mammalian brain (Sikorski, Hebert, & Swain, 2008).

CLA signaling in several tissues involves activation of peroxisome proliferator-activated receptors (PPARs) (Alibin, Kopilas, & Anderson, 2008; Moya-Camarena & Belury, 1999; Moya-Camarena, Vanden Heuvel, Blanchard, Leesnitzer, & Belury, 1999). PPARs belong to a nuclear receptor family of transcription factors that are best known for their ability to regulate fatty acid and triglyceride metabolism (Lemberger, Desvergne, & Wahli, 1996). However, PPAR agonists such as the natural ligand 15-deoxy-Δ-12,14-prostaglandin J2 (15d-PGJ2) (Garcia-Bueno, Caso, Perez-Nievas, Lorenzo, & Leza, 2007; X. Zhao, Ou, Grotta, Waxham, & Aronowski, 2006) and PPARγ-selective agonists, rosiglitazone (Garcia-Bueno, et al., 2007), ciglitazone (X. Zhao, et al., 2006), and troglitazone (Uryu, Harada, Hisamoto, & Oda, 2002) also protect against glutamate excitotoxicity in both cultured neurons and *in vivo*. While CLA-PPAR signaling has not yet been reported in neurons, we hypothesized that CLA is neuroprotective in glutamate excitotoxicity. The objective of the current study was to determine whether physiologically relevant concentrations of CLA protect against glutamate excitotoxicity in primary cortical neuron cultures.

4.2 Materials and Methods

4.2.1 Neuron cultures

Neuron cultures were prepared from embryonic day 16 CD-1 mouse cortices in accordance within guidelines set forth by the *Canadian Council on Animal Care*. Cultures were plated on poly-D-lysine coated plastic at $2.5x10^5$ cells/cm^2 in Neurobasal medium (NB) with B27 supplement (Invitrogen, Carlsbad, CA), 1.2 mM glutamine, and 5% Fetal Bovine Serum (FBS; Hyclone, Logan, UT). The following day (day 1), media was changed to NB with B27 and glutamine. Cytosine arabinofuranoside (2 µM) was added on day 2 to prevent glial proliferation, and replaced on day 3 with NB/B27/glutamine. Cultures were maintained at 37°C/5% CO_2, and given a partial media change of day 6. Cultures were used on day 8 post-culture for all experiments and contained less than 2% glial fibrillary acidic protein immunopositive astrocytes.

4.2.2 Assessment of neuron death

To determine neuron death in response to glutamate and neuroprotection by CLA, neurons were treated with glutamate in NB for 1 hour in the presence of CLA or DMSO vehicle (0.1% DMSO final concentration). Media was changed to NB and cell survival measured 18 hours later. For CLA post-treatment, glutamate exposure was for 1 hour, followed by incubation in NB for 1 to 8 hours, and subsequent exposure to CLA in NB for the balance of 18 hours. Live cells were quantified by assessing intracellular calcein acetoxymethelester (calcein/AM; Roche, Eugene, OR) fluorescence using a Gemini Spectromax fluorescence plate reader with excitation at 485 nm and emission at 530 nm.

Results were normalized to a range between a 0% survival control (1 mM glutamate, 18 hours) and 100% survival (NB control), and accuracy of bulk fluorescence measurements by the plate reader was verified by counting live cells in individual wells in select experiments.

4.2.3 Materials

The mixed CLA used in our experiments (Nu-Chek Prep, Inc, Elysian, MN) contained ~80% *cis*-9, *trans*-11 and *trans*-10, *cis*-12 CLA at an approximate 1:1 ratio as well as trace amounts of other isomers. In addition to the putatively bioactive forms of the molecule (39.1% c9,t11 and 40.7% t10,c12 CLA), the reported composition of this preparation included the following trace isomers: 1.8% *cis*-9, *cis*-11 CLA; 1.3% *cis*-10, *cis*-12 CLA; 1.9% *trans*-9, *trans*-11 and *trans*-10, *trans*-12 CLA; and 1.1% *cis*-9, *cis*-12 linoleic acid. Except where noted, all other reagents were purchased from Sigma Chemical (Oakville, Ontario).

4.3 Results

Exposure of 8-day-old cortical neuron cultures to glutamate (0.1-100 μM) for 1 hour reduced neuronal survival 18 hours after treatment in a concentration-dependent fashion, reaching a maximal death rate of 76 ± 12% at 30 μM glutamate (Fig. 16a-c); control neuron death under these conditions was 22 ± 10%. A glutamate concentration of 3 μM (1 hour) was used to test for neuroprotection by CLA since this concentration

yielded significant yet submaximal neuron death revealed by the dose-response curve in Fig. 16c. At 3 μM glutamate, neuron death was not significantly different than control until beyond 8 hr post-glutamate removal. Survival declined rapidly after this, with significant levels of neuron death evident at 12 and 20 hour time points (Fig. 16d). Neuron death in response to 3 μM glutamate was due to excitotoxic NMDA receptor activation as the NMDA receptor antagonist, MK-801, significantly reduced glutamate-induced reduction of cell survival (Fig. 16e). Inclusion of CLA in the glutamate exposure medium (co-treatment) resulted in a significant reduction of glutamate-induced neuron death at both 10 and 30 μM CLA (Fig. 17a). CLA at 30 μM reduced neuron death produced by glutamate from 73.6 ± 6.5% to 31.7 ± 7.2% ($p<0.01$), corresponding to 81% protection. The CLA neuroprotection dose-response curve was bell-shaped as concentrations both lower (3 μM) and higher (100 μM) than the protective range of CLA failed to protect neurons from glutamate excitotoxicity; CLA (30 μM) did not influence cell survival on its own. We next asked whether CLA is capable of protecting cortical neurons from glutamate exposure when introduced to cultures at various points after removal of glutamate (post-treatment). CLA (30 μM) significantly reduced glutamate-induced neuron death when given at 1, 3 and 5 hours after glutamate treatment (Fig. 17b). The protective effect of CLA was maximal 3 hours post-glutamate, reducing neuronal death from 53.6 ± 3.2% to 22.3 ± 5.7% (73.1 ± 13.3% protection; $p<0.01$ compared to glutamate only control). No protection was observed when CLA was administered 8 hours post-glutamate.

Since the CLA used in the current study is comprised mostly of a 1:1 mixture of the two positional isomers known as *cis*-9, *trans*-11 and *trans*-10, *cis*-12 CLA, we tested

both of these component compounds for neuroprotective effects against glutamate excitotoxicity individually at concentrations (15 μM) similar to those found in the mixture (~12 μM each). *cis*-9, *trans*-11 CLA significantly reduced glutamate-induced neuron death (Fig. 18a), while *trans*-10, *cis*-12 CLA had no significant effect on survival. To eliminate the possibility of a non-specific neuroprotective effect of polyunsaturated fatty acids, we examined the ability of linoleic acid (LA) to reverse glutamate excitotoxicity. LA differs from CLA in that the double bonds are unconjugated (*i.e.* separated by two single bonds). Linoleic acid (30 μM) provided no significant protection of neuronal survival against glutamate exposure (Fig. 18b).

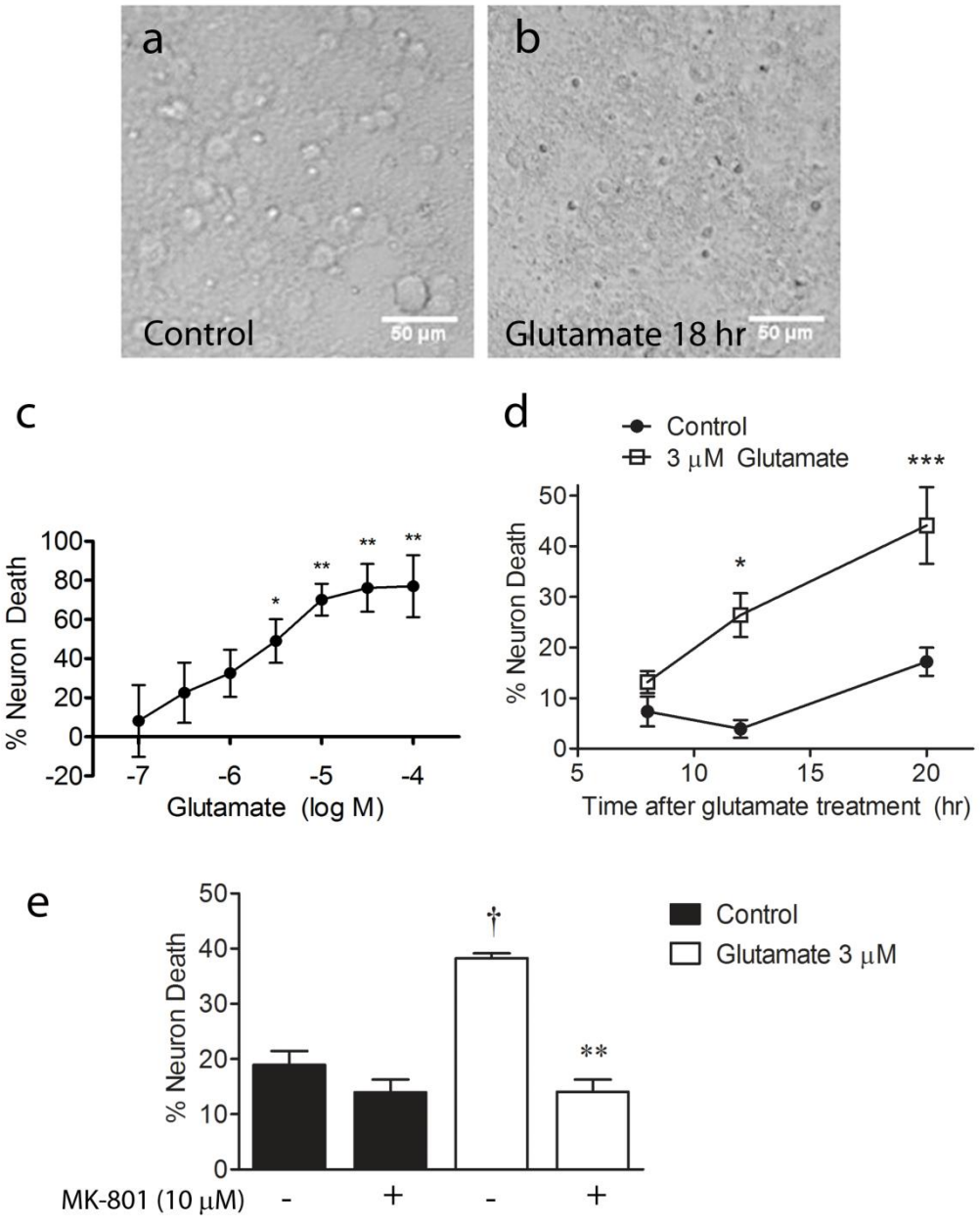

Figure 16. Concentration and time-dependent death of primary cortical neuron cultures by glutamate

Neuron-enriched mouse cortical cultures were exposed to glutamate for 1 hour, and cell death was assayed by quantifying intracellular calcein fluorescence. **a, b**, Phase contrast imaged showing morphological changes in dead and dying neurons (b) compared to

control (a) **c**, Glutamate caused a concentration-dependent reduction in neuron survival 18 hours after exposure. * $p < 0.05$, ** $p < 0.01$ compared with 10^{-7} M glutamate group using one-way analysis of variance (ANOVA) and Dunnett's post-hoc test. **d**, Glutamate (3 μM) reduced survival in a time-dependent manner. * $p < 0.05$, ***$p < 0.001$ compared to control group at the same time point using 2-way ANOVA followed by the Bonferroni post-hoc test. **e**, MK-801 inhibits cell death induced by 3 μM glutamate (1 hr treatment/18 hours later). † $p < 0.05$ compared to control; ** $p < 0.01$ compared to 3 μM glutamate group using 1-way ANOVA and the Student Newman-Keuls test. In all cases, n = 5-7.

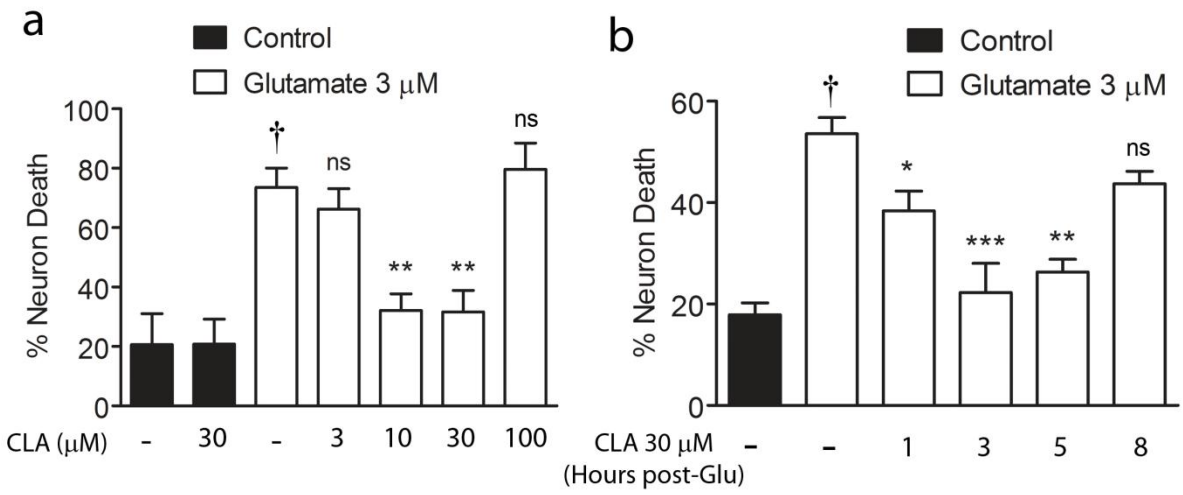

Figure 17. Conjugated Linoleic Acid (CLA) protected neurons from glutamate (Glu) excitotoxicity

A, Mouse cortical neuron cultures were exposed to glutamate with or without CLA for 1 hour, and cell death was assayed by quantifying intracellular calcein fluorescence 18 hours later. Glutamate toxicity (3 μM) was significantly reduced by CLA at 10 and 30 μM but not at 3 and 100 μM. **B**, Cortical neuron cultures were exposed to glutamate (3 μM) for 1 hour. Glutamate was replaced with Neurobasal medium and CLA (30 μM) introduced 1, 3, 5 or 8 hours after glutamate removal. Neuron survival was quantified 18 hours after glutamate removal. Significant neuroprotection was observed at 1 and 3 hours port-glutamate. † $p < 0.01$ compared to control; * $p < 0.05$, ** $p < 0.01$, *** $p < 0.001$, ns $p > 0.05$ compared to control neuron death (3 μM glutamate) using ANOVA with the Student Newman-Keul Test. In all cases, n = 5-7.

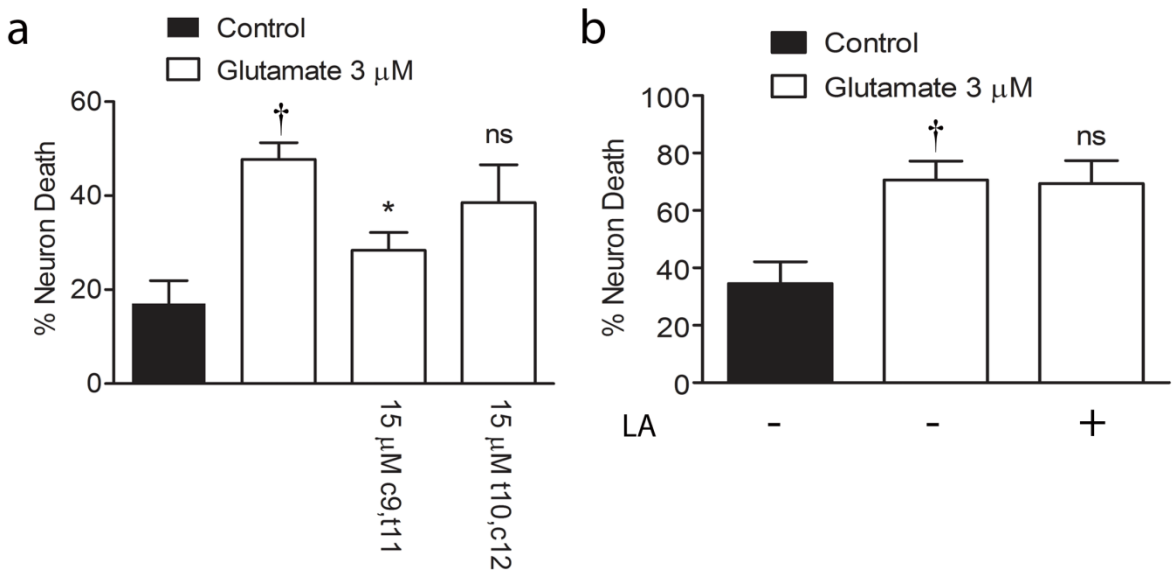

Figure 18. *cis*-9, *trans*-11 CLA is an active neuroprotective CLA isomer

A, *cis*-9, *trans*-11 CLA and *trans*-10, *cis*-12 CLA (15 μM), were co-incubated with glutamate (3 μM) to test for neuroprotective dominance of a single isomer. *cis*-9, *trans*-11 CLA but not *trans*-10, *cis*-9 significantly reduced glutamate-induced neuron death. **B**, Linoleic acid (LA, 30 μM) had no significant effect on neuron survival in glutamate excitotoxicity (3 μM; 1 hour). † $p < 0.01$ compared to control; * $p < 0.05$, ns = $p > 0.05$ compared to control neuron death (glutamate 3 μM) using ANOVA with the Student Newman-Keul Test. In all cases, n = 5-7.

4.4 Discussion

This study demonstrated that CLA protects cultured embryonic cortical neurons from excitotoxic death at concentrations likely attainable by dietary supplementation. Both concurrent CLA/glutamate exposure and CLA exposure up to 5 hours after glutamate treatment significantly protected neurons from excitotoxicity, suggesting potential post-insult pharmacological value for CLA.

CLA was tested for neuroprotective effects in glutamate excitotoxicity previously in a report that found a modest reversal of NMDA receptor-induced neuron death at very high CLA concentrations (500 µM) and no significant protective effect at 100 µM (Joo & Park, 2003). While our observations at these higher CLA concentrations agree with this study, our findings differ by showing more complete neuroprotection at CLA concentrations an order of magnitude lower. In our hands, both 10 and 30 µM CLA reduced neuron death to levels statistically indistinguishable from the control group with no glutamate treatment. The reason for the loss of effect at higher CLA concentrations is not clear but we speculate that it is related to the ability of higher CLA concentrations to reduce protective Bcl-2 expression. This will be explained further in Chapter 5. The finding that lower CLA concentrations (10-30 µM) are capable of neuroprotection in culture is novel and important since these levels are much more likely to be physiologically relevant in humans consuming supplemental CLA. In humans, basal plasma levels of CLA are in the micromolar range (~7 µM) (Herbel, McGuire, McGuire, & Shultz, 1998). Daily supplementation with CLA in healthy male (3.0 g/day) and female (3.9 g/day) volunteers resulted in 3-4-fold increases in plasma CLA over this baseline (Doyle, et al., 2005), and local tissue concentrations easily reach levels 10-fold greater

than plasma concentrations, or up to 200-300 µM (Lai, Torres-Duarte, & Vanderhoek, 2005; Miller, Stanton, & Devery, 2002). Since CLA is taken up by the CNS and present in brain tissue at approximately one fifth the tissue content of adipose tissue in at least one study (Fa, et al., 2005), brain CLA concentrations may be as high as 30-50 µM and thus, our experimental concentrations of CLA (10 and 30 µM) are likely physiologically attainable and relevant. It should be noted that a complete analysis of brain CLA isomer content remains to be performed and it is not clear how different CLA supplement regimens might affect brain CLA content.

Most pharmacological effects of CLA, including those in the present study, have been demonstrated using a mixture of positional and geometric CLA isomers with the main constituents being roughly equal proportions of *cis*-9, *trans*-11-CLA and *trans*-10, *cis*-12-CLA (~40% each). However, there are also reports of disparate pharmacological effects of different isomers (Evans, et al., 2000; Martin & Valeille, 2002; Nagao, et al., 2003; Ryder, et al., 2001). We thus tested whether the neuroprotective effects of CLA in excitotoxicity are mediated by one or both major individual constituent isomers. We found that *cis*-9, *trans*-11 CLA but not *trans*-10, *cis*-12 CLA significantly protected neurons from glutamate-induced death. This is consistent with the cardiovascular disease and metabolic syndrome literature, which reports that *cis*-9, *trans*-11 CLA reduces triglycerides, increases high-density lipoprotein cholesterol, attenuates insulin resistance, and reduces inflammatory response (Lopes, et al., 2008; Moloney, et al., 2007; Nestel, Fujii, & Allen, 2006; Qin, Liu, Lu, Li, & Sun, 2009; Roche, et al., 2002). In contrast, *trans*-10, *cis*-12 CLA increases plasma glucose, triglycerides and LDL:HDL while promoting insulin resistance and enhancing inflammation (Navarro, et al., 2010;

Tholstrup, et al., 2008). More work is needed to elucidate the signaling mechanisms of *cis*-9, *trans*-11 CLA in neurons, but it is encouraging that the neuroprotective effects appear to be conferred by the same isomeric species that is beneficial in other disease states and not by the species that has been demonstrated to have deleterious effects on lipid metabolism and cardiovascular health. We cannot rule out the possibility that a minor isomeric component/s of our commercial CLA preparation is responsible for the neuroprotective effects observed; however, this is unlikely since additional components are present only in trace amounts (<2% total CLA), and thus would have to be extremely potent to produce the magnitude of neuroprotection we observed at 10 and 30 μM CLA. Furthermore, none of the minor CLA isomers have demonstrated significant biological activity to date. Alternatively, the neuroprotective effects of the mixed CLA isomers are more robust than the neuroprotective effects of *cis*-9, *trans*-11 CLA, leaving open the possibility that isomer combinations are required for maximal neuroprotective effect.

Our study demonstrates that a physiologically relevant concentration of CLA protects mouse cortical neurons against glutamate excitotoxicity. These findings provide novel support for the role of this polyunsaturated fatty acid as a functional food or nutraceutical supplement with protective effects against cerebral ischemia and raise the possibility that dietary supplements may produce brain CLA levels sufficient to provide baseline neuroprotection from stroke.

[4]Chapter 5: CLA preserves mitochondrial function and anti-apoptotic balance in neuronal excitotoxicity

[4] Reprinted and adapted with permission by John Wiley and Sons from Hunt WT, Anderson, HD and Anderson CM. (2010) *Protection of cortical neurons from excitotoxicity by treatment with conjugated linoleic acid after glutamate exposure.* J Neurochem. 115(1):123-30. Copyright 2010 by John Wiley and Sons.

5.1 Introduction and Rationale

We made the novel observation that CLA provides impressive neuroprotection in an *in vitro* mouse model of glutamate excitotoxicity (described in Chapter 4), but the mechanism of CLA neuroprotection is unknown. The purpose of this chapter is to use information about CLA signaling in non-CNS tissue/cells to investigate possible neuroprotective mechanisms in brain.

CLA signaling in several tissues involves direct activation of peroxisome proliferator-activated receptors (PPARs) (Alibin, et al., 2008; Moya-Camarena & Belury, 1999; Moya-Camarena, et al., 1999). PPARs belong to a nuclear receptor family of transcription factors that are best known for their ability to regulate fatty acid and triglyceride metabolism (Lemberger, et al., 1996). In brain, PPAR agonists such as the natural ligand 15-deoxy-Δ-12,14-prostaglandin J2 (15d-PGJ2) (Garcia-Bueno, et al., 2007; X. Zhao, et al., 2006) and PPARγ-selective agonists, rosiglitazone (Garcia-Bueno, et al., 2007), ciglitazone (X. Zhao, et al., 2006), and troglitazone (Uryu, et al., 2002) also protect against glutamate excitotoxicity in both cultured neurons and *in vivo*. While CLA-PPAR signaling has not yet been reported in neurons, increased expression of Bcl-2 has been linked to PPARγ activation and neuroprotection (Fuenzalida, et al., 2007). Increased Bcl-2 expression is protective against numerous excitotoxic stimuli (Soane & Fiskum, 2005) by promoting mitochondrial stabilization (Fuenzalida, et al., 2007). Therefore, we hypothesized that CLA is neuroprotective in glutamate excitotoxicity by activating PPARγ mediated expression of Bcl-2 and mitochondrial stabilization. Moreover, since AIF is released from mitochondria with loss of mitochondrial membrane potential and

subsequent permeablization, we further hypothesized that AIF levels would be reduced in the presence of CLA.

5.2 Materials and Methods

5.2.1 Neuron cultures

Neuron cultures were prepared from embryonic day 16 CD-1 mouse cortices in accordance with guidelines set forth by the *Canadian Council on Animal Care*. Cultures were plated on poly-D-lysine coated plastic at $2.5x10^5$ cells/cm^2 in Neurobasal medium (NB) with B27 supplement (Invitrogen, Carlsbad, CA), 1.2 mM glutamine, and 5% Fetal Bovine Serum (FBS; Hyclone, Logan, UT). The following day (day 1), media was changed to NB with B27 and glutamine. Cytosine arabinofuranoside (2 µM) was added on day 2 to prevent glial proliferation, and replaced on day 3 with NB/B27/glutamine. Cultures were maintained at 37°C/5% CO_2, and given a partial media change of day 6. Cultures were used on day 8 post-culture for all experiments and contained less than 2% glial fibrillary acidic protein immunopositive astrocytes.

5.2.2 Assessment of neuron death

Neurons were treated with glutamate in NB for 1 hour in the presence of CLA or Benzyloxycarbonyl-Asp(OMe)-Glu(OMe)-Val-Asp(OMe)-fluormethylketone (Z-DEVD-FMK) (10 µM), followed by incubation for 18 h with Z-DEVD-FMK (10 µM) alone.

Media in control wells was changed to neurobasal medium and cell survival measured 18 hours later. Live cells were quantified by assessing intracellular calcein acetoxymethelester (calcein/AM; Roche, Eugene, OR) fluorescence using a Gemini Spectromax fluorescence plate reader with excitation at 485 nm and emission at 530 nm. Results were normalized to a range between a 0% survival control (1 mM glutamate, 18 hours) and 100% survival (NB control).

5.2.3 Western blot

Cytoplasmic fractions were prepared after treatments by removing media, rinsing each well with cold-PBS pH 7.4, and then collecting cells by gentle scraping in cold PBS. Cells were centrifuged at 300 x g for 5 minutes and supernatant was expelled. Pellet was re-suspended in cold STE Buffer and put through a series of freeze/thaw cycles using liquid N_2, in order to ensure cell lysis of outer-membrane. Next, cells were centrifuged at 20,800 x g for 15 minutes to ensure all cellular contents, besides the cytoplasmic fraction, would pellet. Supernatant contained the cytoplasmic fraction. However, confirmation was obtained by collecting and re-suspending the pellet containing the mitochondrial fraction in lysis buffer (2% SDS, 50mM TRIS, with protease inhibitor cocktail pH 7.4) and performing western blots with both fractions collected using cytochrome c oxidase Antibody, COX IV (Cell Signaling Technology, Pickering, ON #4844), according to the method previously described. Protein concentrations were determined using a BCA kit and samples prepared for quantification of cytoplasmic AIF. Homogenates (10 µg) were separated on 12% polyacrylamide gels and transferred to PVDF membranes. Membranes

were exposed overnight (4°C) to a mouse monoclonal anti-Bcl-2 (Santa Cruz Biotechnology, sc-7382, 1:100) or rabbit polyclonal anti-AIF (Cell Signaling Technology, #4642, 1:1000), washed and then exposed for 1 hour (room temperature) to a horse-radish peroxidase linked anti-mouse/rabbit IgG (1:2000). Again, membranes were washed and the ECL Plus chemiluminescence kit was used to visualize immunoreactive bands with a Fluor-STM MultiImager (Bio-Rad). Membranes were probed with a mouse monoclonal anti-β-actin antibody (Sigma-Aldrich, A5441), used for a loading control.

5.2.4 Mitochondrial membrane potential imaging

The fluorescent probe 5,5′,6,6′-tetrachloro-1,1′,3,3′ tetraethylbenzimidazolylcarbo-cyanine iodide (JC-1) was used to investigate mitochondrial membrane potential ($\Delta\Psi_m$) in primary neurons. Cells were loaded with JC-1 for 30 min at 37°C as per manufacturer's protocol, and images were acquired using a Zeiss LSM-510 confocal microscope. Samples were excited at 488 nm for monomer fluorescence and 540 nm for JC-1 aggregate fluorescence. Emission fluorescence images were recorded at 530 nm for monomer and 590 nm for JC-1 aggregates. The ratio of the aggregate to monomer fluorescence was measured as an index of changes in $\Delta\Psi_m$. Mitochondrial membrane depolarization was indicated by a reduction in the red/green fluorescence-intensity ratio. The JC-1 fluorescence ratio between red and green was normalized to the control ratio. Each experimental group was repeated in duplicate or triplicate wells per plate and averaged to give a single value per experiment.

5.2.5 Materials

The mixed CLA used in our experiments (Nu-Chek Prep, Inc, Elysian, MN) contained ~80% *cis*-9, *trans*-11 and *trans*-10, *cis*-12 CLA at an approximate 1:1 ratio as well as trace amounts of other isomers. In addition to the putatively bioactive forms of the molecule (39.1% c9,t11 and 40.7% t10,c12 CLA), the reported composition of this preparation included the following trace isomers: 1.8% *cis*-9, *cis*-11 CLA; 1.3% *cis*-10, *cis*-12 CLA; 1.9% *trans*-9, *trans*-11 and *trans*-10, *trans*-12 CLA; and 1.1% *cis*-9, *cis*-12 linoleic acid. Benzyloxycarbonyl-Asp(OMe)-Glu(OMe)-Val-Asp(OMe)-fluormethylketone (Z-DEVD-FMK) was purchased from Tocris bioscience (Ellisville, Missouri). Protein inhibitor cocktail tablets and BCA protein assay kits were purchased from Roche Diagnostics (Mannheim, Germany) and Pierce (Rockford, Illinois), respectively. Amersham ECL kits were purchased from GE Life Sciences (Piscataway, New Jersey). JC-1 was purchased from the Cayman Chemical Company (Ann Arbor, Michigan). Except where noted, all other reagents were purchased from Sigma Chemical (Oakville, Ontario).

5.3 Results

To investigate the mechanism of CLA neuroprotection in glutamate toxicity, we first assessed the mechanism of low dose (3 μM) glutamate mediated neuron death using the pan-caspase inhibitor, Z-DEVD-FMK. The purpose of this was to provide clues as to whether excitotoxic apoptotic death followed the intrinsic or extrinsic paths (discussed in

section 1.3.1). Z-DEVD-FMK had no significant effect on the level of glutamate-induced neuron death (Fig. 19A), indicating our glutamate excitotoxicity paradigm causes caspase-independent neuron death. Accordingly, we hypothesized that reduced cell survival is associated with mitochondrial release of AIF. This was confirmed by our observation that glutamate (3 μM) increased cytosolic AIF levels (Fig. 19B). Based on these observations we decided to investigate events upstream of AIF translocation, including changes in mitochondrial membrane potential and expression of anti-apoptotic Bcl-2 family members (S. W. Yu, et al., 2002).

We first examined expression of Bcl-2, an anti-apoptotic factor that stabilizes mitochondrial membrane potential and limits release of pro-death factors such as cytochrome c and apoptosis-inducing factor (for review, see (Brenner & Mak, 2009)). Individually, neither glutamate nor CLA affected Bcl-2 p26 expression after 6 hours (Fig. 20a); however, when CLA was combined with our 1 hour glutamate treatment paradigm, a 2-fold increase in Bcl-2 expression 6 hours after glutamate exposure resulted (Fig. 20b). In agreement, dissipation of mitochondrial membrane potential by glutamate was restricted by CLA, as indicated by ratiometric imaging of cultures using the dye, JC-1. Representative photographs show that the ratio of mitochondrial JC-1 aggregate (red) to cytosolic JC-1 monomer (green) was reduced 8 hours after glutamate treatment (Fig. 21e, f) compared to the healthy control cultures (Fig. 21a, b). This decline was reversed by CLA (Fig. 21e, f), and CLA by itself had no significant effect (Fig. 21c, d). The sum of these data are presented in Fig. 21i.

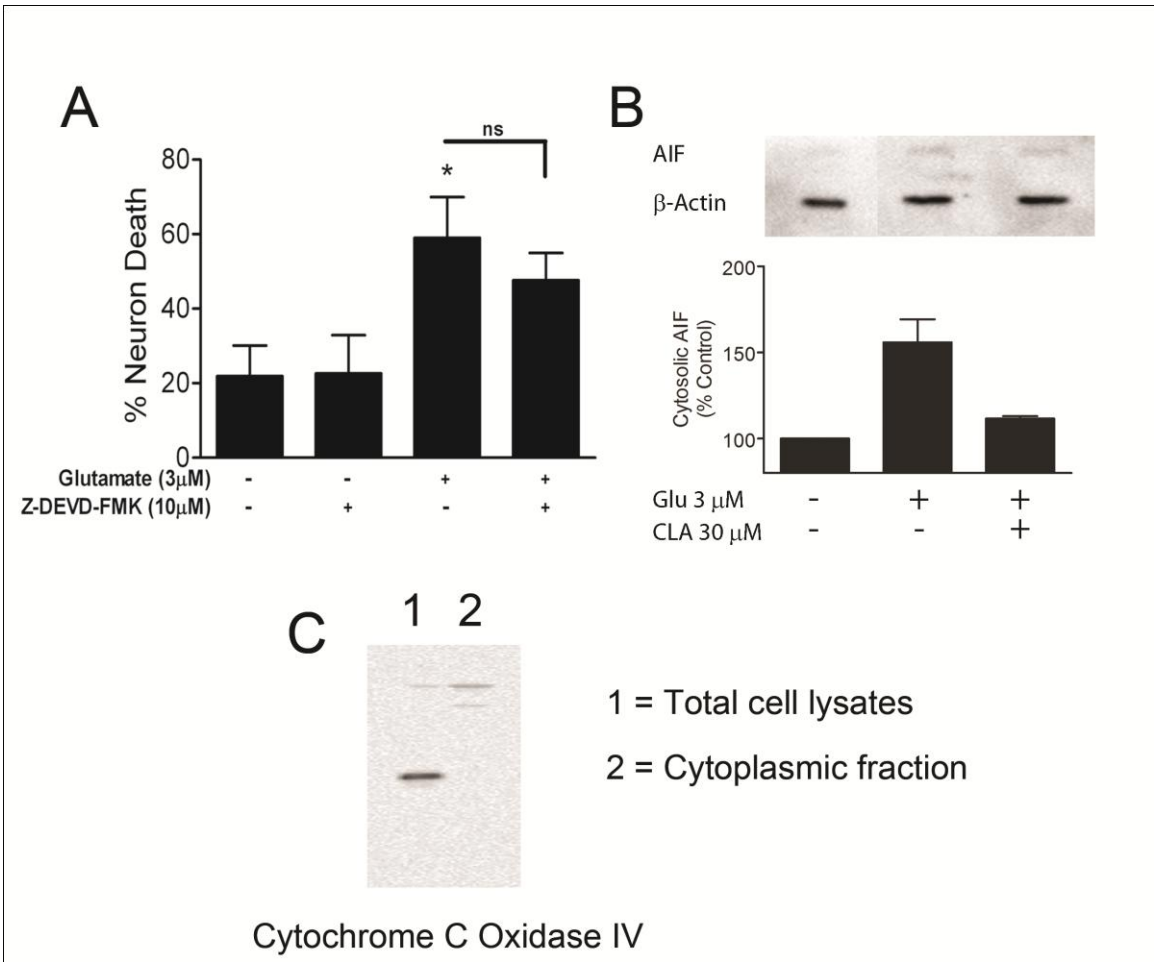

Figure 19. Glutamate (3 μM) mediated death is not caspase dependent

(A) Mouse-cortical neurons were co-treated with Benzyloxycarbonyl-Asp(OMe)-Glu(OMe)-Val-Asp(OMe)-fluormethylketone (Z-DEVD-FMK) (10 μM) and glutamate (3 μM) for 1 hour, followed by incubation for 18 h with Z-DEVD-FMK (10 μM) alone. Cell death was assayed by quantifying intracellular calcein fluorescence retained in live cells as compared with controls. No significant differences were observed between the glutamate (3 μM) neurons and those treated with Z-DEVD-FMK, using ANOVA and Tukey's Test. n = 8. (B) **CLA blocks glutamate induced increases in AIF.** CLA (30 μM) was co-incubated with glutamate (3 μM) for 60 min, and cell homogenates were prepared for western blot 6 hours later with antibodies for AIF and β-actin. A

representative blot showing the relative expression levels of AIF and β-actin in each experimental condition is shown and represents the cumulative result of 3 sample replicates. CLA significantly reduced the AIF/actin ratio in the presence of glutamate. * $p < 0.05$ compared to glutamate/0 CLA, using ANOVA with the Student Newman-Keul Test. (C) **Separation of cytoplasmic fraction from total cell lysates.** Cell homogenates were prepared and cytoplasmic fraction collected as previously described. A representative blot showing the relative expression levels of Cox IV in the total cell lysates compared to the cytoplasmic fraction confirm no mitochondrial contaminants.

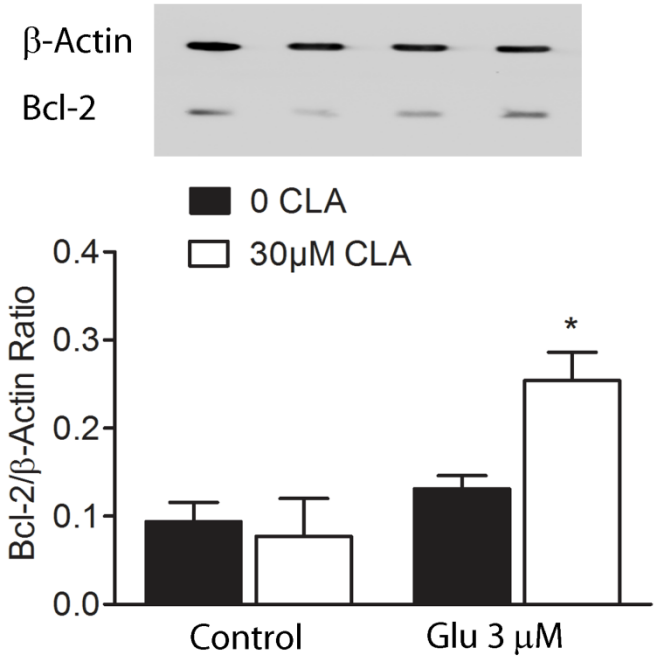

Figure 20. CLA enhances neuronal Bcl-2 levels

CLA (30 μM) was co-incubated with glutamate (3 μM) for 60 min, and cell homogenates were prepared for western blot 6 hours later with antibodies for Bcl-2 p26 and β-actin. A representative blot is shown to indicate the relative expression levels of Bcl-2 and β-actin in each experimental conditions. The plot below represents the cumulative results of 4 sample replicates. CLA significantly increased the Bcl-2/actin ratio in the presence of glutamate. * $p < 0.05$ compared to glutamate/0 CLA, using ANOVA with the Student Newman-Keul Test. In all cases, n = 5-7.

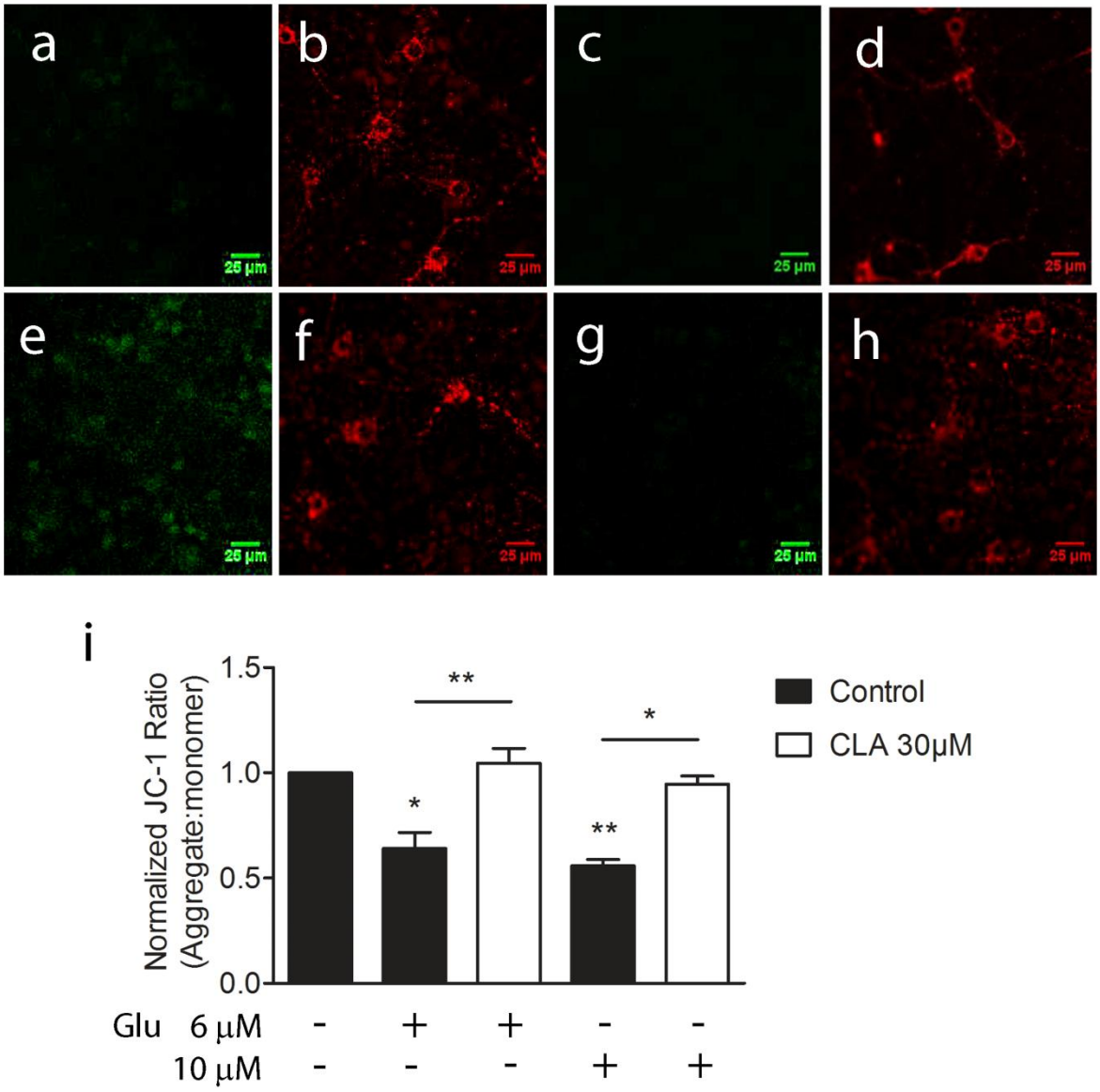

Figure 21. CLA reverses glutamate-induced mitochondrial membrane depolarization

CLA (30 µM) was incubated alone or with glutamate (6 or 10 µM) for 60 min, and cells were loaded with the dye JC-1 8 hours later. The ratio of JC-1 aggregate (red) to JC-1 monomer (green) was assessed. Untreated cells (a, b) and cells treated with 30 µM CLA only (c, d) are characterized by healthy mitochondria indicated by JC-1 aggregate fluorescence. Treatment with glutamate (e, f) increased monomer fluorescence, while

CLA co-treatment (g, h) reversed this trend. **i**, Cumulative data expressing 4 sample replicates indicate that CLA significantly protects mitochondrial membrane potential from glutamate-induced dissipation at 8 hours. * $p < 0.05$, ** $p < 0.01$ compared to control or as indicated using ANOVA with the Student Newman-Keul Test.

5.4 Discussion

This study suggests that CLA protects cultured embryonic cortical neurons from excitotoxic death by protecting mitochondrial integrity. CLA enhanced Bcl-2 levels and stabilized mitochondrial membrane potential, suggesting that it blocks death pathways resulting from enhanced mitochondrial permeability. There are three lines of evidence that CLA stabilizes mitochondrial function. First, CLA roughly doubles Bcl-2 levels when given to glutamate-treated cultures, compared to glutamate treatment alone. Mitochondrial membrane integrity is maintained by a balance between antiapoptotic Bcl-2 family members (Bcl-2 and Bcl-xl) and proapoptotic members like Bax and Bid; thus, CLA-induced enhancement of Bcl-2 levels is likely protective. CLA activates PPARs resulting in neuroprotective effects (Kapadia, Yi, & Vemuganti, 2008; Y. Zhao, Patzer, Herdegen, Gohlke, & Culman, 2006), and there is evidence that PPARs are neuroprotective by enhancing neuronal Bcl-2 levels in brain ischemia characterized by elevated glutamate levels (Fuenzalida, et al., 2007). Thus, mechanistically our data are consistent with an activator effect of CLA at PPARs, although we did not determine whether neuroprotection by CLA is dependent on PPARs directly; this is a logical future direction. While our finding is supportive of the conclusion that CLA protects from excitotoxicity by enhancing Bcl-2 expression, our results are complex. One might expect that glutamate would reduce Bcl-2 expression on its own, that CLA would increase Bcl-2 expression on its own and that CLA would reverse glutamate-induced downregulation in combination. In fact, we found no significant effect of CLA or glutamate on Bcl-2 expression. We speculate that the lack of glutamate effect is related to the relatively low glutamate concentration we are using as other groups report that glutamate concentrations

at least an order of magnitude higher are required to reduce Bcl-2 expression (Montpied, Weller, & Paul, 1993). Despite no indication of changes in Bcl-2 expression with either glutamate or CLA alone, the combination of CLA and glutamate in our hands produced a significant increase in Bcl-2 expression, consistent with a protective effect of CLA on Bcl-2 only when glutamate is present. Interestingly, the literature suggests the same bell-shaped dose-response for the effect of CLA on Bcl-2 that we observed for neuroprotection. Concentrations of CLA consistent with those showing reduced neuroprotective effects in our hands ($\geq$ 100 μM) have been shown to reduce Bcl-2 expression (Ochoa, et al., 2004).

The second line of evidence for CLA-induced mitochondrial stabilization is a direct demonstration of mitochondrial membrane potential preservation by CLA from JC-1 imaging experiments showing that glutamate-induced expulsion of positively-charged dye aggregates to yield cytosolic monomers was reduced by CLA. This is the first demonstration of an effect of CLA on mitochondrial membrane potential. From these experiments we cannot conclude whether CLA-induced Bcl-2 enhancement is required for mitochondrial protection. However, it is noteworthy that unlike its lack of effect on Bcl-2 expression alone, glutamate in this case, does depolarize mitochondrial membranes on its own. Thus, it is likely that the effect of Bcl-2 is not the only factor acting to influence membrane potential. One possibility is that glutamate up-regulates pro-apoptotic factors such as Bax, Bad, and BNIP3 as shown previously (Kim, Chang, Chen, Rapoport, & Rao, 2009; Z. Zhang, et al., 2011), tipping the balance toward apoptosis, while CLA counters these factors with increased expression of Bcl-2.

The third piece of evidence that CLA stabilizes mitochondrial membrane potential is that CLA reduced glutamate-induced increases in AIF. AIF is a pro-death factor that mediates nuclear condensation and programmed cell death. We found that AIF is released from the mitochondria and likely mediates glutamate-induced neuron death in our *in vitro* model of excitotoxicity. AIF is released into the cytosol from the mitochondria upon depolarization and permeabilization (S. W. Yu, Wang, Dawson, & Dawson, 2003), thus retention of mitochondrial AIF (inferred by decreased cytosolic levels) indicates that CLA protected mitochondrial structural integrity and function.

Overall, we made important novel discoveries showing that CLA stabilizes mitochondrial function in neurons. Our model was based on glutamate excitotoxicity. However mitochondrial dysfunction is a common underlying occurrence in the deleterious cascade of events that underpins nearly all neurodegenerative disorders. Thus CLA has broad therapeutic potential.

Chapter 6: General Discussion

6.1 Summary of Findings

The overall focus of the works presented in this thesis was to identify novel neuroprotective pathways in neurodegeneration. Neurodegenerative disorders are becoming increasingly prevalent in our society. As we follow the demographic shift of the "babyboom" generation, we will continue to see a dramatic rise in the number of people who are diagnosed with neurodegenerative disorders. The Alzheimer Society of Canada predicts the number of people diagnosed with Alzheimer's disease to double over the next 25 years (The Alzheimer Society of Canada, 2011).

PARP-1 is important in excitotoxicity and we hypothesized that it is also important in Aβ-induced neuron death, seeking to identify a unifying mechanistic role for PARP-1 in multiple brain disorders that would accentuate the importance of new PARP-1-based therapeutics. We were surprised to find a limited role for PARP-1 in Aβ-induced death. The likely reason for this is that PARP-2 offers redundant and compensatory ADP-ribosylation or that PARP-1 plays no role at all. This is an important finding, as a large portion of the literature makes the assumption that non-selective inhibitors of PARP-1/2 are protective in various models by inhibiting PARP-1. While there are certain cases where both PARP inhibitors and selective PARP-1 deletion are protective, our data show that reducing activity of both PARP-1 and PARP-2 may be required in some neurodegeneration models. This is supported by other observations in our lab showing that PARP-2 is critical for development of neurological signs of experimental allergic encephalomyelitis (EAE) in mice (Kamboj et al., in preparation).

Our interest in PARP-1 extended beyond its role in Aβ toxicity to its role in cellular bioenergetic decline. It has long been reported in fibroblasts (Herceg & Wang, 1999) and other non-neuronal cells that pathological PARP activation causes NAD^+ depletion due to excessive NAD^+-dependent ADP-ribosylation, but the nature of this depletion had not been characterized in neurons or astrocytes, and it was unclear whether cells die of simple starvation, as was largely assumed until about 5 years ago, or whether substrate depletion leads to mitochondrial-mediated cell suicide. Since NAD^+ and ATP are the primary adenine nucleotides of interest in energy metabolism, one of our goals was to define the temporal relationship between declines in NAD^+ and ATP levels, as well as the extent of depletion and recovery of each. We developed 2 HPLC methods that allow detection of NAD^+ and ATP, as well as ADP and AMP simultaneously in the same sample. We used direct PARP activation by DNA alkylation in astrocytes, which suffer PARP-mediated toxicity, as a model and reported for the first time a comprehensive description of the time-line and severity of declines of each adenine nucleotide. We also confirmed loss of the total adenine nucleotide pool, thus differentiating PARP-induced bioenergetic depletion from bioenergetic depletion in brain ischemia or hypoxia, which is characterized by ATP loss and concomitant increases in AMP levels and activation of AMP Kinase. These results provided novel nucleotide separation techniques valuable for PARP research and a critical baseline description of PARP-induced adenine nucleotide depletion in neural cells. These results were an integral part of a published manuscript (Tang, et al., 2010) showing that PARP-induced bioenergetic depletion severely inhibits glutamate uptake capacity by astrocytes.

Our results from Chapter 3, looking at PARP-induced changes in astrocyte bioenergetics and survival, also provide preliminary data that would fuel the remainder of my thesis work. CLA prevented a portion of astrocyte death induced by PARP activation. Since PARP is activated in glutamate neurotoxicity, this prompted the hypothesis that CLA protects neurons from simulated stroke. This observation that CLA protected astrocytes from PARP toxicity, coupled with the lack of neuroprotection by the PARP-$1^{-/-}$ genotype in Aβ toxicity, precipitated a change in direction away from PARP for this thesis. Now focus was placed on the exciting idea that CLA, which humans can ingest in dietary or supplement form, might be neuroprotective in glutamate excitotoxicity. We made the important discovery that CLA was able to rescue cultured neurons from glutamate induced death, even when given up to 5 hours after removal of the glutamate injury, at levels likely achievable in humans by taking available supplements. We also characterized the mechanistic nature of CLA neuroprotection (Chapter 5), showing that CLA increases Bcl-2 expression and stabilizes mitochondrial membrane potential. All of these are novel observations that kindle interest in CLA as a therapeutic for human brain injury and neurodegeneration characterized by excitotoxicity, including stroke, trauma, ALS, Alzheimer's disease, Huntington's etc.

Our findings suggest that CLA may hold potential as a therapeutic for neurodegeneration and stroke for many reasons. First, delivery of a therapeutic to the tissue of interest is of paramount importance for its efficacy and has posed a major hurdle for drug makers investigating novel CNS drugs. CLA crosses the blood brain barrier and is metabolized in the brain, allowing for the possibility that local concentrations of CLA could reach between 30 μM and 50 μM (Fa, et al., 2005), which is similar to where we

observed therapeutic benefit in our in vitro model. Second, therapeutics currently available for treatment of stroke and Alzheimer's disease either show limited clinical benefits or are plagued by a myriad of adverse effects. For example, tissue plasminogen activator (TPA) which is used to treat acute ischemic stroke, has a narrow therapeutic window and thus has been useful in less than 5% of candidate patients (Armstead, et al., 2010). Similarly, memantine is the only drug approved for moderate to advanced stages of AD but is not effective in all patients, produces only modest beneficial effects in patients in whom it is efficacious and is associated (Osborn & Saunders, 2010) and has numerous adverse effects that may limit its use. These examples underscore the need for novel safe and effective therapies. CLA is ingested naturally as part of a balanced diet or taken in pharmacological doses as a dietary supplement for weight loss and has proven to be well tolerated with minor gasterointestinal disturbances as the most common complaint. Given our recent results, it is tempting to speculate that CLA already on the market could be a useful alternative treatment for neurodegenerative disorders. Though this story is in its early stages, with substantially more animal work required for proof of concept and progression to other pre-clinical models, the prospects of CLA offering beneficial effects against several disorders looks promising. One issue that will be critical will be determining which mix of CLA isomers offers the most beneficial effects. There are reports that the two most abundant isomers, cis9, trans11 and trans10, cis12 CLA have opposite effects in several systems and that they therefore have functionally-antagonistic effects when administered together (Tricon, et al., 2004). Our results suggest that cis9, trans11 CLA may be the neuroprotective isomer, suggesting that supplementation of this isomer may be more beneficial than the standard isomeric

mixture. Again, more studies are required to establish isomeric differences. Another critical issue will be dosing; the question to be addressed is whether dietary CLA is sufficient to provide salutary effects against neurodegeneration, or whether large pharmacological doses obtained through supplementation are required. Lastly, in the case of stroke research, it is important to remember that although our post-injury administration paradigm produced significant neuroprotection with CLA, we must juxtapose these findings with the reality that many promising therapeutics have proven ineffective in humans despite showing promise in animal models (Jonas, Aiyagari, Vieira, & Figueroa, 2001). Performance of meta-analysis based on other human clinical trials with CLA in other organ systems may provide insight into putative benefits of CLA in the CNS. However, clinical trials with CLA in brain disorders are necessary to provide more clarity and ultimately, dictate whether our observed *in vitro* benefits will translate to benefits in humans.

6.2 Future Directions

With regard to our experiments focused on PARP-1, we implicated other mediators of amyloid-β induced neuron death. One such mediator is PARP-2 which has been shown to offer compensatory ADP-ribosylation in PARP-$1^{-/-}$ models (Kamboj et al., in preparation). We hypothesize that PARP-2 is compensating for loss of PARP-1 and thus future studies may be performed employing inducible double knockouts for PARP-1 and PARP-2 since deletion of both is embryonic lethal. By inducing the double knockout upon exposure to amyoid-β insult, we expect to see neuroprotection.

With regard to our work with CLA, future studies could focus on PPAR signaling to provide further evidence for the mechanisms underlying protection. We hypothesize that CLA is signaling through PPARγ and thus, increasing expression of Bcl-2. This signaling mechanism has been shown to be responsible for Bcl-2 up-regulation by rosaglitazone (Fuenzalida, et al., 2007). Electrophoretic mobility shift assays (EMSA) for PPARγ binding by CLA could be performed in order to test this hypothesis. In addition, post-transcriptional gene silencing using shRNA/RNAi may be used to knock-down expression of PPARs and provide insight into CLA signaling.

Animal feeding studies may also provide further evidence of beneficial effects of CLA in neurodegeneration or stroke. As the natural next phase, establishing a *proof of concept* for the efficacy of CLA in an animal model would provide momentum for the further study of CLA in humans. This may be achieved by examining the effects of CLA on histological markers of neurodegeneration. Based on PPAR protection in AD models (d'Abramo, Ricciarelli, Pronzato, & Davies, 2006; Heneka & O'Banion, 2007), we hypothesize that CLA will positively impact mouse models of cognitive impairment by reducing the plaque formation and possibly by reducing infarct volumes in mouse models of Alzheimer's disease and stroke, respectively. To test this hypothesis, we could compare immunohistochemistry staining for markers of neurodegeneration such as plaque formation between a mouse model of Alzheimer's disease and wild-type mice, while feeding them therapeutic doses of CLA. Analysis at various time-points while the animals age may provide evidence of a beneficial effect over time while also providing insight into possible preventative benefits of taking CLA regularly. In the stroke model, middle cerebral artery occlusion (MCAO) may be performed in CLA fed vs. non-fed

animals or even post-MCAO administration of CLA to look for post-treatment protection from cell death. This would further substantiate our initial findings of post-treatment protection (Hunt, Kamboj, Anderson, & Anderson, 2010). Feeding studies have been performed in other disease models with CLA such as atherosclerosis and have even shown translational benefits in humans (Bhattacharya, et al., 2006).

References

Akahoshi, A., Goto, Y., Murao, K., Miyazaki, T., Yamasaki, M., Nonaka, M., et al. (2002). Conjugated linoleic acid reduces body fats and cytokine levels of mice. *Biosci Biotechnol Biochem, 66*(4), 916-920.

Alano, C. C., Garnier, P., Ying, W., Higashi, Y., Kauppinen, T. M., & Swanson, R. A. (2010). NAD+ depletion is necessary and sufficient for poly(ADP-ribose) polymerase-1-mediated neuronal death. *J Neurosci, 30*(8), 2967-2978.

Alano, C. C., Tran, A., Tao, R., Ying, W., Karliner, J. S., & Swanson, R. A. (2007). Differences among cell types in NAD(+) compartmentalization: a comparison of neurons, astrocytes, and cardiac myocytes. *J Neurosci Res, 85*(15), 3378-3385.

Alibin, C. P., Kopilas, M. A., & Anderson, H. D. (2008). Suppression of cardiac myocyte hypertrophy by conjugated linoleic acid: role of peroxisome proliferator-activated receptors alpha and gamma. *J Biol Chem, 283*(16), 10707-10715.

Ame, J. C., Spenlehauer, C., & de Murcia, G. (2004). The PARP superfamily. *Bioessays, 26*(8), 882-893.

Anderson, C. M., Norquist, B. A., Vesce, S., Nicholls, D. G., Soine, W. H., Duan, S., et al. (2002). Barbiturates induce mitochondrial depolarization and potentiate excitotoxic neuronal death. *J Neurosci, 22*(21), 9203-9209.

Anderson, C. M., & Swanson, R. A. (2000). Astrocyte glutamate transport: review of properties, regulation, and physiological functions. *Glia, 32*(1), 1-14.

Arbones-Mainar, J. M., Navarro, M. A., Guzman, M. A., Arnal, C., Surra, J. C., Acin, S., et al. (2006). Selective effect of conjugated linoleic acid isomers on atherosclerotic lesion development in apolipoprotein E knockout mice. *Atherosclerosis, 189*(2), 318-327.

Armstead, W. M., Ganguly, K., Kiessling, J. W., Riley, J., Chen, X. H., Smith, D. H., et al. (2010). Signaling, delivery and age as emerging issues in the benefit/risk ratio outcome of tPA For treatment of CNS ischemic disorders. *J Neurochem, 113*(2), 303-312.

Arundine, M., & Tymianski, M. (2003). Molecular mechanisms of calcium-dependent neurodegeneration in excitotoxicity. *Cell Calcium, 34*(4-5), 325-337.

Balazs, R. (2006). Trophic effect of glutamate. *Curr Top Med Chem, 6*(10), 961-968.

Bauman, D. E., Baumgard, L. H., Corl, B. A., & Griinari, J. M. (2000). Biosynthesis of conjugated linoleic acid in ruminants. *Journal of Animal Science, 77*, 1-15.

Beal, M. F. (1995). Aging, energy, and oxidative stress in neurodegenerative diseases. *Ann Neurol, 38*(3), 357-366.

Benveniste, H., Drejer, J., Schousboe, A., & Diemer, N. H. (1984). Elevation of the extracellular concentrations of glutamate and aspartate in rat hippocampus during transient cerebral ischemia monitored by intracerebral microdialysis. *J Neurochem, 43*(5), 1369-1374.

Bezprozvanny, I., & Mattson, M. P. (2008). Neuronal calcium mishandling and the pathogenesis of Alzheimer's disease. *Trends Neurosci, 31*(9), 454-463.

Bhattacharya, A., Banu, J., Rahman, M., Causey, J., & Fernandes, G. (2006). Biological effects of conjugated linoleic acids in health and disease. *J Nutr Biochem, 17*(12), 789-810.

Blazquez, C., Woods, A., de Ceballos, M. L., Carling, D., & Guzman, M. (1999). The AMP-activated protein kinase is involved in the regulation of ketone body production by astrocytes. *J Neurochem, 73*(4), 1674-1682.

Bliss, T. V., & Gardner-Medwin, A. R. (1973). Long-lasting potentiation of synaptic transmission in the dentate area of the unanaestetized rabbit following stimulation of the perforant path. *J Physiol, 232*(2), 357-374.

Bowling, A. C., & Beal, M. F. (1995). Bioenergetic and oxidative stress in neurodegenerative diseases. *Life Sci, 56*(14), 1151-1171.

Braak, H., & Braak, E. (1994). Morphological criteria for the recognition of Alzheimer's disease and the distribution pattern of cortical changes related to this disorder. *Neurobiol Aging, 15*(3), 355-356; discussion 379-380.

Brenner, D., & Mak, T. W. (2009). Mitochondrial cell death effectors. *Curr Opin Cell Biol, 21*(6), 871-877.

Brown, J. M., Boysen, M. S., Jensen, S. S., Morrison, R. F., Storkson, J., Lea-Currie, R., et al. (2003). Isomer-specific regulation of metabolism and PPARgamma signaling by CLA in human preadipocytes. *J Lipid Res, 44*(7), 1287-1300.

Camandola, S., & Mattson, M. P. (2010). Aberrant subcellular neuronal calcium regulation in aging and Alzheimer's disease. *Biochim Biophys Acta*.

Castillo, J., Dávalos, A., Naveiro, J., & Noya, M. (1996). Neuroexcitatory amino acids and their relation to infarct size and neurological deficit in ischemic stroke. *Stroke, 27*(6), 1060-1065.

Cavone, L., Aldinucci, A., Ballerini, C., Biagioli, T., Moroni, F., & Chiarugi, A. (2011). PARP-1 inhibition prevents CNS migration of dendritic cells during EAE, suppressing the encephalitogenic response and relapse severity. *Mult Scler*.

Chapman, A. G. (2000). Glutamate and epilepsy. *J Nutr, 130*(4S Suppl), 1043S-1045S.

Cheng, A., Wang, S., Cai, J., Rao, M. S., & Mattson, M. P. (2003). Nitric oxide acts in a positive feedback loop with BDNF to regulate neural progenitor cell proliferation and differentiation in the mammalian brain. *Dev Biol, 258*(2), 319-333.

Choi, D. W. (1985). Glutamate neurotoxicity in cortical cell culture is calcium dependent. *Neurosci Lett, 58*(3), 293-297.

Choi, D. W. (1988). Glutamate neurotoxicity and diseases of the nervous system. *Neuron, 1*(8), 623-634.

Choi, D. W. (1992). Excitotoxic cell death. *J Neurobiol, 23*(9), 1261-1276.

Conn, P. J., & Pin, J. P. (1997). Pharmacology and functions of metabotropic glutamate receptors. *Annu Rev Pharmacol Toxicol, 37*, 205-237.

Corder, E. H., Saunders, A. M., Strittmatter, W. J., Schmechel, D. E., Gaskell, P. C., Small, G. W., et al. (1993). Gene dose of apolipoprotein E type 4 allele and the risk of Alzheimer's disease in late onset families. *Science, 261*(5123), 921-923.

Corona, J. C., Tovar-y-Romo, L. B., & Tapia, R. (2007). Glutamate excitotoxicity and therapeutic targets for amyotrophic lateral sclerosis. *Expert Opin Ther Targets, 11*(11), 1415-1428.

Cosi, C., & Marien, M. (1999). Implication of poly (ADP-ribose) polymerase (PARP) in neurodegeneration and brain energy metabolism. Decreases in mouse brain NAD+ and ATP caused by MPTP are prevented by the PARP inhibitor benzamide. *Ann N Y Acad Sci, 890*, 227-239.

Coyle, J. T., & Puttfarcken, P. (1993). Oxidative stress, glutamate, and neurodegenerative disorders. *Science, 262*(5134), 689-695.

Crescentini, G., & Stocchi, V. (1984). Fast reversed-phase high-performance liquid chromatographic determination of nucleotides in red blood cells. *J Chromatogr, 290*, 393-399.

d'Abramo, C., Ricciarelli, R., Pronzato, M. A., & Davies, P. (2006). Troglitazone, a peroxisome proliferator-activated receptor-gamma agonist, decreases tau phosphorylation in CHOtau4R cells. *J Neurochem, 98*(4), 1068-1077.

Dawson, V. L., & Dawson, T. M. (2004). Deadly conversations: nuclear-mitochondrial cross-talk. *J Bioenerg Biomembr, 36*(4), 287-294.

Dingledine, R., Borges, K., Bowie, D., & Traynelis, S. F. (1999). The glutamate receptor ion channels. *Pharmacol Rev, 51*(1), 7-61.

Dirnagl, U., Iadecola, C., & Moskowitz, M. A. (1999). Pathobiology of ischaemic stroke: an integrated view. *Trends Neurosci, 22*(9), 391-397.

Doyle, L., Jewell, C., Mullen, A., Nugent, A. P., Roche, H. M., & Cashman, K. D. (2005). Effect of dietary supplementation with conjugated linoleic acid on markers of calcium and bone metabolism in healthy adult men. *Eur J Clin Nutr, 59*(3), 432-440.

Dudek, S. M., & Bear, M. F. (1992). Homosynaptic long-term depression in area CA1 of hippocampus and effects of N-methyl-D-aspartate receptor blockade. *Proc Natl Acad Sci U S A, 89*(10), 4363-4367.

Estrada Sanchez, A. M., Mejia-Toiber, J., & Massieu, L. (2008). Excitotoxic neuronal death and the pathogenesis of Huntington's disease. *Arch Med Res, 39*(3), 265-276.

Evans, M., Geigerman, C., Cook, J., Curtis, L., Kuebler, B., & McIntosh, M. (2000). Conjugated linoleic acid suppresses triglyceride accumulation and induces apoptosis in 3T3-L1 preadipocytes. *Lipids, 35*(8), 899-910.

Fa, M., Diana, A., Carta, G., Cordeddu, L., Melis, M. P., Murru, E., et al. (2005). Incorporation and metabolism of c9,t11 and t10,c12 conjugated linoleic acid (CLA) isomers in rat brain. *Biochim Biophys Acta, 1736*(1), 61-66.

Fonnum, F. (1984). Glutamate: a neurotransmitter in mammalian brain. *J Neurochem, 42*(1), 1-11.

Forder, J. P., & Tymianski, M. (2009). Postsynaptic mechanisms of excitotoxicity: Involvement of postsynaptic density proteins, radicals, and oxidant molecules. *Neuroscience, 158*(1), 293-300.

Frykholm, P., Andersson, J. L., Valtysson, J., Silander, H. C., Hillered, L., Persson, L., et al. (2000). A metabolic threshold of irreversible ischemia demonstrated by PET in a middle cerebral artery occlusion-reperfusion primate model. *Acta Neurol Scand, 102*(1), 18-26.

Fuenzalida, K., Quintanilla, R., Ramos, P., Piderit, D., Fuentealba, R. A., Martinez, G., et al. (2007). Peroxisome proliferator-activated receptor gamma up-regulates the Bcl-2 anti-apoptotic protein in neurons and induces mitochondrial stabilization

and protection against oxidative stress and apoptosis. *J Biol Chem, 282*(51), 37006-37015.

Galluzzi, L., Blomgren, K., & Kroemer, G. (2009). Mitochondrial membrane permeabilization in neuronal injury. *Nat Rev Neurosci, 10*(7), 481-494.

Gan, L., & Mucke, L. (2008). Paths of convergence: sirtuins in aging and neurodegeneration. *Neuron, 58*(1), 10-14.

Garcia-Bueno, B., Caso, J. R., Perez-Nievas, B. G., Lorenzo, P., & Leza, J. C. (2007). Effects of peroxisome proliferator-activated receptor gamma agonists on brain glucose and glutamate transporters after stress in rats. *Neuropsychopharmacology, 32*(6), 1251-1260.

Gaullier, J. M., Halse, J., Hoye, K., Kristiansen, K., Fagertun, H., Vik, H., et al. (2005). Supplementation with conjugated linoleic acid for 24 months is well tolerated by and reduces body fat mass in healthy, overweight humans. *J Nutr, 135*(4), 778-784.

Goodwin, P. M., Lewis, P. J., Davies, M. I., Skidmore, C. J., & Shall, S. (1978). The effect of gamma radiation and neocarzinostatin on NAD and ATP levels in mouse leukaemia cells. *Biochim Biophys Acta, 543*(4), 576-582.

Ha, Y. L., Grimm, N. K., & Pariza, M. W. (1987). Anticarcinogens from fried ground beef: heat-altered derivatives of linoleic acid. *Carcinogenesis, 8*(12), 1881-1887.

Hara, M. R., & Snyder, S. H. (2007). Cell signaling and neuronal death. *Annu Rev Pharmacol Toxicol, 47*, 117-141.

Hardingham, G. E. (2009). Coupling of the NMDA receptor to neuroprotective and neurodestructive events. *Biochem Soc Trans, 37*(Pt 6), 1147-1160.

Heneka, M. T., & O'Banion, M. K. (2007). Inflammatory processes in Alzheimer's disease. *J Neuroimmunol, 184*(1-2), 69-91.

Hengartner, M. O. (2000). The biochemistry of apoptosis. *Nature, 407*(6805), 770-776.

Herbel, B. K., McGuire, M. K., McGuire, M. A., & Shultz, T. D. (1998). Safflower oil consumption does not increase plasma conjugated linoleic acid concentrations in humans. *Am J Clin Nutr, 67*(2), 332-337.

Herceg, Z., & Wang, Z. Q. (1999). Failure of poly(ADP-ribose) polymerase cleavage by caspases leads to induction of necrosis and enhanced apoptosis. *Mol Cell Biol, 19*(7), 5124-5133.

Hertz, L. (2008). Bioenergetics of cerebral ischemia: a cellular perspective. *Neuropharmacology, 55*(3), 289-309.

Houseknecht, K. L., Vanden Heuvel, J. P., Moya-Camarena, S. Y., Portocarrero, C. P., Peck, L. W., Nickel, K. P., et al. (1998). Dietary conjugated linoleic acid normalizes impaired glucose tolerance in the Zucker diabetic fatty fa/fa rat. *Biochem Biophys Res Commun, 244*(3), 678-682.

Huber, A., Bai, P., de Murcia, J. M., & de Murcia, G. (2004). PARP-1, PARP-2 and ATM in the DNA damage response: functional synergy in mouse development. *DNA Repair (Amst), 3*(8-9), 1103-1108.

Hunt, W. T., Kamboj, A., Anderson, H. D., & Anderson, C. M. (2010). Protection of cortical neurons from excitotoxicity by conjugated linoleic acid. *J Neurochem, 115*(1), 123-130.

Jonas, S., Aiyagari, V., Vieira, D., & Figueroa, M. (2001). The failure of neuronal protective agents versus the success of thrombolysis in the treatment of ischemic stroke. The predictive value of animal models. *Ann N Y Acad Sci, 939*, 257-267.

Joo, N. E., & Park, C. S. (2003). Inhibition of excitotoxicity in cultured rat cortical neurons by a mixture of conjugated linoleic acid isomers. *Pharmacol Res, 47*(4), 305-310.

Kapadia, R., Yi, J. H., & Vemuganti, R. (2008). Mechanisms of anti-inflammatory and neuroprotective actions of PPAR-gamma agonists. *Front Biosci, 13*, 1813-1826.

Kauppinen, T. M., Suh, S. W., Berman, A. E., Hamby, A. M., & Swanson, R. A. (2009). Inhibition of poly(ADP-ribose) polymerase suppresses inflammation and promotes recovery after ischemic injury. *J Cereb Blood Flow Metab, 29*(4), 820-829.

Kauppinen, T. M., & Swanson, R. A. (2007). The role of poly(ADP-ribose) polymerase-1 in CNS disease. *Neuroscience, 145*(4), 1267-1272.

Kelley, N. S., Hubbard, N. E., & Erickson, K. L. (2007). Conjugated linoleic acid isomers and cancer. *J Nutr, 137*(12), 2599-2607.

Kennedy, A., Chung, S., LaPoint, K., Fabiyi, O., & McIntosh, M. K. (2008). Trans-10, cis-12 conjugated linoleic acid antagonizes ligand-dependent PPARgamma activity in primary cultures of human adipocytes. *J Nutr, 138*(3), 455-461.

Kennedy, A., Martinez, K., Schmidt, S., Mandrup, S., LaPoint, K., & McIntosh, M. (2010). Antiobesity mechanisms of action of conjugated linoleic acid. *J Nutr Biochem, 21*(3), 171-179.

Kerr, J. F., Wyllie, A. H., & Currie, A. R. (1972). Apoptosis: a basic biological phenomenon with wide-ranging implications in tissue kinetics. *Br J Cancer, 26*(4), 239-257.

Kim, H. W., Chang, Y. C., Chen, M., Rapoport, S. I., & Rao, J. S. (2009). Chronic NMDA administration to rats increases brain pro-apoptotic factors while decreasing anti-Apoptotic factors and causes cell death. *BMC Neurosci, 10*, 123.

Kohr, G. (2006). NMDA receptor function: subunit composition versus spatial distribution. *Cell Tissue Res, 326*(2), 439-446.

Kowalska, A. (2004). Genetic basis of neurodegeneration in familial Alzheimer's disease. *Pol J Pharmacol, 56*(2), 171-178.

Kramer, J. K., Parodi, P. W., Jensen, R. G., Mossoba, M. M., Yurawecz, M. P., & Adlof, R. O. (1998). Rumenic acid: a proposed common name for the major conjugated linoleic acid isomer found in natural products. *Lipids, 33*(8), 835.

Lai, K. L., Torres-Duarte, A. P., & Vanderhoek, J. Y. (2005). 9-trans, 11-trans-CLA: antiproliferative and proapoptotic effects on bovine endothelial cells. *Lipids, 40*(11), 1107-1116.

Lau, A., & Tymianski, M. (2010). Glutamate receptors, neurotoxicity and neurodegeneration. *Pflugers Arch*.

Lee, K. N., Kritchevsky, D., & Pariza, M. W. (1994). Conjugated linoleic acid and atherosclerosis in rabbits. *Atherosclerosis, 108*(1), 19-25.

Lemberger, T., Desvergne, B., & Wahli, W. (1996). Peroxisome proliferator-activated receptors: a nuclear receptor signaling pathway in lipid physiology. *Annu Rev Cell Dev Biol, 12*, 335-363.

Li, X., Klaus, J. A., Zhang, J., Xu, Z., Kibler, K. K., Andrabi, S. A., et al. (2010). Contributions of poly(ADP-ribose) polymerase-1 and -2 to nuclear translocation of apoptosis-inducing factor and injury from focal cerebral ischemia. *J Neurochem, 113*(4), 1012-1022.

Lijtmaer, H., Fuld, P. A., & Katzman, R. (1976). Letter: Prevalence and malignancy of Alzheimer disease. *Arch Neurol, 33*(4), 304.

Liu, Y., Wong, T. P., Aarts, M., Rooyakkers, A., Liu, L., Lai, T. W., et al. (2007). NMDA receptor subunits have differential roles in mediating excitotoxic neuronal death both in vitro and in vivo. *J Neurosci, 27*(11), 2846-2857.

Lopes, P. A., Martins, S. V., Pinho, M. S., Alfaia, C. M., Fontes, C. M., Rodrigues, P. O., et al. (2008). Diet supplementation with the cis-9,trans-11 conjugated linoleic acid isomer affects the size of adipocytes in Wistar rats. *Nutr Res, 28*(7), 480-486.

Loscher, C. E., Draper, E., Leavy, O., Kelleher, D., Mills, K. H., & Roche, H. M. (2005). Conjugated linoleic acid suppresses NF-kappa B activation and IL-12 production in dendritic cells through ERK-mediated IL-10 induction. *J Immunol, 175*(8), 4990-4998.

Love, S., Barber, R., & Wilcock, G. K. (1999). Increased poly(ADP-ribosyl)ation of nuclear proteins in Alzheimer's disease. *Brain, 122 (Pt 2)*, 247-253.

Mandir, A. S., Poitras, M. F., Berliner, A. R., Herring, W. J., Guastella, D. B., Feldman, A., et al. (2000). NMDA but not non-NMDA excitotoxicity is mediated by Poly(ADP-ribose) polymerase. *J Neurosci, 20*(21), 8005-8011.

Mark, L. P., Prost, R. W., Ulmer, J. L., Smith, M. M., Daniels, D. L., Strottmann, J. M., et al. (2001). Pictorial review of glutamate excitotoxicity: fundamental concepts for neuroimaging. *AJNR Am J Neuroradiol, 22*(10), 1813-1824.

Martin, J. C., & Valeille, K. (2002). Conjugated linoleic acids: all the same or to everyone its own function? *Reprod Nutr Dev, 42*(6), 525-536.

Mattson, M. P. (2003). Excitotoxic and excitoprotective mechanisms: Abundant targets for the prevention and treatment of neurodegenerative disorders. *NeuroMolecular Medicine, 3*(2), 65-94.

Mattson, M. P. (2007). Calcium and neurodegeneration. *Aging Cell, 6*(3), 337-350.

Mattson, M. P. (2008). Glutamate and neurotrophic factors in neuronal plasticity and disease. *Ann N Y Acad Sci, 1144*, 97-112.

Mattson, M. P., Cheng, B., Davis, D., Bryant, K., Lieberburg, I., & Rydel, R. E. (1992). beta-Amyloid peptides destabilize calcium homeostasis and render human cortical neurons vulnerable to excitotoxicity. *J Neurosci, 12*(2), 376-389.

Mattson, M. P., Dou, P., & Kater, S. B. (1988). Outgrowth-regulating actions of glutamate in isolated hippocampal pyramidal neurons. *J Neurosci, 8*(6), 2087-2100.

Mattson, M. P., Duan, W., Chan, S. L., Cheng, A., Haughey, N., Gary, D. S., et al. (2002). Neuroprotective and neurorestorative signal transduction mechanisms in brain aging: modification by genes, diet and behavior. *Neurobiol Aging, 23*(5), 695-705.

McGeer, P. L., & McGeer, E. G. (1998). Mechanisms of cell death in Alzheimer disease--immunopathology. *J Neural Transm Suppl, 54*, 159-166.

McLeod, R. S., LeBlanc, A. M., Langille, M. A., Mitchell, P. L., & Currie, D. L. (2004). Conjugated linoleic acids, atherosclerosis, and hepatic very-low-density lipoprotein metabolism. *Am J Clin Nutr, 79*(6 Suppl), 1169S-1174S.

Miller, A., Stanton, C., & Devery, R. (2002). Cis 9, trans 11- and trans 10, cis 12-conjugated linoleic acid isomers induce apoptosis in cultured SW480 cells. *Anticancer Res, 22*(6C), 3879-3887.

Mitchell, P. L., & McLeod, R. S. (2008). Conjugated linoleic acid and atherosclerosis: studies in animal models. *Biochem Cell Biol, 86*(4), 293-301.

Moloney, F., Toomey, S., Noone, E., Nugent, A., Allan, B., Loscher, C. E., et al. (2007). Antidiabetic effects of cis-9, trans-11-conjugated linoleic acid may be mediated via anti-inflammatory effects in white adipose tissue. *Diabetes, 56*(3), 574-582.

Montpied, P., Weller, M., & Paul, S. M. (1993). N-methyl-D-aspartate receptor agonists decrease protooncogene bcl-2 mRNA expression in cultured rat cerebellar granule neurons. *Biochem Biophys Res Commun, 195*(2), 623-629.

Moreno, H., Wu, W. E., Lee, T., Brickman, A., Mayeux, R., Brown, T. R., et al. (2007). Imaging the Abeta-related neurotoxicity of Alzheimer disease. *Arch Neurol, 64*(10), 1467-1477.

Moya-Camarena, S. Y., & Belury, M. A. (1999). CLA and PPARgamma activation. *J Nutr, 129*(11), 2106.

Moya-Camarena, S. Y., Vanden Heuvel, J. P., Blanchard, S. G., Leesnitzer, L. A., & Belury, M. A. (1999). Conjugated linoleic acid is a potent naturally occurring ligand and activator of PPARalpha. *J Lipid Res, 40*(8), 1426-1433.

Nagao, K., Inoue, N., Wang, Y. M., Hirata, J., Shimada, Y., Nagao, T., et al. (2003). The 10trans,12cis isomer of conjugated linoleic acid suppresses the development of hypertension in Otsuka Long-Evans Tokushima fatty rats. *Biochem Biophys Res Commun, 306*(1), 134-138.

Nakamura, Y. K., Flintoff-Dye, N., & Omaye, S. T. (2008). Conjugated linoleic acid modulation of risk factors associated with atherosclerosis. *Nutr Metab (Lond), 5*, 22.

Nakanishi, T., Koutoku, T., Kawahara, S., Murai, A., & Furuse, M. (2003). Dietary conjugated linoleic acid reduces cerebral prostaglandin E(2) in mice. *Neurosci Lett, 341*(2), 135-138.

Navarro, M. A., Badimon, L., Rodriguez, C., Arnal, C., Noone, E. J., Roche, H. M., et al. (2010). Trans-10,cis-12-CLA dysregulate lipid and glucose metabolism and induce hepatic NR4A receptors. *Front Biosci (Elite Ed), 2*, 87-97.

Nedergaard, M., Takano, T., & Hansen, A. J. (2002). Beyond the role of glutamate as a neurotransmitter. *Nat Rev Neurosci, 3*(9), 748-755.

Nestel, P., Fujii, A., & Allen, T. (2006). The cis-9,trans-11 isomer of conjugated linoleic acid (CLA) lowers plasma triglyceride and raises HDL cholesterol concentrations but does not suppress aortic atherosclerosis in diabetic apoE-deficient mice. *Atherosclerosis, 189*(2), 282-287.

Nicholls, D. G. (2004). Mitochondrial dysfunction and glutamate excitotoxicity studied in primary neuronal cultures. *Curr Mol Med, 4*(2), 149-177.

Nicholls, D. G. (2008). Oxidative stress and energy crises in neuronal dysfunction. *Ann N Y Acad Sci, 1147*, 53-60.

Niizuma, K., Yoshioka, H., Chen, H., Kim, G. S., Jung, J. E., Katsu, M., et al. (2010). Mitochondrial and apoptotic neuronal death signaling pathways in cerebral ischemia. *Biochim Biophys Acta, 1802*(1), 92-99.

Ochoa, J. J., Farquharson, A. J., Grant, I., Moffat, L. E., Heys, S. D., & Wahle, K. W. (2004). Conjugated linoleic acids (CLAs) decrease prostate cancer cell proliferation: different molecular mechanisms for cis-9, trans-11 and trans-10, cis-12 isomers. *Carcinogenesis, 25*(7), 1185-1191.

Olney, J. W. (1986). Inciting excitotoxic cytocide among central neurons. *Adv Exp Med Biol, 203*, 631-645.

Olney, J. W. (Ed.). (1974). *Toxic effects of glutamate and related amino acids on the developing central nervous system*. New York: John Wiley & Sons, Inc.

Osborn, G. G., & Saunders, A. V. (2010). Current treatments for patients with Alzheimer disease. *J Am Osteopath Assoc, 110*(9 Suppl 8), S16-26.

Pacher, P., & Szabo, C. (2005). Role of poly(ADP-ribose) polymerase-1 activation in the pathogenesis of diabetic complications: endothelial dysfunction, as a common underlying theme. *Antioxid Redox Signal, 7*(11-12), 1568-1580.

Palmquist, D. L., Lock, A. L., Shingfield, K. J., & Bauman, D. E. (2005). Biosynthesis of conjugated linoleic acid in ruminants and humans. *Adv Food Nutr Res, 50*, 179-217.

Pariza, M. W., Ashoor, S. H., Chu, F. S., & Lund, D. B. (1979). Effects of temperature and time on mutagen formation in pan-fried hamburger. *Cancer Lett, 7*(2-3), 63-69.

Park, Y., Albright, K. J., Liu, W., Storkson, J. M., Cook, M. E., & Pariza, M. W. (1997). Effect of conjugated linoleic acid on body composition in mice. *Lipids, 32*(8), 853-858.

Paschen, W., Olah, L., & Mies, G. (2000). Effect of transient focal ischemia of mouse brain on energy state and NAD levels: no evidence that NAD depletion plays a major role in secondary disturbances of energy metabolism. *J Neurochem, 75*(4), 1675-1680.

Pieper, A. A., Blackshaw, S., Clements, E. E., Brat, D. J., Krug, D. K., White, A. J., et al. (2000). Poly(ADP-ribosyl)ation basally activated by DNA strand breaks reflects glutamate-nitric oxide neurotransmission. *Proc Natl Acad Sci U S A, 97*(4), 1845-1850.

Pieper, A. A., Verma, A., Zhang, J., & Snyder, S. H. (1999). Poly (ADP-ribose) polymerase, nitric oxide and cell death. *Trends Pharmacol Sci, 20*(4), 171-181.

Platt, S. R. (2007). The role of glutamate in central nervous system health and disease--a review. *Vet J, 173*(2), 278-286.

Qin, H., Liu, Y., Lu, N., Li, Y., & Sun, C. H. (2009). cis-9,trans-11-Conjugated Linoleic Acid Activates AMP-Activated Protein Kinase in Attenuation of Insulin Resistance in C(2)C(12) Myotubes. *J Agric Food Chem*.

Querfurth, H. W., & LaFerla, F. M. (2010). Alzheimer's disease. *N Engl J Med, 362*(4), 329-344.

Rauk, A. (2008). Why is the amyloid beta peptide of Alzheimer's disease neurotoxic? *Dalton Trans*(10), 1273-1282.

Reynolds, C. M., & Roche, H. M. (2010). Conjugated linoleic acid and inflammatory cell signalling. *Prostaglandins Leukot Essent Fatty Acids, 82*(4-6), 199-204.

Reynolds, I. J., & Hastings, T. G. (1995). Glutamate induces the production of reactive oxygen species in cultured forebrain neurons following NMDA receptor activation. *J Neurosci, 15*(5 Pt 1), 3318-3327.

Riederer, P., & Hoyer, S. (2006). From benefit to damage. Glutamate and advanced glycation end products in Alzheimer brain. *J Neural Transm, 113*(11), 1671-1677.

Riel, R. R. (1963). Physico-chemical characteristics of Canadian milk fat unsaturated fatty acids. *J. Dairy Sci., 46*, 102-106.

Ringseis, R., Muller, A., Herter, C., Gahler, S., Steinhart, H., & Eder, K. (2006). CLA isomers inhibit TNFalpha-induced eicosanoid release from human vascular smooth muscle cells via a PPARgamma ligand-like action. *Biochim Biophys Acta, 1760*(2), 290-300.

Riserus, U., Arner, P., Brismar, K., & Vessby, B. (2002). Treatment with dietary trans10cis12 conjugated linoleic acid causes isomer-specific insulin resistance in obese men with the metabolic syndrome. *Diabetes Care, 25*(9), 1516-1521.

Riserus, U., Vessby, B., Arnlov, J., & Basu, S. (2004). Effects of cis-9,trans-11 conjugated linoleic acid supplementation on insulin sensitivity, lipid peroxidation, and proinflammatory markers in obese men. *Am J Clin Nutr, 80*(2), 279-283.

Ritzenthaler, K. L., McGuire, M. K., Falen, R., Shultz, T. D., Dasgupta, N., & McGuire, M. A. (2001). Estimation of conjugated linoleic acid intake by written dietary assessment methodologies underestimates actual intake evaluated by food duplicate methodology. *J Nutr, 131*(5), 1548-1554.

Roche, H. M., Noone, E., Sewter, C., Mc Bennett, S., Savage, D., Gibney, M. J., et al. (2002). Isomer-dependent metabolic effects of conjugated linoleic acid: insights from molecular markers sterol regulatory element-binding protein-1c and LXRalpha. *Diabetes, 51*(7), 2037-2044.

Ryder, J. W., Portocarrero, C. P., Song, X. M., Cui, L., Yu, M., Combatsiaris, T., et al. (2001). Isomer-specific antidiabetic properties of conjugated linoleic acid. Improved glucose tolerance, skeletal muscle insulin action, and UCP-2 gene expression. *Diabetes, 50*(5), 1149-1157.

Sattler, R., Charlton, M. P., Hafner, M., & Tymianski, M. (1998). Distinct influx pathways, not calcium load, determine neuronal vulnerability to calcium neurotoxicity. *J Neurochem, 71*(6), 2349-2364.

Selkoe, D. J. (2002). Deciphering the genesis and fate of amyloid beta-protein yields novel therapies for Alzheimer disease. *J Clin Invest, 110*(10), 1375-1381.

Selkoe, D. J. (2004). Alzheimer disease: mechanistic understanding predicts novel therapies. *Ann Intern Med, 140*(8), 627-638.

Sheline, C. T., Behrens, M. M., & Choi, D. W. (2000). Zinc-induced cortical neuronal death: contribution of energy failure attributable to loss of NAD(+) and inhibition of glycolysis. *J Neurosci, 20*(9), 3139-3146.

Shigeri, Y., Seal, R. P., & Shimamoto, K. (2004). Molecular pharmacology of glutamate transporters, EAATs and VGLUTs. *Brain Res Brain Res Rev, 45*(3), 250-265.

Sikorski, A. M., Hebert, N., & Swain, R. A. (2008). Conjugated Linoleic Acid (CLA) inhibits new vessel growth in the mammalian brain. *Brain Res, 1213*, 35-40.

Soane, L., & Fiskum, G. (2005). Inhibition of mitochondrial neural cell death pathways by protein transduction of Bcl-2 family proteins. *J Bioenerg Biomembr, 37*(3), 179-190.

Sodhi, R. K., Singh, N., & Jaggi, A. S. (2010). Poly(ADP-ribose) polymerase-1 (PARP-1) and its therapeutic implications. *Vascul Pharmacol, 53*(3-4), 77-87.

Soel, S. M., Choi, O. S., Bang, M. H., Yoon Park, J. H., & Kim, W. K. (2007). Influence of conjugated linoleic acid isomers on the metastasis of colon cancer cells in vitro and in vivo. *J Nutr Biochem, 18*(10), 650-657.

Strosznajder, J. B., Jesko, H., & Strosznajder, R. P. (2000). Effect of amyloid beta peptide on poly(ADP-ribose) polymerase activity in adult and aged rat hippocampus. *Acta Biochim Pol, 47*(3), 847-854.

Suh, S. W., Aoyama, K., Alano, C. C., Anderson, C. M., Hamby, A. M., & Swanson, R. A. (2007). Zinc inhibits astrocyte glutamate uptake by activation of poly(ADP-ribose) polymerase-1. *Mol Med, 13*(7-8), 344-349.

Suzuki, M., Nelson, A. D., Eickstaedt, J. B., Wallace, K., Wright, L. S., & Svendsen, C. N. (2006). Glutamate enhances proliferation and neurogenesis in human neural progenitor cell cultures derived from the fetal cortex. *Eur J Neurosci, 24*(3), 645-653.

Takuma, H., Tomiyama, T., Kuida, K., & Mori, H. (2004). Amyloid beta peptide-induced cerebral neuronal loss is mediated by caspase-3 in vivo. *J Neuropathol Exp Neurol, 63*(3), 255-261.

Tanaka, S., Takehashi, M., Iida, S., Kitajima, T., Kamanaka, Y., Stedeford, T., et al. (2005). Mitochondrial impairment induced by poly(ADP-ribose) polymerase-1 activation in cortical neurons after oxygen and glucose deprivation. *J Neurochem, 95*(1), 179-190.

Tang, K. S., Suh, S. W., Alano, C. C., Shao, Z., Hunt, W. T., Swanson, R. A., et al. (2010). Astrocytic poly(ADP-ribose) polymerase-1 activation leads to bioenergetic depletion and inhibition of glutamate uptake capacity. *Glia, 58*(4), 446-457.

Terpstra, A. H., Javadi, M., Beynen, A. C., Kocsis, S., Lankhorst, A. E., Lemmens, A. G., et al. (2003). Dietary conjugated linoleic acids as free fatty acids and triacylglycerols similarly affect body composition and energy balance in mice. *J Nutr, 133*(10), 3181-3186.

Tholstrup, T., Raff, M., Straarup, E. M., Lund, P., Basu, S., & Bruun, J. M. (2008). An oil mixture with trans-10, cis-12 conjugated linoleic acid increases markers of inflammation and in vivo lipid peroxidation compared with cis-9, trans-11 conjugated linoleic acid in postmenopausal women. *J Nutr, 138*(8), 1445-1451.

Tricon, S., Burdge, G. C., Kew, S., Banerjee, T., Russell, J. J., Jones, E. L., et al. (2004). Opposing effects of cis-9,trans-11 and trans-10,cis-12 conjugated linoleic acid on blood lipids in healthy humans. *Am J Clin Nutr, 80*(3), 614-620.

Uryu, S., Harada, J., Hisamoto, M., & Oda, T. (2002). Troglitazone inhibits both post-glutamate neurotoxicity and low-potassium-induced apoptosis in cerebellar granule neurons. *Brain Res, 924*(2), 229-236.

Uttara, B., Singh, A. V., Zamboni, P., & Mahajan, R. T. (2009). Oxidative stress and neurodegenerative diseases: a review of upstream and downstream antioxidant therapeutic options. *Curr Neuropharmacol, 7*(1), 65-74.

VanDongen, A. M. (Ed.). (2009). *Biology of the NMDA receptor*: CRC Press.

Verderio, C., Bruzzone, S., Zocchi, E., Fedele, E., Schenk, U., De Flora, A., et al. (2001). Evidence of a role for cyclic ADP-ribose in calcium signalling and neurotransmitter release in cultured astrocytes. *J Neurochem, 78*(3), 646-657.

Wang, Y., & Qin, Z. H. (2010). Molecular and cellular mechanisms of excitotoxic neuronal death. *Apoptosis*.

Yagami, T., Takahara, Y., Ishibashi, C., Sakaguchi, G., Itoh, N., Ueda, K., et al. (2004). Amyloid beta protein impairs motor function via thromboxane A2 in the rat striatum. *Neurobiol Dis, 16*(3), 481-489.

Yashiro, K., & Philpot, B. D. (2008). Regulation of NMDA receptor subunit expression and its implications for LTD, LTP, and metaplasticity. *Neuropharmacology, 55*(7), 1081-1094.

Yelamos, J., Schreiber, V., & Dantzer, F. (2008). Toward specific functions of poly(ADP-ribose) polymerase-2. *Trends Mol Med, 14*(4), 169-178.

Ying, W., Garnier, P., & Swanson, R. A. (2003). NAD+ repletion prevents PARP-1-induced glycolytic blockade and cell death in cultured mouse astrocytes. *Biochem Biophys Res Commun, 308*(4), 809-813.

Yu, S. W., Wang, H., Dawson, T. M., & Dawson, V. L. (2003). Poly(ADP-ribose) polymerase-1 and apoptosis inducing factor in neurotoxicity. *Neurobiol Dis, 14*(3), 303-317.

Yu, S. W., Wang, H., Poitras, M. F., Coombs, C., Bowers, W. J., Federoff, H. J., et al. (2002). Mediation of poly(ADP-ribose) polymerase-1-dependent cell death by apoptosis-inducing factor. *Science, 297*(5579), 259-263.

Yu, Y., Correll, P. H., & Vanden Heuvel, J. P. (2002). Conjugated linoleic acid decreases production of pro-inflammatory products in macrophages: evidence for a PPAR gamma-dependent mechanism. *Biochim Biophys Acta, 1581*(3), 89-99.

Zeng, J., Yang, G. Y., Ying, W., Kelly, M., Hirai, K., James, T. L., et al. (2007). Pyruvate improves recovery after PARP-1-associated energy failure induced by oxidative stress in neonatal rat cerebrocortical slices. *J Cereb Blood Flow Metab, 27*(2), 304-315.

Zhang, J., Dawson, V. L., Dawson, T. M., & Snyder, S. H. (1994). Nitric oxide activation of poly(ADP-ribose) synthetase in neurotoxicity. *Science, 263*(5147), 687-689.

Zhang, Z., Shi, R., Weng, J., Xu, X., Li, X. M., Gao, T. M., et al. (2011). The proapoptotic member of the Bcl-2 family Bcl-2 / E1B-19K-interacting protein 3 is a mediator of caspase-independent neuronal death in excitotoxicity. *FEBS J, 278*(1), 134-142.

Zhao, X., Ou, Z., Grotta, J. C., Waxham, N., & Aronowski, J. (2006). Peroxisome-proliferator-activated receptor-gamma (PPARgamma) activation protects neurons from NMDA excitotoxicity. *Brain Res, 1073-1074*, 460-469.

Zhao, Y., Patzer, A., Herdegen, T., Gohlke, P., & Culman, J. (2006). Activation of cerebral peroxisome proliferator-activated receptors gamma promotes neuroprotection by attenuation of neuronal cyclooxygenase-2 overexpression after focal cerebral ischemia in rats. *FASEB J, 20*(8), 1162-1175.